# A New Multisampling-Based Non-Coherent FSK Receiver Using Parametric Spectrum Estimators

by

Wael Hasan A. Shehadah

A Thesis Presented to the

FACULTY OF THE COLLEGE OF GRADUATE STUDIES

KING FAHD UNIVERSITY OF PETROLEUM & MINERALS

DHAHRAN, SAUDI ARABIA

In Partial Fulfillment of the
Requirements for the Degree of

**MASTER OF SCIENCE**

In

**ELECTRICAL ENGINEERING**

July, 1992

# A new multisampling-based non-coherent FSK receiver using parametric spectrum estimators

Shehadah, Wael Hasan Awadallah, M.S.

King Fahd University of Petroleum and Minerals (Saudi Arabia), 1992

# A NEW MULTISAMPLING-BASED NON-COHERENT FSK RECEIVER USING PARAMETRIC SPECTRUM ESTIMATORS

BY


## WAEL HASAN A. SHEHADAH


A Thesis Presented to the

FACULTY OF THE COLLEGE OF GRADUATE STUDIES

KING FAHD UNIVERSITY OF PETROLEUM & MINERALS

DHAHRAN, SAUDI ARABIA

In Partial Fulfillment of the
Requirements for the Degree of

## MASTER OF SCIENCE
## In
## ELECTRICAL ENGINEERING



July 1992

**KING FAHD UNIVERSITY OF PETROLEUM AND MINERALS**
**DHAHRAN, SAUDI ARABIA**

**COLLEGE OF GRADUATE STUDIES**

This thesis, written by ***WAEL HASAN AWADALLAH SHEHADAH*** under the direction of his Thesis Advisor and approved by his Thesis Committee, has been presented to and accepted by the Dean of the College of Graduate Studies, in partial fulfillment of the requirements for the degree of ***MASTER OF SCIENCE*** in ***ELECTRICAL ENGINEERING.***

***THESIS COMMITTEE***

***Dr. M. S. El-Hennawey (Chairman)***

***Dr. M. Bettayeb (Member)***

***Dr. S. Abdul Jawad (Member)***

***Dr. K. Biyari (Member)***

***Department Chairman***

***Dean, College of Graduate Studies***

# الإهداء

إلى والدي الحبيبين ..

اللذين لم أجد من هو أحق منهما بالإهداء

إلى أبي الذي علمني وجهني نحو القراءة والبحث والاطلاع وما فتئ يشجعني

إليه أهدي هذا الجهد الذي هو ثمرة من ثمار تربيته وغرسه

وإلى أمي التي ما انفكت تدعو لي وترعاني

إليهما وإلى إخوتي وأخواتي وكل من أطعمه أبي أهدي هذا العمل

وأسأل الله أن يحفظهما

وأن يرحمهما كما ربياني صغيراً

بسم الله الرحمن الرحيم

# وَقُل رَّبِّ زِدْنِي عِلْماً

(طه - ١١٤)

In the name of Allah, the Beneficient, the Merciful

*"And say: My Lord! Increase me in Knowledge!"*

**(Taha - 114)**

**To My Beloved Parents,**

**To My Brothers and Sisters,**

**And To Those Who Shared Their Care And Concern**

# ACKNOWLEDGMENT

All thanks and praises are due first and last to ALLAH, the almighty God, for the strength and courage he gave me to complete this Master Thesis.

Acknowledgment is due to *King Fahd University of Petroleum and Minerals* for support of this research.

I would like to express my deep appreciation to *Dr. M. Samy El-Hennawey*, my thesis advisor, for his patient guidance and his generous support for this research.

I would like, also, to express my gratefulness to the other committee members, *Dr. Mammar Bettayeb*, *Dr. Khalid Biyari*, and *Dr. Samir Abdul Jauwad*, for their valuable suggestions and helpful remarks.

Finally, special thanks, are due to the *Electrical Engineering Department*, *Dr. Abdullah Al-Shehri*, Chairman of Electrical Engineering Department, and *Dr. Talal Halawani*, for all the support and all the help that was extended, during the Master program.

# خلاصة

## مستقبل جديد لموجات مضمنات التردد الرقمية

## غير المتابعة متعدد القياسات


الأســـــم: وائل حسن عوض الله شحاده

التخصص: هـنـدســـــة كـهـربـائـيـــــة

التاريـــخ: يوليو ١٩٩٢



تعتبر مشكلة استقبال الأشارات في البيئات التي تتسم بسرعة تغير مكونات الموجات المستقبلة المتعددة طرق الوصول المتضائلة (مثل بيئات أجواء بعض الكواكب السيارة و البيئات التي قد تحيط بالمستقبلات المستخدمة في الوسائل المتنقلة)، من المشاكل التي تتلقى اهتماما متزايدا في الوقت الحاضر، لتزايد الحاجة للعمل في هذه البيئات و تحت تلك الظروف.

و لقد تم في هذه الرسالة، يتم طرح بنية جديدة لمستقبل مستحدث للموجات المضمنة الرقمية المتغيرة التردد الغير متابعة، ليعمل في هذه البيئات، و يلقب بالمستقبل المتعدد ترددات القياسات. وعلى عكس المستقبلات التقليدية الأخرى من نفس الفئة يقوم هذا المستقبل بتغيير تردد أخذ القياسات في كل فرع من فروعه، حيث يستخدم ترددا متغيرا لكل فرع من الفروع – بدلا من أن يستخدم نفس التردد لكل الفروع كما يحدث في المستقبلات الأخرى. هذا التردد يعادل أربعة أضعاف التردد الرئيس المستخدم للتضمين في الأشارة الرئيسة المرسلة من الفرع المعادل لذلك الفرع. بعد ذلك يتم تقدير التردد في الاشارة المستقبلة، وحساب مقدار الخطأ في تقدير التردد في كل فرع من فروع المستقبل. ويتم اختيار تردد الفرع الذي تم اكتشاف أصغر كمية خطأ فيه على أن اشارته هي الأشارة المرسلة.

ولقد قورن أداء هذا المستقبل الجديد بأداء المستقبلات التقليدية الأخرى التي تم اقتراحها سابقا للقيام بالعمل في تلك البيئات تحت نفس الحالات، ووجد أن المستقبل الجديد المقترح يتفوق على تلك المستقبلات في الأداء و مستوى دقة الارسال.



ماجستير العلوم

جامعة الملك فهد للبترول والمعادن

الظهران، المملكة العربية السعوديه

يوليو ١٩٩٢

# ABSTRACT

## A NEW MULTISAMPLING-BASED NON-COHERENT FSK RECEIVER USING PARAMETRIC SPECTRUM ESTIMATORS

**By:** Wael Hasan Awadallah Shehadah
**Major Field:** Electrical Engineering
**Date:** July 1992

The problem of detection of signals in fast multipath fading channels is increasingly gaining more attention, to achieve better performances, faster and more reliable communications, at the receivers.

In this thesis, a new FSK receiver structure, which is dubbed: the Multisampler receiver, is proposed to work in fast multipath fading channels. Contrary to the other conventional FSK receivers, this receiver samples the received signals of non-resolvable fast multipath fading channels at a distinct sampling rate in each of its branches. The sampling rate of a certain branch, is a four-fold of one of the transmitted frequencies in the transmitted frequency set. The received frequency is then estimated using a parametric estimator, in each branch. The error in frequency estimation is calculated. The magnitudes of estimation errors of all the branches are compared to each other, and the branch with the lowest error magnitude is decided in favor of.

The multisampler receiver is compared to other conventional receivers, to determine its performance. The multisampler receiver is found to give the best results for the realistic cases of fast multipath fading channels.

MASTER OF SCIENCE

KING FAHD UNIVERSITY OF PETROLEUM AND MINERALS
DHAHRAN, SAUDI ARABIA

July 1992

# CONTENTS

# LIST OF FIGURES

# LIST OF TABLES

# Chapter I
# INTRODUCTION

## 1.1 Overview

Ever since man existed on Earth, he tried to communicate with other people using different techniques. The communications techniques have varied over time. Each of the techniques has had its own advantages as well as its limitations. When the industrial revolution started to take place a couple of hundred years ago, the physical and abstract sciences have remarkably developed. The field of communications has benefited very much from these developments. Many new discoveries have taken place, since then.

There are two main disciplines, in which developments have taken place in modern communications systems. These are the analog and digital domains. It was not until recently that digital communication has received the proper attention. This was a result of the rapid growth in the computer industry, and the need for more accurate and more secure ways of communication.

Digital modulation is the process by which digital symbols are transformed into waveforms that are compatible with the characteristics of the channel. In the case of *baseband modulation*, these waveforms are pulses, but in the case of *bandpass modulation* the desired information signal modulates a sinusoid called a *carrier wave*, or simply a *carrier*. For radio transmission, the carrier is con-

verted to an electromagnetic (EM) field for propagation to the desired destination.

As the signal is transmitted, it is corrupted with noise, generally plagued with impairments, non-linearities and time-invariances and in some cases, with fading. The task of the demodulator or detector is to retrieve the symbol stream from the received waveform, as nearly error free as possible, not withstanding the distortion to which the signal may have been subjected. This signal distortion has two primary causes. The first is filtering effects of the transmitter, channel, and receiver. A non-ideal system transfer function causes symbol "smearing," which can produce *intersymbol interference*. The second cause for signal distortion is the noise that is produced by a variety of sources, such as galaxy noise, amplifier noise, and unwanted signals from other sources. The unavoidable cause of noise is the thermal motion of electrons in any conducting media, which adds to the received signal.

When it is required to transmit data over a *band-pass channel*, it is necessary to modulate the incoming data onto a carrier wave (usually sinusoidal) with fixed frequency limits imposed by the channel. The channel may be a microwave radio link, or a satellite channel, etc. The carrier sinusoid has just three features that can be used to distinguish it from other sinusoids: amplitude, frequency, and phase. In any event, the modulation process involves switching or keying the amplitude, frequency, or phase of the carrier in accordance with the incoming data. Thus there are, essentially, three methods of basic signalling techniques known as *amplitude-shift keying* (ASK), *frequency-shift keying(FSK)*, and *phase shift keying(PSK)*, which may be viewed as special cases of amplitude modulation, frequency modulation, and phase modulation, respectively.

Ideally, FSK and PSK signals have a constant envelope. This feature makes them impervious to amplitude non-linearities, as encountered in microwave radio links and satellite channels. Accordingly, we find that in practice, FSK and PSK signals are much more widely used than ASK signals.

Both Phase Shift Keying (PSK), and Frequency Shift Keying (FSK) transmission schemes, detected coherently or non-coherently, can be used for multipath detection. However, on fast fading channels, the time variations are sufficiently fast to preclude the implementation of coherent detection. In such cases, the use of DPSK or FSK, with non-coherent detection (NCFSK), becomes a necessity. Although PSK modulation scheme offer a 3 dB advantage over FSK, the latter is used more often in communication systems that are designed to work in multipath fading environments. This is because the FSK is much less susceptible to multipath distortion than the PSK, where loss of coherence is a major problem.

Orthogonal FSK with noncoherent detection is appropriate for both slow and fast fading multipath channels. In this technique, the different M messages are distinguished from each other, by transmitting one of M sinusoidal waves that differ in frequency by a fixed amount. The use of orthogonal FSK scheme with non-coherent detection, at the receiver becomes more appropriate for channels which fade fast enough to impede the establishment of a phase reference. For this reason, our attention will be focused on the FSK modulation scheme. And since the new method applied in this thesis is based on the estimation of the frequency content of the received signal, NCFSK modulation scheme will be used in the course of this thesis.

## 1.2 Statement of the Problem:

In this thesis, the main work will be focused at the receiver part. The behavior of the receivers under multipath fast fading situations is studied. In this section, a brief review of some of the existent conventional receivers is presented. Then, the problem tackled in this thesis is formulated.

The Quadrature Receiver (QR) is the most commonly used non-coherent FSK receiver. When the received signal is a continuous wave (CW) signal corrupted with additive white Gaussian noise (AWGN) with zero mean, the QR gives the optimum results. However, when the received CW signals are corrupted with non-resolvable fast fading multipath, the performance of the QR is degraded.

Multipath channels are more complex than classical (AWGN, or linear filter with AWGN) channels. They are generally described as: channels having random time-variant impulse response channels [1]. This characterization serves as a model for signal transmission over many radio channels such as shortwave ionospheric radio communication in the 3 to 30 MHz frequency band (HF), tropospheric scatter (beyond-the-horizon) radio communication in the 300 to 3000-MHz frequency band (UHF), 3000- to 30,000-MHz frequency band (SHF), and ionospheric forward scatter in the 30- to 300-MHz frequency band (VHF). The time variant impulse responses of these channels are a consequence of the constantly changing physical characteristics of the media. For example, the ions in the ionospheric layers that reflect the signals transmitted in high frequency (HF) band are always in motion. To the user of the channel, the motion of the ions appears to be random. Consequently, if the same signal is transmit-

ted at HF in two widely separated time intervals, the two received signals will not only be different, but the difference will be random rather than deterministic.

To overcome this degradation problem with the QR operating in non-resolvable fast fading multipath channels, Higgins has suggested a parallel interconnection of the quadrature receiver (QR) that is matched to the discontinuities' intervals in [2]. He assumed that the discontinuities take place in the middle of the symbol duration exactly, and proposed a receiver, which he called the Parallel Quadrature Receiver (PQR). He, then, compared the performance of this receiver (PQR) to the QR, or equivalently, the Single Quadrature Receiver (SQR). It was concluded that the PQR outperforms the SQR significantly for the case of existence of one phase discontinuity in the middle of symbol duration. However, the SQR performs slightly better in the case of no phase discontinuity existent in the duration of the symbol.

However, non-resolvable fast multipath fading signals, are different from the case used by Higgins in [2]. In many realistic situations, the occurrence and location of occurrence of phase discontinuities within a certain symbol duration due to non-resolvable multipath fading channel is completely random.

In many real situations, the occurrence and location of occurrence of phase discontinuities within a certain symbol duration is completely random. This depends on many factors. Some of these are the complexity of the reflecting mechanism, as well as the medium through which the transmission is taking place. For simplicity, Higgins [2], assumed that the signal duration is divided into two equal time intervals, with the correlation characteristics between the

two signal parts being specified by a correlation coefficient. In real world, however, the discontinuity distribution of the received signal scheme is not known. The phase discontinuity of the received signal might not take place at the middle of the symbol duration exactly. On the contrary, it might take place at some other place within the symbol duration. For example, it could happen at 1/3, 1/4, or 4/5 of the symbol duration. In addition, the phase discontinuities might not occur at all in one symbol duration. On the other hand, they could occur for a certain number of times in one symbol duration, and for a different number of times in the next symbol's duration, and so on. This gives rise to the randomness of the phase discontinuities number and their position during the consecutive symbol intervals.

This problem happens to be a real life situation, especially for receivers that are exposed to work in unknown environments. It can, also, happen to receivers of the mobile radios, and to stationary receiver units that are surrounded by rapidly changing environment. For example, in 1975, the National Aeronautics and Space Agency (NASA), launched two unmanned space-craft, Christened Viking I and II, to carry out a series of experiments designed to find traces of biological life as it may exist, or might have existed, on Mars. Each of these space-crafts consisted of two connected sections - an Orbiter and Lander - which separate in the Martian Orbital flight. A non-coherent FSK modulation scheme was used for the Lander - Orbiter channel, because of the existing multi-path problems of Mars [3].

This problem creates the need for a receiver structure that will be immune to phase discontinuities within the symbol duration as well as to the random

phase of the signal. The performance of both the SQR and the PQR receivers is degraded significantly under such cases. This problem creates the need for a receiver structure that is immune or at least less sensitive to phase discontinuities within the symbol duration, as well as to the random phase of the signal.

## 1.3 Thesis Contribution

In this thesis, a number of contributions are made. These contributions can be listed as follows:

1. The Digital Frequency-Locked Loop (DFLL) proposed in [8] is used as a non-resolvable multipath receiver. The DFLL is studied under the two cases presented by Higgins in [2], as well as the new proposed cases.
2. A new non-coherent simple FSK receiver, with a better performance, in fast fading multipath environments, than the SQR and PQR receivers, is proposed. It is tested under all cases, and its performance is compared with that of the conventional SQR and PQR receivers. The new receiver is called the Multisampler Receiver (MSR). It uses the concept of changing the sampling frequency to make the best estimate of the received frequency, instead of changing the frequency of the device to try to lock to the received frequency (like the DFLL). The work presented in this part of the thesis is new and has never been investigated before.

## 1.4 Thesis Organization:

In chapter 2 of this thesis, the conventional SQR and PQR receivers are studied in detail. A review of the work done by previous researchers in this field is presented. Then, simulations of the SQR and PQR under different (old and new) test cases are presented.

In chapter 3, the DFLL receiver is reviewed. It is used as a non-resolvable multipath receiver. The behavior of the DFLL under different fast fading cases is presented. It is then compared to that of the conventional SQR and PQR.

Chapter 4 introduces the idea of changing the sampling frequency, and how it is used to propose the new Multisampler Receiver. Then, the different tests that were carried on the previous receivers are carried on this receiver. Its performance is, then, compared to that of the SQR, and PQR.

Chapter 5 summarizes the work done in this thesis and presents the conclusions drawn from this research. In addition, it discusses some suggestions for future work.

Finally, the programs and subroutines used to simulate the different receivers are included in Appendix A. Futhermore, Appendices B and C discuss the generation of the Rayleigh amplitudes and the received signal's noise, respectively.

# Chapter II
# PERFORMANCE OF CONVENTIONAL FSK RECEIVERS IN FAST MULTIPATH FADING CHANNELS

## 2.1 Introduction

Many receivers were proposed and implemented for both analog and digital modulation domains. In the digital modulation domain, many receivers were proposed and implemented for different modulation schemes: ASK, PSK, and FSK. In some cases more than one receiver were proposed and implemented. The multiplicity of these receivers stemmed from the need to overcome a certain problem, or the need to find a better solution to a certain case or situation, in the communication system.

As we are investigating the fast multipath fading channels, our attention will be focused on some FSK receivers with noncoherence for the reasons mentioned in the preceding chapter. The most common one of these receivers is the so called *Quadrature Receiver*. It has been referred to as the *Single Quadrature Receiver*, (SQR) as opposed to the *Parallel Quadrature Receiver*, (PQR), which is a parallel interconnection of quadratures operating over different time intervals

of the symbol duration [2]. These two receivers are referred to as the convention al receivers within the course of this thesis.

In this chapter, a quick overview of the transmitted and received FSK signal structure is provided. Then, some literature review of the work done on the SQR and PQR is carried out. Next, a simulation of the behavior of the SQR and PQR under reported test cases of fast fading channels is performed. The deficiencies and problems associated with both conventional receivers are then discussed. After that, the new cases that represent the real situation of fast multipath fading channels are listed. These cases will be used to test both the conventional receivers, as well as the new Multi-Sampler Receiver, in later chapters of this thesis. Finally, a simulation of the behavior of the SQR, and PQR receivers is carried out, to study the behavior of these two receivers under multipath cases. The outcome of this simulation will be used for comparison purposes later in this thesis.

## 2.2 Transmitted FSK Signal Structure

An FSK modulation scheme for M messages is achieved by transmitting one of M frequencies that can be described by

$$s_i(t) = \begin{cases} \sqrt{\frac{2E_s}{T_s}}\cos(2\pi f_i t) & ;\ 0 \le t \le T_s \\ 0 & ;\ elsewhere \end{cases} \qquad (2.1)$$

where $i = 1, 2, \ldots, M$, $T_s$ is the period of the symbol and $E_s$ is the transmitted signal energy per symbol, and the transmitted frequency equals

$$f_i = \frac{n_c + i}{T_s} \tag{2.2}$$

for some fixed integer $n_c$ and $i = 1, 2, \ldots, M$. From Eqn. (2.1), we observe directly that the different M signals are orthogonal, but not normalized to have unit energy. We therefore deduce that the most useful form for the set of orthogonal basis functions is

$$\varphi_i(t) = \begin{cases} \sqrt{\frac{2}{T_s}} \cos(2\pi f_i t) & ; 0 \le t \le T_s \\ 0 & ; \text{elsewhere} \end{cases} \tag{2.3}$$

where $i = 1, 2, \ldots, M$. Correspondingly, the coefficient $s_{ij}$ for $i = 1, 2, \ldots, M$, and $j = 1, 2, \ldots, M$, is defined by

$$\begin{aligned} s_{ij} &= \int_0^{T_s} s_i(t)\, \varphi_j(t)\, dt \\ &= \int_0^{T_s} \sqrt{\frac{2E_s}{T_s}} \cos(2\pi f_i t) \sqrt{\frac{2}{T_s}} \cos(2\pi f_j t) \end{aligned} \tag{2.4}$$

Then,

$$s_{ij} = \begin{cases} \sqrt{E_s} & ; i = j \\ 0 & ; i \neq j \end{cases} \tag{2.5}$$

Thus, an FSK system is characterized by having a signal space that is N-dimensional (N = M), with M message points. The M message points are defined by the signal vectors

$$s_1 = \begin{bmatrix} \sqrt{E_s} \\ 0 \\ \cdot \\ \cdot \\ \cdot \\ 0 \end{bmatrix}, \quad s_2 = \begin{bmatrix} 0 \\ \sqrt{E_s} \\ 0 \\ \cdot \\ \cdot \\ \cdot \\ 0 \end{bmatrix},$$

$$s_i = \begin{bmatrix} 0 \\ 0 \\ \cdot \\ \cdot \\ \cdot \\ 0 \\ \sqrt{E_s} \\ 0 \\ \cdot \\ \cdot \\ \cdot \\ 0 \end{bmatrix}, \quad \cdots$$

$$\text{and } s_M = \begin{bmatrix} 0 \\ 0 \\ \cdot \\ \cdot \\ \cdot \\ 0 \\ \sqrt{E_s} \end{bmatrix} \qquad (2.6)$$

The received vector x has M elements, $x_1, x_2, \ldots, x_M$, that are defined by, respectively,

$$x_1 = \int_0^{T_s} x(t)\varphi_1(t)dt \quad ,$$

$$x_2 = \int_0^{T_s} x(t)\varphi_2(t)dt \quad ,$$

.

.

.

$$x_i = \int_0^{T_s} x(t)\varphi_i(t)dt \quad , \tag{2.7}$$

.

.

.

and

$$x_M = \int_0^{T_s} x(t)\varphi_M(t)dt \quad .$$

where x(t) is the received signal , and it depends on the transmitted symbol. In the next section, a brief idea will be given about the FSK receiver structures, in order to be prepare for the presentation of the problems associated with the operation of these receivers, in multipath fast fading channels.

## 2.3 FSK Receiver Structures

In an ideal communication system, the information-bearing signal can be made completely known at the receiver. However, in practice, it is often found that in addition to the uncertainty due to the additive noise, there is an additional uncertainty due to the randomness of certain signal parameters. The usual cause of this uncertainty is distortion in the transmission medium, as well as fading.

### 2.3.1 Coherent FSK Detection

The coherent binary FSK receiver's primary function is to recover the noisy received FSK waves. A binary receiver such as the one shown in Fig. 2.1, would be suitable for a binary signal reception scheme. It consists of two correlators with a common input. These correlators multiply the incoming signals, with the locally generated coherent signals $\varphi_1(t)$ and $\varphi_2(t)$. The correlator outputs are then entered in full period integrators. After that, the two outputs are subtracted from one another, and the the output is entered in a decision device. This device will compare the input to a certain threshold. If the input is greater than that threshold, then the decision device will decide in favor of the signal 1, and if it is less than this threshold, then it will favor the signal 0.

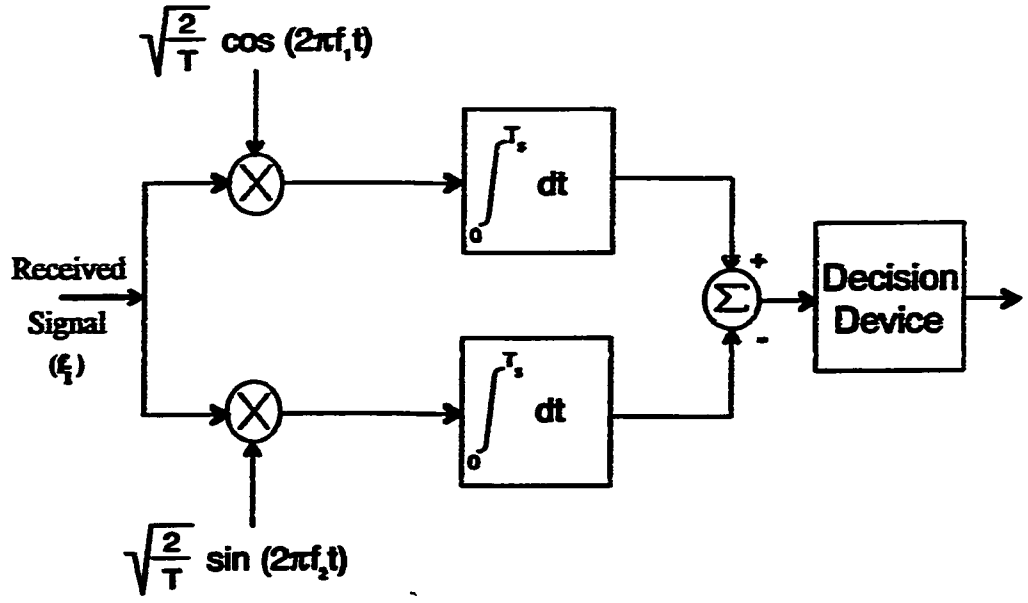


*Figure* 2.1: Block Diagram of a Binary Coherent FSK Receiver.

## 2.3.2 Non Coherent FSK Detection

When no provision is made to synchronize the phase with the transmitter, the received signal will, for additive white gaussian noise (AWGN) channel, be of the form

$$x(t) = \sqrt{\frac{2E_s}{T_s}}\cos(2\pi f_i t + \theta) + w(t) \qquad ; 0 \le t \le T_s \qquad (2.8)$$

where $w(t)$ is the sample function of white Gaussian noise process of zero mean and power spectral density of $N_o/2$. The phase $\theta$ is unknown, and it is usually considered to be the sample value of a random variable, uniformly distributed between 0 and $2\pi$ radians. This implies a complete lack of the knowledge of the phase. A digital communication receiver characterized in this way is said to be *noncoherent.*

Non-coherent detection of FSK signals has originated because of the randomness of the phase of the received signal. This may cause the phase of the received signal to change in a way that the receiver cannot follow. Synchronization with the phase of the transmitted carrier may then be too costly, and the designer may simply choose to disregard the phase information of the received signal at the expense of some degradation in the performance of the system.

Different kinds of receivers have been proposed for the detection of non-coherent FSK (NCFSK) signals. Among these, is the so-called *quadrature receiver* shown in Fig. 2.2(a). Indeed, this receiver is optimum in the sense that it realizes the detection of the NCFSK signals with the minimum probability of error [4]. There are two equivalent forms of the quadrature receiver. The first form is easily obtained by replacing each correlator in Fig. 2.2(a) with a corre-

sponding equivalent matched filter [4]. This alternative form of quadrature receiver is shown in Fig. 2.2(b). Another alternative form of the quadrature receiver is shown in Fig. 2.2(c). The quadrature receiver's performance is optimum when the amplitude and phase of the received signal are constant but unknown(i.e., coherent signal) and the background noise is white Gaussian noise with zero mean [4].

The general structure of a noncoherent M-ary Orthogonal Keyed (MOK) receiver consisting of M matched filters followed by envelope detectors and a largest-of decision is shown in Fig. 2.3 [5].

In practical NCFSK systems, it is often found that in addition to the uncertainty due to the additive noise of a receiver, there is an additional uncertainty due to the randomness of certain signal parameters. Perhaps the most common random signal parameter is the phase which is especially true for narrow-band signals. For example, transmission over a multiplicity of paths of different and variable lengths, or rapidly varying delays in the propagating medium from transmitter to receiver may cause these multipath returns to overlap (i.e., non-resolvable multipath). When this happens the composite echo has a random time-varying phase and amplitude over the signal duration. This mismatch that exists between the random time-varying parameters of the echo and fixed parameters of the sine and cosine multipliers in the quadrature receiver, causes a degradation in the detection performance.

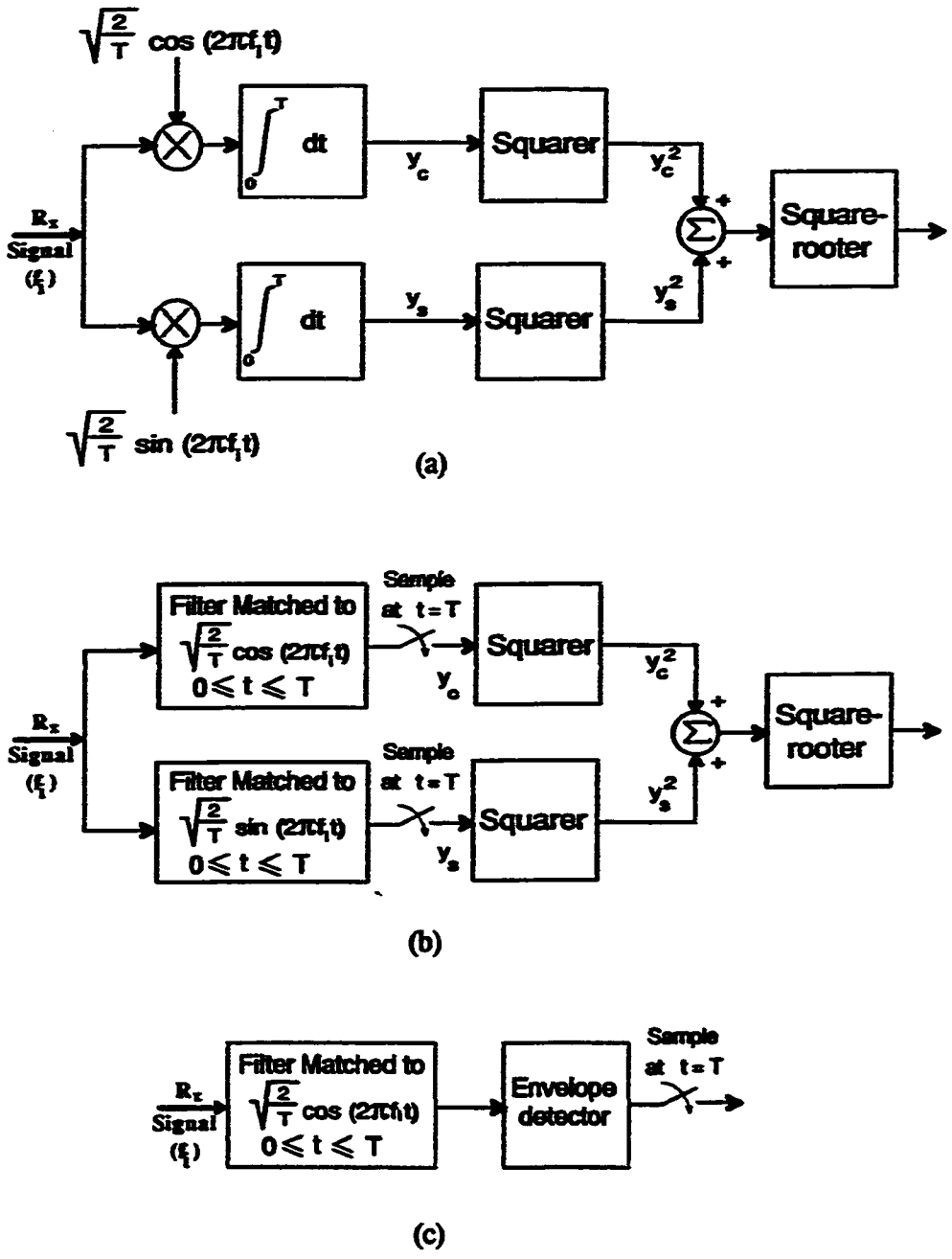


*Figure 2.2*: Non-Coherent receivers. (a) Quadrature receivers using correlators. (b) Quadrature receiver using matched filters. (c) Another equivalent form of the quadrature receiver based on envelope detection.

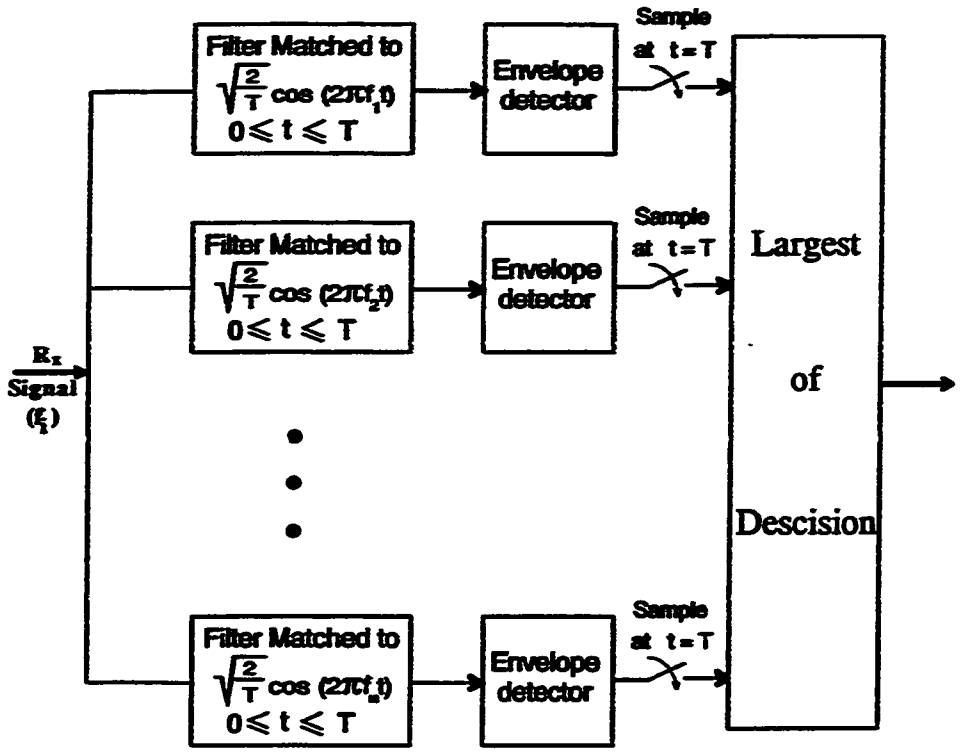


*Figure 2.3*: Noncoherent MOK Recievers.

## 2.4 Characterization of Multipath Channels

As the different receivers being studied in this thesis are tested under multipath reception situations, this section is dedicated to give a brief idea about the characteristics of multipath channels.

One characteristic of a multipath medium is the time spread introduced in the signal which is transmitted through the channel. A second characteristic is due to the time variations in the structure of the medium. As a result of such time variations, the nature of the multipath varies with time. Moreover, as the name of the channel implies, multipath channels have multiple propagation paths. Associated with each path is a propagation delay and an attenuation factor. Both propagation delays, and attenuation factors are time- variant as a result of changes in the structure of the medium. Thus, for some channels, such as the tropospheric scatter channel, it is more appropriate to view the received signal as a continuum of multipath components. In most radio transmission media, the attenuation and phase shift associated with one path delay, is uncorrelated with the attenuation and phase shift associated with another path delay. This is usually called *uncorrelated scattering.*

The above mentioned delays, time-variances, attenuations, and multipath receptions, have been modeled mathematically by many researchers of this field, to be able to study the behavior of different receivers in such cases, and to be able to improve the existing receivers. When the impulse response of a multipath fading channel is modeled as a zero mean complex-valued gaussian process, the envelope of such a response at any instant of time is Rayleigh distributed [1]. In this case, the channel is said to be a *Rayleigh Fading Channel.* A Rayleigh probability density function can be written as follows:

$$f_v(v) = \begin{cases} v \exp\left(-\frac{v^2}{2}\right) & ; v \geq 0 \\ 0 & ; \text{elsewhere} \end{cases} \qquad (2.9)$$

The above equation represents a normalized Rayleigh distribution form, and can be plotted as shown in Fig. 2.4 [4].

In the event that there are fixed scatters or signal reflectors in the medium, in addition to randomly moving scatters, the impulse response of the multipath channel can no longer be modeled as having zero mean [1]. In this case, the envelope of this response has a Rician distribution, and the channel is said to be a *Rician Fading Channel.* In our treatment of the channel in of this thesis, we consider only the Rayleigh-distributed envelope statistics, as it appears to be a realistic one. Rayleigh-distributed envelope fading has been observed often on HF and troposcatter channels. As a consequence, this channel model has been widely accepted [1].

In [6], Higgins investigated the performance degradation in the quadrature receiver for CW signals corrupted by multipath. He showed that the output SNR depends on the correlation characteristics of the input signal. Higgins determined theoretically, the performance of the quadrature receiver, in terms of output signal-to-noise ratio, when the input signal is postulated to be narrow-band, with Rayleigh distributed amplitude and uniformly distributed phase fluctuations in time, and the background noise is white Gaussian with zero-mean. He assumed that the input signal model is the well-known "fast fading" model representing the received signal when the transmit signal is a sinusoid.

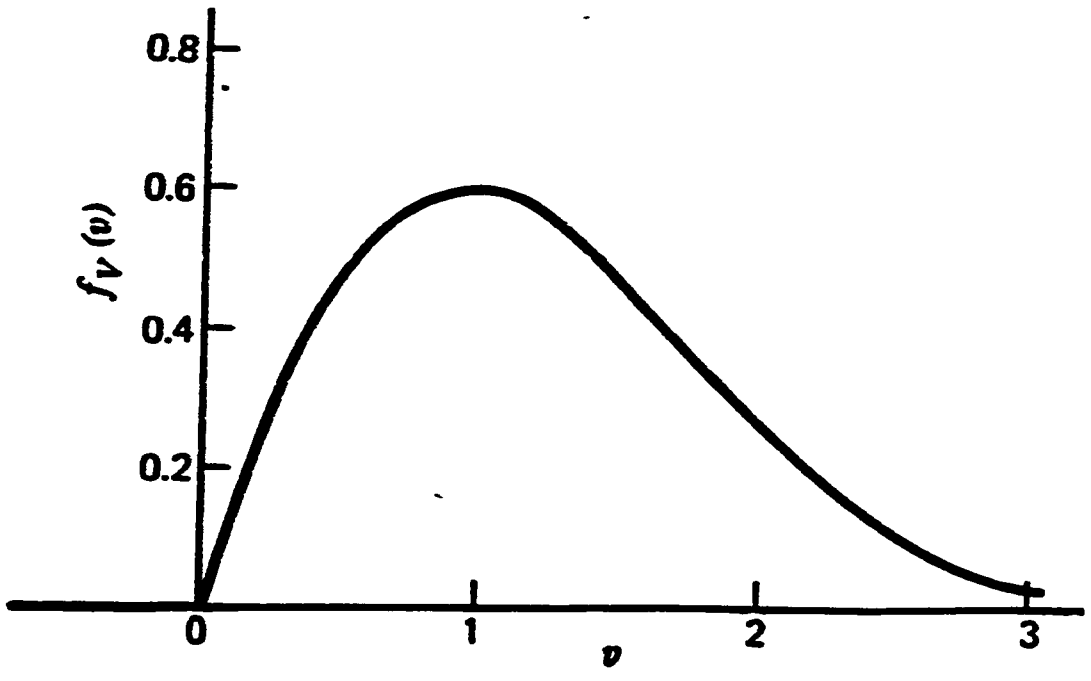


*Figure 2.4*: Rayliegh Distribution [4].

When a detection system is operating in a multipath environment, the parameters of the transmit phase may be affected to such an extent, that a degradation is included in the detection performance of the receiver. In his subsequent paper [2], Higgins considered the input signal to be modeled as a piecewise constant approximation to the familiar "slow fading" Gaussian signal that is corrupted with a background white Gaussian noise. Then, he suggested a parallel interconnection of quadrature receivers, and derived their Receiver Operating Characteristics (ROCs). The integration times of the component quadrature receivers in this processor correspond to successive intervals of constant (but unknown) amplitude and phase shift. Then, the results of this new processor were compared to the single quadrature receiver results. It was assumed that the signal coherence times are known a *priori*. In [2], Higgins assumed that the signal duration is divided into two equal time intervals as shown in Fig. 2.6. The signal correlation characteristics between intervals are specified by the correlation coefficient, ρ. Higgins formulated in [2], the correlation between the two signal parts as:

$$\rho = \frac{cov[s_1(t) \cdot s_2(t)]}{\{var[s_1(t)] \cdot var[s_2(t)]\}^{1/2}} \quad , \tag{2.10}$$

where $s_i(t)$ represents the signal over interval i. The performance of each receiver was examined when the signal parts are completely uncorrelated (i.e., $\rho = 0$), and when they are completely correlated (i.e., $\rho = 1$). He showed that when $\rho = 0$, the parallel quadrature receiver combination provided a substantially improved detection capability over the single quadrature receiver. However, when $\rho = 1$, the capability is only slightly diminished relative to the single quad-

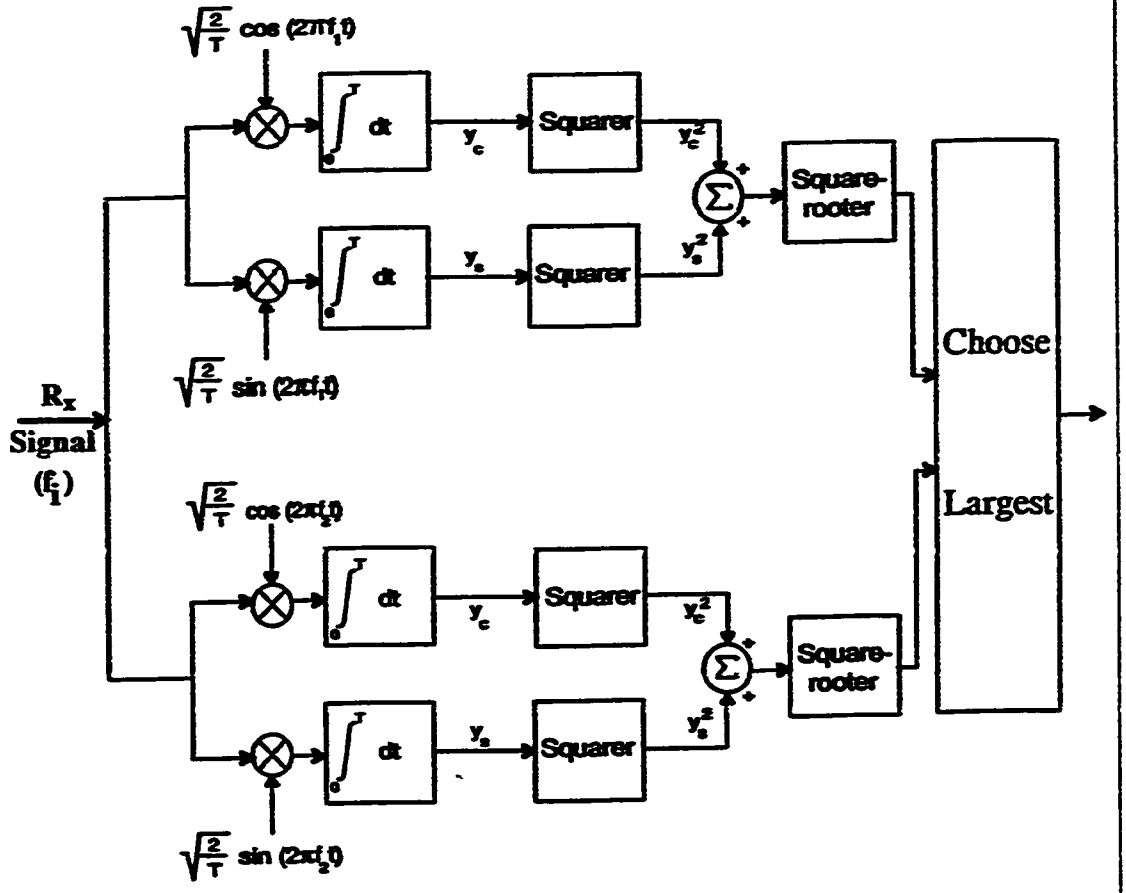


*Figure 2.5:* Single Quadrature Receiver.

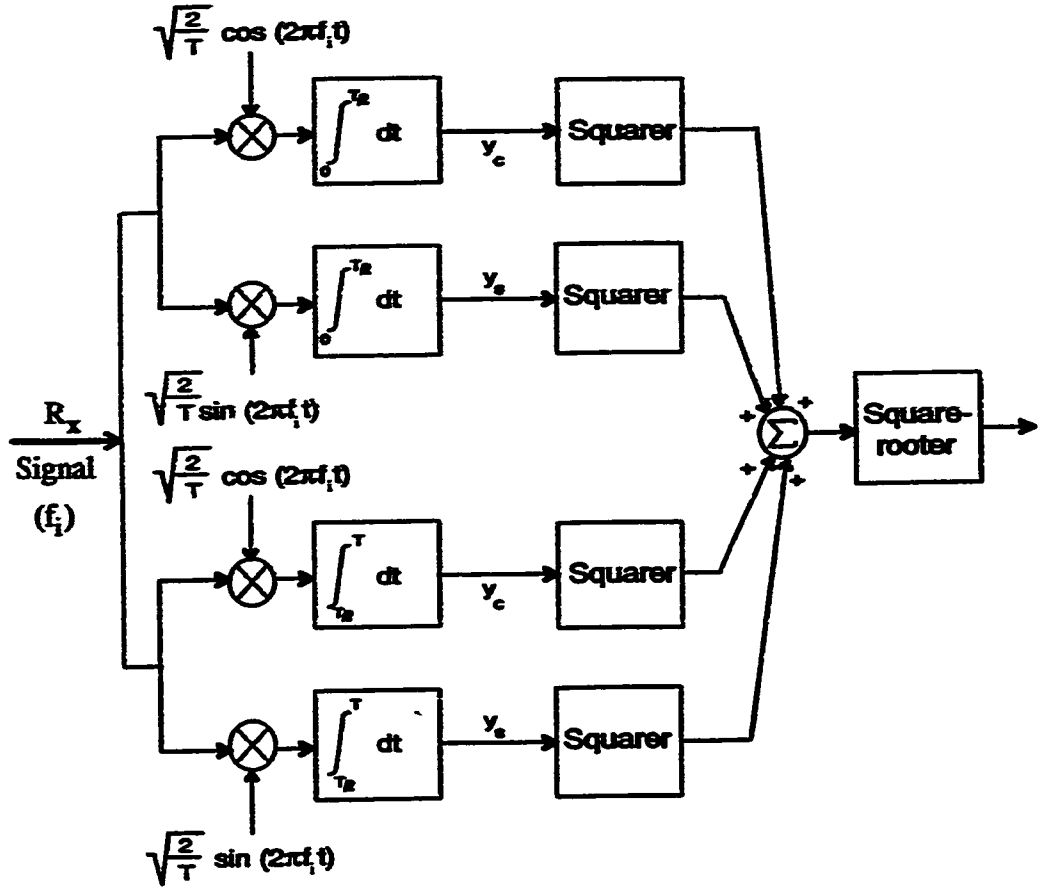


*Figure 2.6:* The Parallel Quadrature Receiver.

rature receiver case. Simulation of these cases and other ones will be presented later in this chapter.

In [5], Friederichs presented a general error analysis for the noncoherent M-ary orthogonal keyed (MOK) receiver in the presence of AWGN noise interference. Moreover, he gave relations to well-known formulae which apply to broad-band white Gaussian noise environment.

In [7], Al-Hussaini generalized the work done by Higgins in [2], and investigated its suitability to an M-ary NCFSK communications system. M-ary single and parallel quadrature receiver systems are shown in Fig. 2.7 and Fig. 2.8, respectively. He derived expressions for the probability of error for both, the single quadrature receiver (SQR) and the parallel quadrature receiver (PQR).

In a non-resolvable multipath reception, the received signal $s(t)$, postulated to be narrowband and Gaussian, has the form

$$s(t) = V(t)\cos(2\pi f_i t + 0) + w(t) \qquad ; \text{for } 0 \le t \le T_b \tag{2.11}$$

where V(t), the envelope, is a Rayleigh distributed random process, $w(t)$ is the sample function of white Gaussian noise process of zero mean and power spectral density of of $N_o/2$, and $0(t)$, the phase, is a uniformly distributed random process. Based on this model, Al-Hussaini has formulated expressions for both, the SQR and the PQR, for complete correlation and for uncorrelation cases. For the SQR case, Al-Husaini showed that for the case of $\rho = 0$, the input to the receiver has a probability density function (*pdf*) that represents a *gamma distribution* with *two* degrees of freedom, yielding a probability of error ($P_e$) of the form [7]

$$P_e = 1 - \sum_{i=0}^{M-1} (-1)^i \binom{M-1}{i} \frac{1}{1 + i(1 + SNR)} \qquad . \tag{2.12}$$

On the other hand, for the case of $\rho = 1$, he derived an expression for $P_e$ of the form

$$P_e = 1 - \sum_{i=0}^{M-1} (-1)^i \binom{M-1}{i} \frac{1}{1+i(1+2 \cdot SNR)} \tag{2.13}$$

which is 3 dB worse than that of the case of $\rho = 0$.

In addition, Al-Hussaini investigated in [7] the performance of the PQR for the same cases. In the case of $\rho = 0$, he deduced that the *pdf* of the input to the receiver in this case has a *gamma distribution* with *four* degrees of freedom. Accordingly, this yields a $P_e$ of the form

$$P_e = 1 - \sum_{i=0}^{M-1} (-1)^i \binom{M-1}{i} \sum_{j=0}^{i} \binom{i}{j} \frac{(i-j+1)!\,(1+SNR)^{i-j}}{[1+i(1+SNR)]^{i-j+2}} \tag{2.14}$$

Moreover, this receiver would for the case of $\rho = 1$, yield a $P_e$ of the form

$$P_e = 1 - \sum_{i=0}^{M-1} (-1)^i \binom{M-1}{i} \sum_{j=0}^{i} \frac{i!}{(i-j)!} \frac{1}{2 \cdot SNR} \left[ \frac{(2 \cdot SNR+1)^{j+1}}{[1+i(1+2 \cdot SNR)]^{j+1}} - \frac{1}{(1+j)^{j+1}} \right] \tag{2.15}$$

These expressions have been simulated in this thesis, and were found to match the theoritically-based graphs given by Al-Hussaini in [7]. In the next section, the problems associated with operation of both the SQR, and PQR in non-resolvable multipath reception will be discussed, and some test cases will be proposed. These test cases will be used in the simulation and comparison of the behavior of the SQR, and PQR to other receivers.

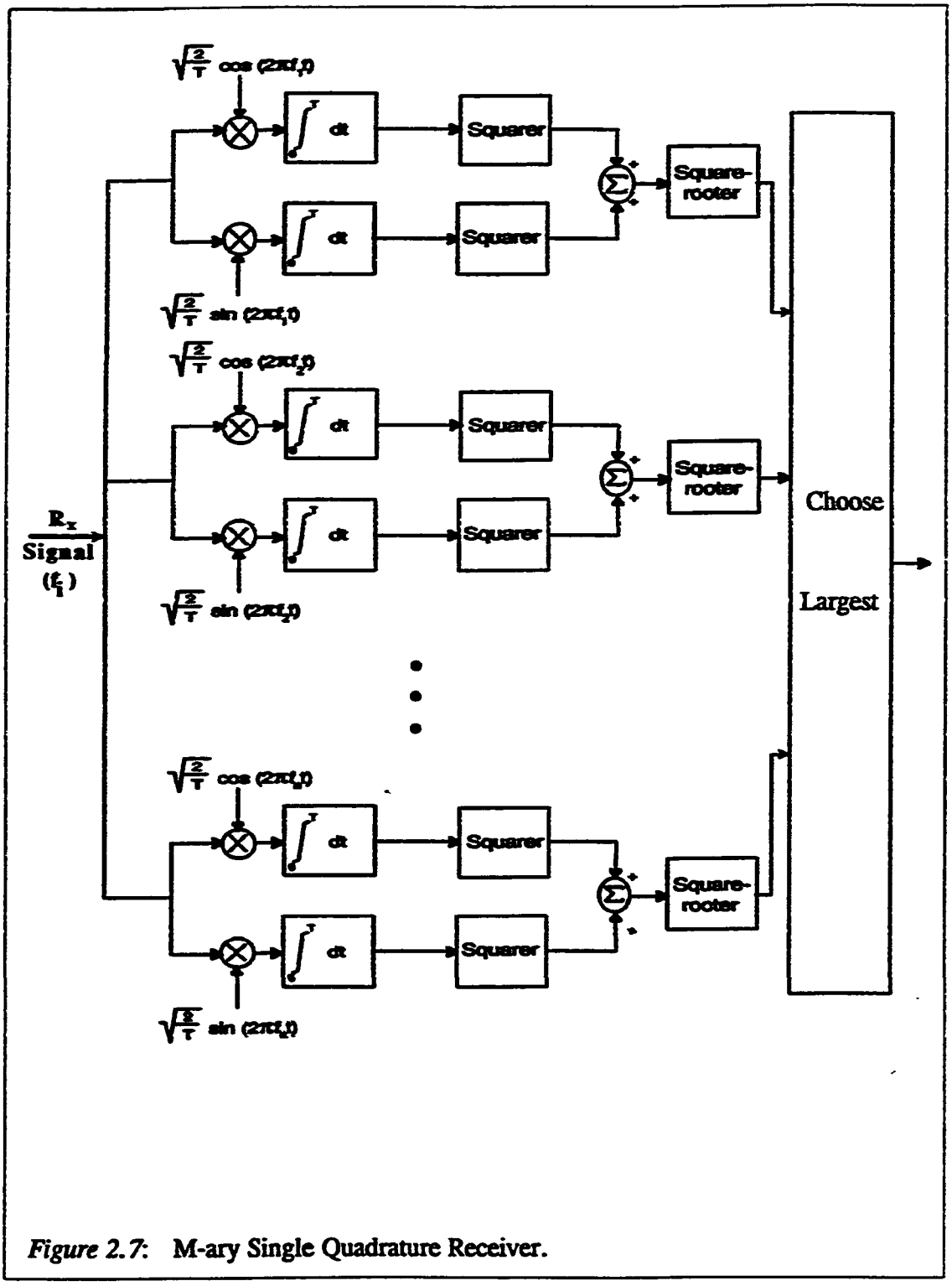


*Figure 2.7*: M-ary Single Quadrature Receiver.

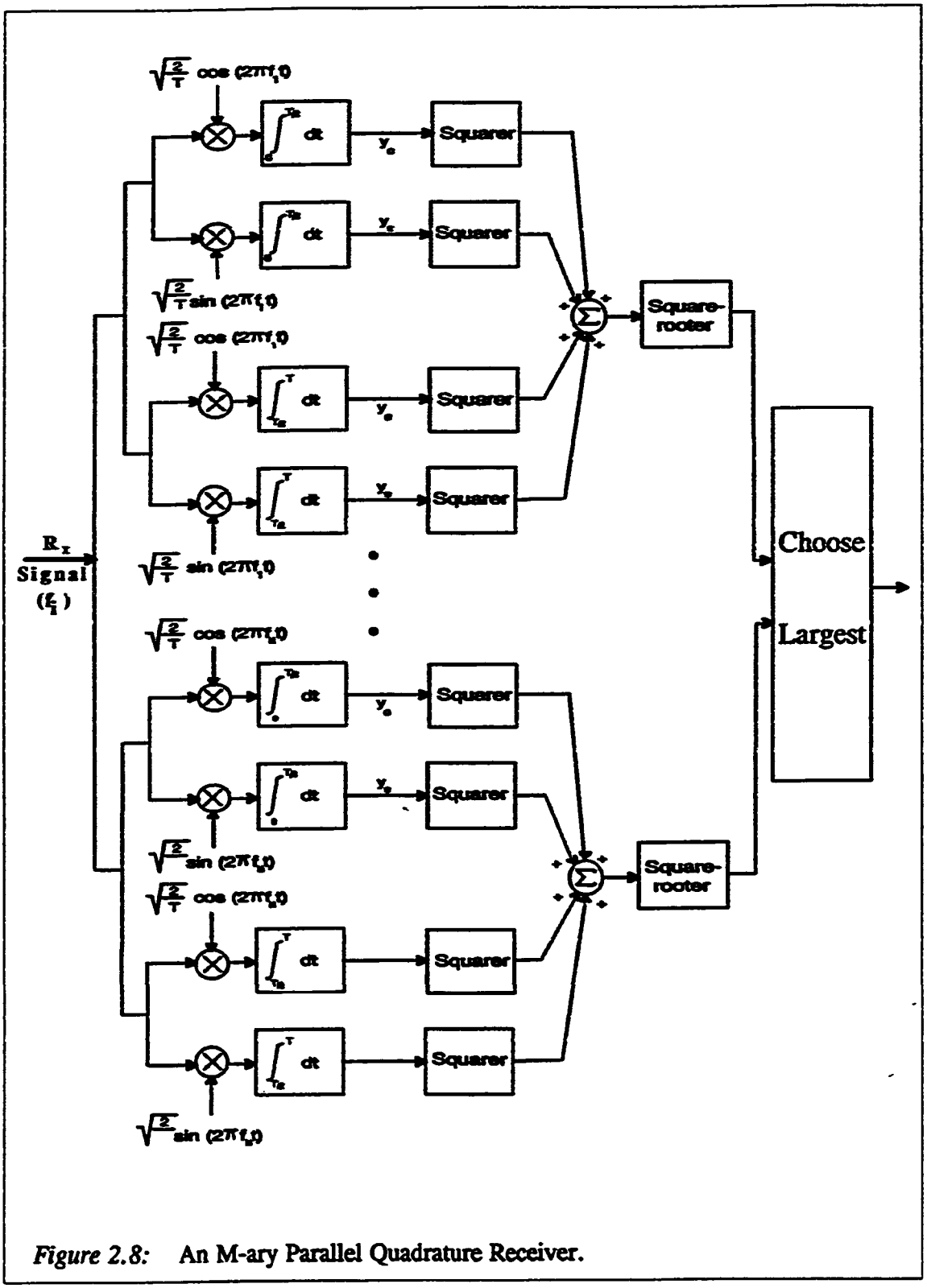


*Figure 2.8:* An M-ary Parallel Quadrature Receiver.

Although the PQR receiver outperforms greatly the SQR on the performance in the case of $\rho = 0$, it is still a very limited solution to the problem of phase discontinuities. The PQR will operate optimally when the locations of occurrences of discontinuities are known a priori. In the case that Higgins used, the PQR will fail to operate optimally, if the location of occurrence of the discontinuity is changed from the middle of the symbol period. In the next section, the problems of the SQR, and PQR are exhibited. Moreover, some realistic cases are proposed to find out more about the behavior of the receivers (SQR, and PQR) under such cases.

## 2.5 Problems of the Conventional SQR and PQR Configurations

As has been mentioned in the first chapter of this thesis, in reality the occurrence and location of occurrence of phase discontinuities within a certain symbol duration is completely random in many situations. This depends on many factors. Some of these are the complexity of the reflecting mechanism, as well as the medium through which the transmission is taking place. In [2], for simplicity, Higgins assumed that the signal duration is divided into two equal time intervals, with the correlation characteristics between the two signal parts being specified by the correlation coefficient, $\rho$ as given in Eqn. (2.10). In real world, however, the discontinuity distribution of the received signal scheme is not known. The phase discontinuity of the received signal might not take place at

the middle of the symbol duration exactly. On the contrary, it might take place at some other place within the symbol duration. For example, it could happen at 1/3, 1/4, or 4/5 of the symbol duration. In addition, the phase discontinuities might not occur at all in one symbol duration. On the other hand, they could occur for a certain number of times in one symbol duration, and for a different number of times in the next symbol duration, and so on. This gives rise to the randomness of the phase discontinuities number and their position during the consecutive bit intervals.

This problem happens to be a real life situation, especially for receivers which are exposed to operate in unknown environments. It can, also, occur to receivers of the mobile radios, and to stationary receiver units that are surrounded by rapidly changing environment. This problem creates the need for a receiver structure which is immune to phase discontinuities within the signal bit duration as well as to the random phase of the signal.

A study of these realistic cases, is carried out here, and is simulated to observe the effect on the behavior of both the conventional SQR, and the PQR. The discontinuities are generated in a similar way in which the $\rho = 0$ case is generated. In other words, the computer program is implemented in a way to imbed a uniformly distributed phase discontinuity at specific locations within the bit duration. The amplitude of the different segments within the bit duration is, also, Rayliegh distributed.

Different tests are implemented. The phase discontinuity occurrence frequency and location are varied. The first of these tests, consisted of having one phase discontinuity within the bit duration. However, its location is random.

This means that instead of fixing the discontinuity in the middle of the bit duration (as Higgins did), the discontinuity could take place anywhere within the bit duration. In the following, the tested cases are discussed in detail.

## 2.6 Test Cases

In addition to the two cases ($\rho = 1$ and $\rho = 0$), that were used by both Higgins [2], and Al-Husaini [5], three new cases are introduced in this thesis. These new cases concentrate on the fast fading non-resolvable multipath channels. They have been implemented to study the behavior of both the conventional SQR, and PQR receivers, as well as the other receivers that will be discussed in the course of this thesis, under different multipath reception situations. In the following, a detailed explanation of these test cases, as well as the two original cases, is provided for convenience.

1. *Case 1:* $\rho = 1$: In this case, the received symbol is modeled to have a random phase that is uniformly distributed between 0 and $2\pi$. It is modeled to be corrupted with AWGN, and to have a Rayleigh distributed envelope, as a result of a multipath signal detection. However, the signal does not have any kind of phase discontinuities. In other words, the signal is supposed to have a continuous phase and a constant envelope within one symbol duration.
2. *Case 2:* $\rho = 0$: In this case, the received symbol is modeled to start with a random phase that is uniformly-distributed between 0 and $2\pi$. In the

middle of the symbol duration exactly, the phase is changed to another value according to a uniform distribution. The phase stays constant within each segment of the symbol duration. But, it is different from one segment to the other. In addition, the envelope of the symbol is Rayleigh-distributed. The two segments are assumed to be completely uncorrelated. This case is referred to . sometimes, as the case of one fixed phase discontinuity within the symbol duration, within the course of this thesis, because it is fixed to take place in the middle of the symbol duration, and it has to occur in each received symbol.

3. *Case 3: One Random Phase Discontinuity:* This case is similar to the $\rho = 0$ case, but with one difference. Instead of the phase discontinuity taking place at the middle of the symbol duration exactly, it can take place in any location within the symbol duration. This means that the symbol duration will still have two segments that are completely uncorrelated. However, these two segments are of an unknown duration. Once again, the phase discontinuity has to take place within one symbol duration, in this test case.

4. *Case 4: Maximum of Three Random Discontinuities:* In this case, not only is the location of occurrence of phase discontinuities variable, but also the number of phase discontinuities. That is, any number of phase discontinuities could occur within the symbol duration, from 0 to 3 discontinuities. The number of segments within the symbol duration ranges from 1 to 4, depending on the number of phase discontinuities. The phase of each segment is random with a uniform-distribution between 0

and 2 π. The amplitude of each segment within the symbol duration is Rayleigh distributed. For a certain percentage of time, this case reduces to one of the first three cases: $\rho = 1$, $\rho = 0$, or one random discontinuity case. The number of discontinuities that take place within the symbol duration is a discrete uniformly distributed random variable between 0 and 3.

5. *Case 5: Maximum of Six Random Discontinuities:* This case is similar to case 4, but with the exception that the number of discontinuities that take place within the symbol duration can have a maximum of 6. This means that a maximum of seven segments of a random duration can take place within the bit symbol duration. Again, for a certain percentage of time this case reduces to one of previous four cases. The amplitude of the different segments is random with a Rayleigh distribution. Each of the segments within the symbol duration has a random uniformly distributed phase between 0 and 2 π. The number of discontinuities within the symbol duration is uniformly distributed between 0 and 6.

## 2.7 Simulation of the Single and the Parallel Quadrature Receivers

Two FORTRAN computer programs (see Appendix A) are developed to simulate both the SQR and PQR. This was done not only to see how accurate the formulae given by Al-Hussaini in [7] are, but also to be used for comparison purposes, with the proposed receivers, as well as, to study the behavior of these two receivers under different real life situations. These simulation programs were carried out on an IBM 370/3090 digital computer mainframe system.

The computer simulation is implemented in the following sequence.

1. Generate the frequencies that are to be used in the simulation, depending on the dimension and the number of messages:

$$M = N \quad ,$$

where M is the number of messages in the signal space to be used, and N is the number of dimensions of that signal space. The frequencies of that signal space are orthogonal. For that purpose and for the sake of simulation, 16 orthogonal frequencies have been chosen. The center frequency of these messages is $f_c = 75Hz$. Moreover, the frequency bandwidth was chosen to be equal to 6 Hz; i.e. $2 \cdot \delta f = 6\ Hz$.

2. Generate the pseudo random message sequence using a pseudo random message generator that employs the CCITT V.32 modem generating ploynomial. This generator employs a 23 stage shift register, and the input to the first memory is given by the following relation:

$$X(1) = X(1) + X(5) + X(23) \quad .$$

where X(I) represnts the state of memory I, and the operator + represents a modulo-two addition.

3. Generate a Rayleigh distributed amplitude sequence that will serve as the amplitude sequence for the random message sequence that will be used for the simulation purposes. A derivation of the Rayleigh distribution is presented in Appendix B.

4. Depending on whether there will be any phase discontinuities in a certain symbol duration, or there will not be any, a special procedure will take care of the generation of the phase discontinuities that will be uniformly distributed between zero and 2 π. Then, this procedure will apply these discontinuities to the specific samples in the symbol duration.

5. The messages are, then, entered in a channel. They are assumed to be sampled at a certain rate and are corrupted with a noise sequence. This noise is Gaussian distributed according to the distribution:

$$f_X(x) = \frac{1}{\sqrt{2\pi}\sigma_n} \exp\left(-\frac{x^2}{2\sigma_n^2}\right) \tag{2.16}$$

with zero mean and a power spectral density of $N_o/2$. The power spectral density is dependent on the signal to noise ratio (SNR). The SNR is defined as:

$$\text{SNR} = 10 \log\left(\frac{E_s}{N_o}\right) \tag{2.17}$$

where $E_s$ is the symbol's energy, and $N_o$ is the power spectral density of the noise. The computer-generated noise sequence variance ( $\sigma_n^2$ ) is related to the power spectral density as follows:

$$\sigma_n^2 = \frac{N_o f_s}{2} \quad , \tag{2.18}$$

where $f_s$ is the sampling rate. The relation between $\sigma_n^2$ is presented in Appendix C. This relation is used in the simulation.

6. At this stage, the symbols have already been simulated as if they have been passed through a multipath fast fading channel, and are being received. The receiver section consists of three parts. The first part is the correlator. This receiver section correlates the received samples (multiplies them) with a sequence of a certain frequency. The value of this frequency depends on the branch that the received sequence is being correlated with. The sequence gets correlated with both a sine and a cosine sequence in each branch, depending on the certain branch's frequency (see Fig. 2.2(a)).

7. Next, the correlated sequences are entered into the second part of the receiver. This is the integrator. For the SQR, the correlated sequences are integrated over the full symbol period (from 0 to $T_s$, where $T_s$ is the symbol's period). After that, the resultant value is squared, and both the squared values of the sine and the cosine parts are summed to give a certain overall output of that branch. In the case of the PQR, however, the correlated sequences are integrated over the first half of the symbol's period and the result is squared, and then the second part is integrated over the second half of the symbol's period. Again the result is squared and the four outputs of the two cosine and the two sine parts of the certain branch are summed to give an overall output value of that branch.

8. The last part of the receiver is the decision device. This device is a procedure that finds out the largest value among all the the output values of the branches. It then decides in favor of that branch.

The results of the simulation of both the SQR and the PQR are shown below. Figures 2.9 and Fig. 2.10 show the probability of error ( $P_e$). plotted versus the signal to noise ratio (SNR), for both the SQR and the PQR, respectively. The performance of the SQR and PQR is shown for the M-ary signaling case, where M = 2, 4, 8, and 16. Results in Fig. 2.9, and Fig. 2.10, are redrawn in Fig. 2.11, and Fig. 2.12, respectively, but with the correlation factor $\rho$ being fixed for each figure. It can be seen that the SQR behavior for the case of no phase discontinuities taking place within the duration of the symbol (i.e. $\rho = 1$), is better than the case of one phase discontinuity taking place at the middle of the signal duration ( $\rho = 0$), by 3 dB as expected. On the other hand, it can be seen from Fig. 2.10, that the $P_e$ curves are much lower (better) in the case of no correlation ( $\rho = 0$), than they are in the case of ( $\rho = 1$), for the PQR. This agrees with what Al-Hussaini [7] and Higgins [6] have concluded.

Figure 2.11, shows a comparison between the SQR and the PQR outputs in the M-ary signal space for $\rho = 1$. It can be seen clearly that the SQR behaves slightly better than the PQR in this case. However, looking at the performance of both receivers for $\rho = 0$, Fig. 2.12 shows clearly, that the PQR significantly outperforms the SQR. This result agrees again with what was found earlier by both Higgins [6], and Al-Husaini [7].

Next, we fix M = 2 (binary) and we include the aforementioned realistic cases. The results of the test for both the Single Quadrature Receiver, and the Parallel Quadrature Receiver are compared to the two previous cases of $\rho = 0$, and $\rho = 1$, in Fig. 2.13 and Fig. 2.14, respectively. It can be seen from Fig. 2.13, that the SQR behaves slightly better for the case of one random discontinuity, than in the case of a fixed discontinuity in the middle ( $\rho = 0$) case. However, the performance of the SQR for no discontinuity case ($\rho = 1$), is still better than any behavior with any kind of discontinuity in the signal.

On the other hand, Fig. 2.14 shows that the performance of the PQR is degraded in the case of one random discontinuity than the behavior in case of one fixed discontinuity in the middle ($\rho = 0$). However, this is still better than that for the case of no phase discontinuity ($\rho = 1$).

Moreover, Fig. 2.15 and Fig. 2.16, show the performance of the two receivers for two more cases. The first case is the possibility of occurrence of up to three phase discontinuities within one symbol duration at random locations. The second case is the possibility of occurrence of up to six random phase discontinuities within one symbol duration. In Fig. 2.15 and Fig. 2.16, all the previous cases tested are included in the same figure for the sake of comparison.

It is clearly seen how the performance of both the SQR and the PQR is degraded in these real life situations. The same thing applies to the case of M-ary signaling situations. Figures 2.17, Fig. 2.18, and 2.19 show the SQR performance for M = 4, M = 8, and M = 16, respectively. On the other hand, Fig. 2.20, Fig. 2.21, and Fig. 2.22, show the performance of the PQR for the same cases. Figures 2.23 through 2.25 compare the performance of the SQR to that of

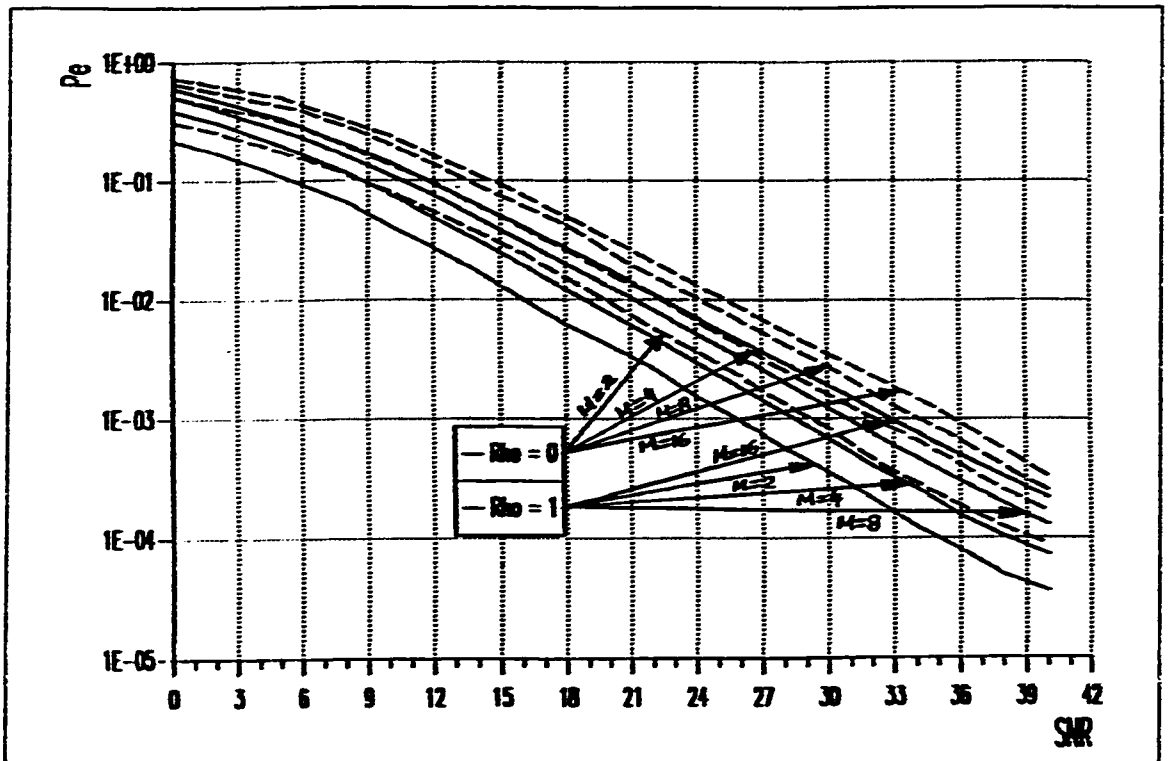


*Fig 2.9*: Single Quadrature Receiver Performance for M = 2, 4, 8, 16.

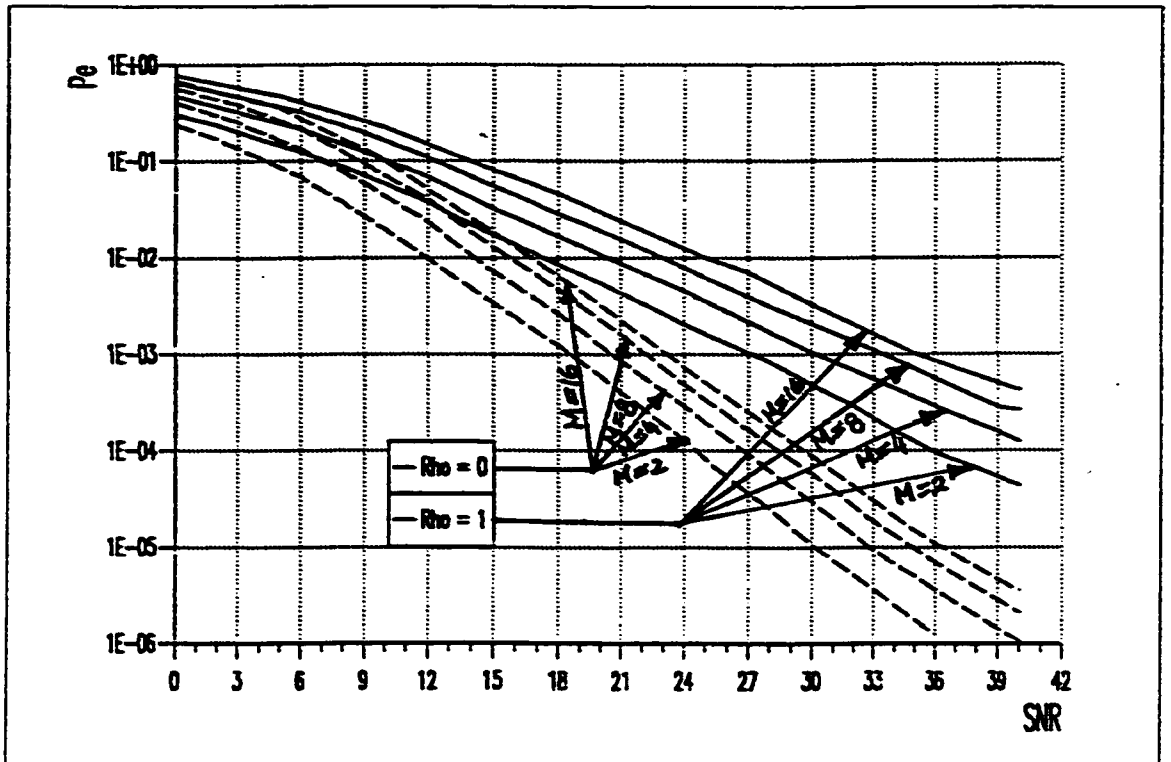


*Fig 2.10*: Parallel Quadrature Receiver Performance for M = 2, 4, 8, 16.

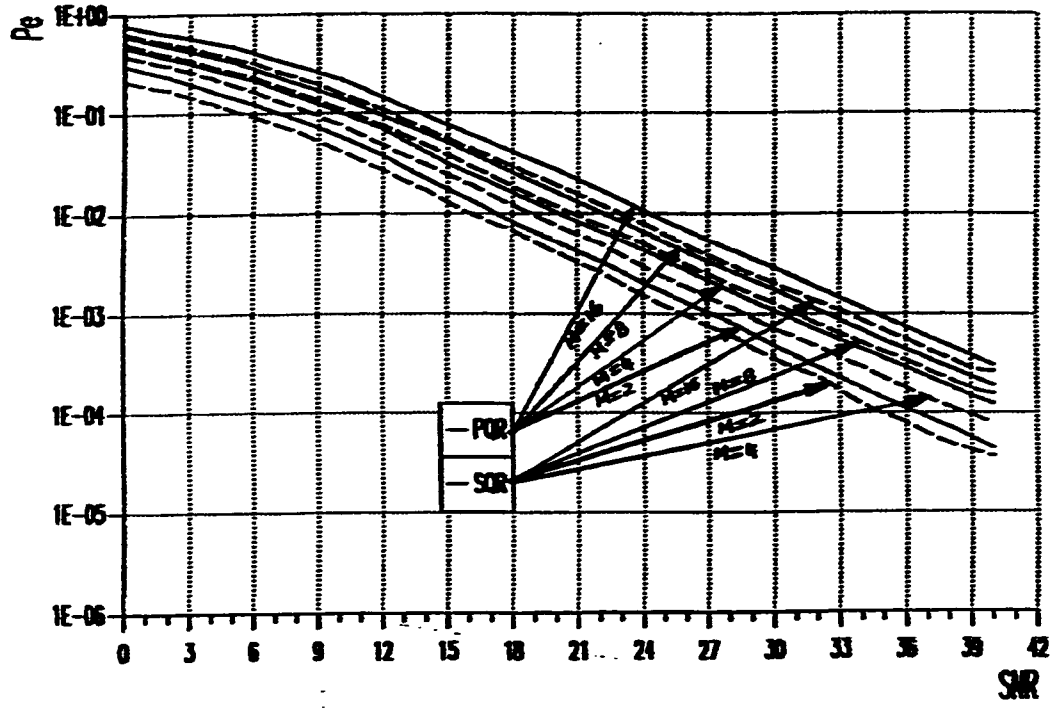


*Fig 2.11*: SQR Versus PQR Performance for M = 2, 4, 8, 16, when ρ = 1.

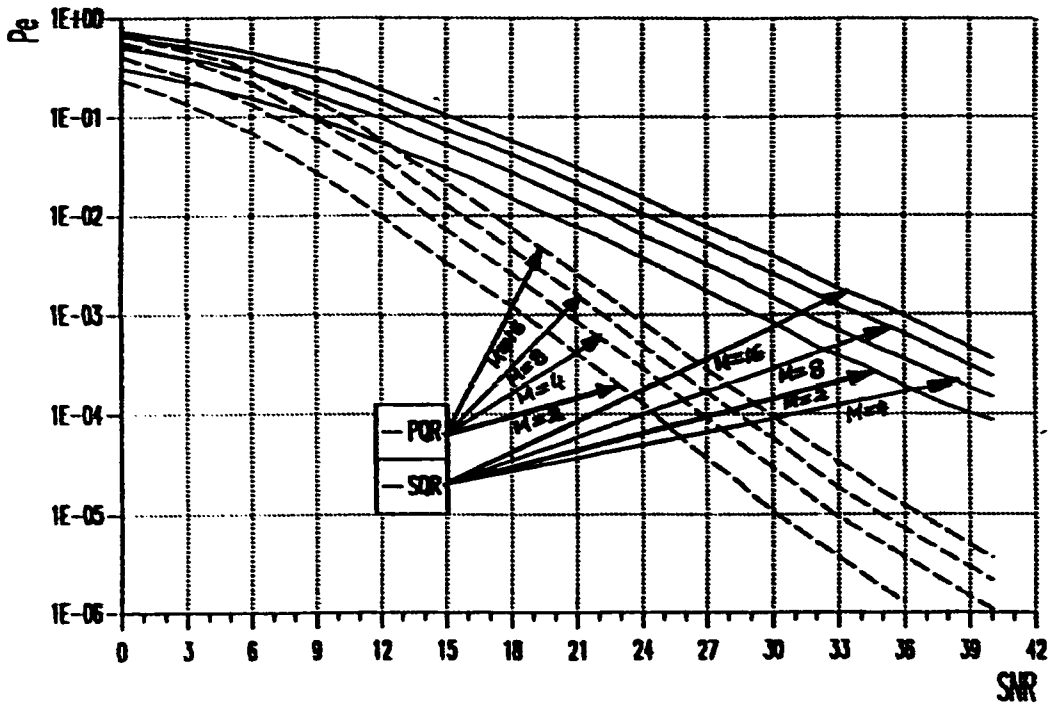


*Fig 2.12*: SQR Versus PQR Performance for M = 2, 4, 8, 16, when ρ = 0.

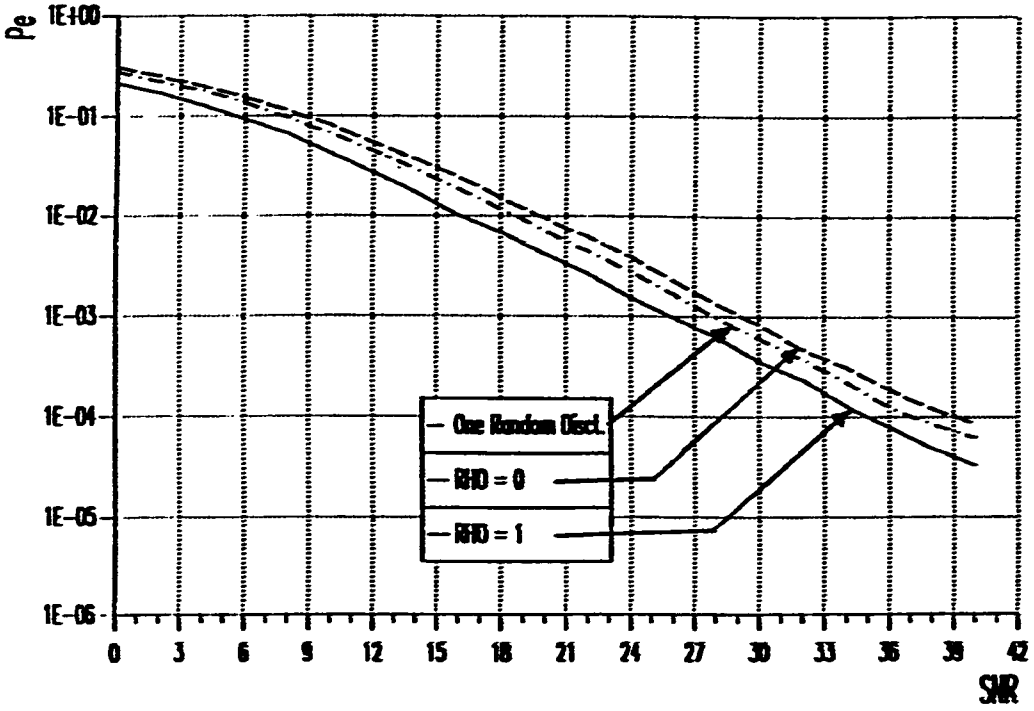


*Fig 2.13*: SQR Performance for M = 2.

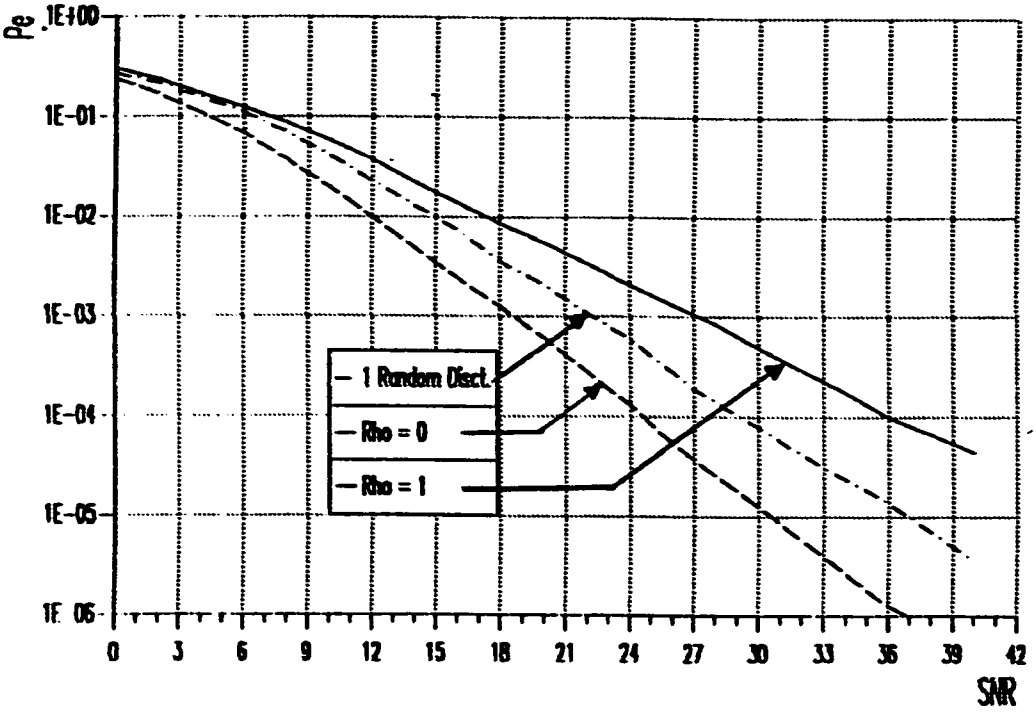


*Fig 2.14*: PQR Performance for M = 2.

the PQR for the three new test cases. It can be seen clearly that the PQR has a better perfomance for all the new test cases. This means that PQR is a better receiver for non-resolvable multipath signals than the SQR.

It is to be noted that in Figures 2.17 through 2.25 and also in any $P_e$ curve with M-ary signaling in the remainder of this thesis, the SNR of the horizontal axis is the ratio between the symbol energy and the additive noise power spectral density $N_o$ as indicated in Eqn. 2.17. This is not usually the case found in the literature where $E_s$ is replaced by the energy per bit $E_b$ However, we use here the former notation in accordance with reference [7], which is of our concern for comparison.

In all cases, but the case of no occurrence of phase discontinuities the performance of the PQR is better than that of the SQR. In other words, the PQR outperforms the SQR if there is any occurrence of phase discontinuities, regardless of the frequency or position of occurrence of phase discontinuities.

This problem happens to be a real life situation, especially for receivers that are exposed to work in an unknown environment. It can also happen to receivers of mobile radios, to the stationary radio units that are surrounded by rapidly changing environment. This problem creates the need for a receiver structure that is immune, or at least less sensitive to discontinuities within the symbol duration as well as to the random phase of the signal.

In [8], Al-Jamaan has proposed a new Digital Frequency Locked Loop (DFLL) receiver. He has shown that this DFLL is concerned mainly with the frequency of the incoming signal, and that it is immune to the phase of the signal. He has tested his new DFLL for wideband frequency-modulated speech sig-

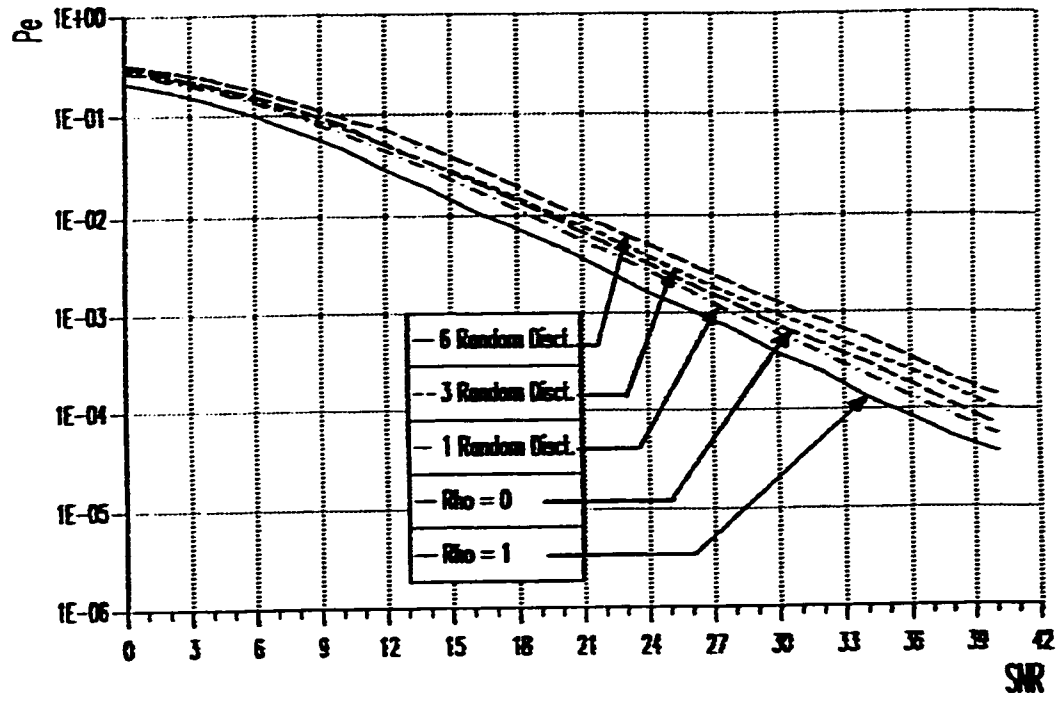


*Fig 2.15*: SQR Performance for M = 2, Under All Five Test Cases.

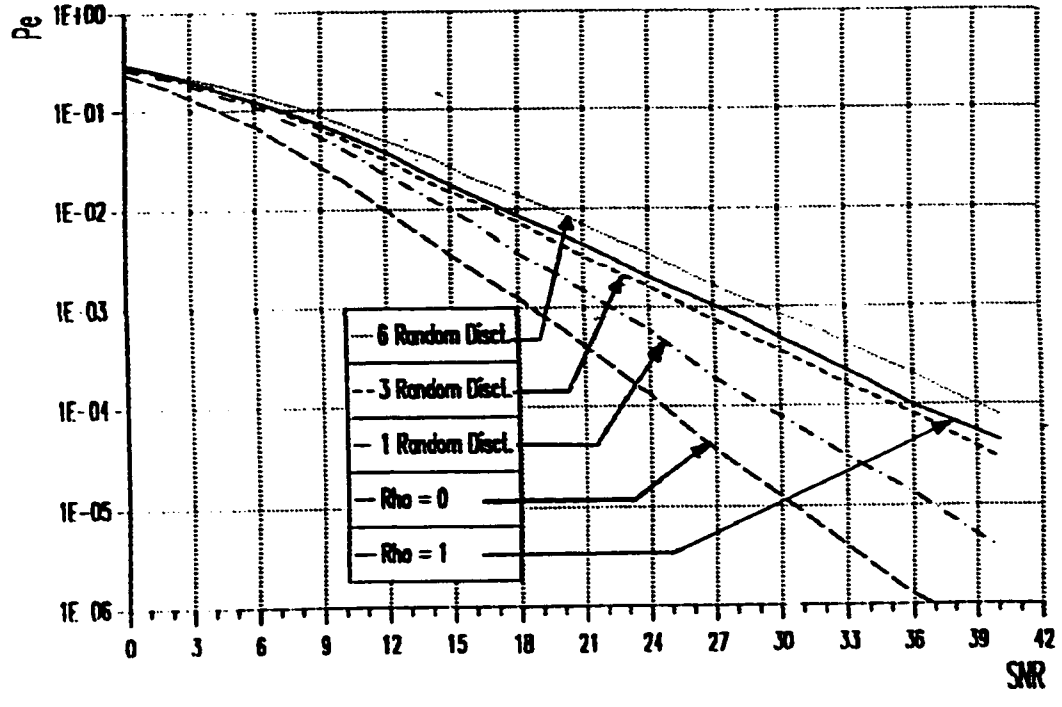


*Fig 2.16*: PQR Performance for M = 2, Under All Five Test Cases.

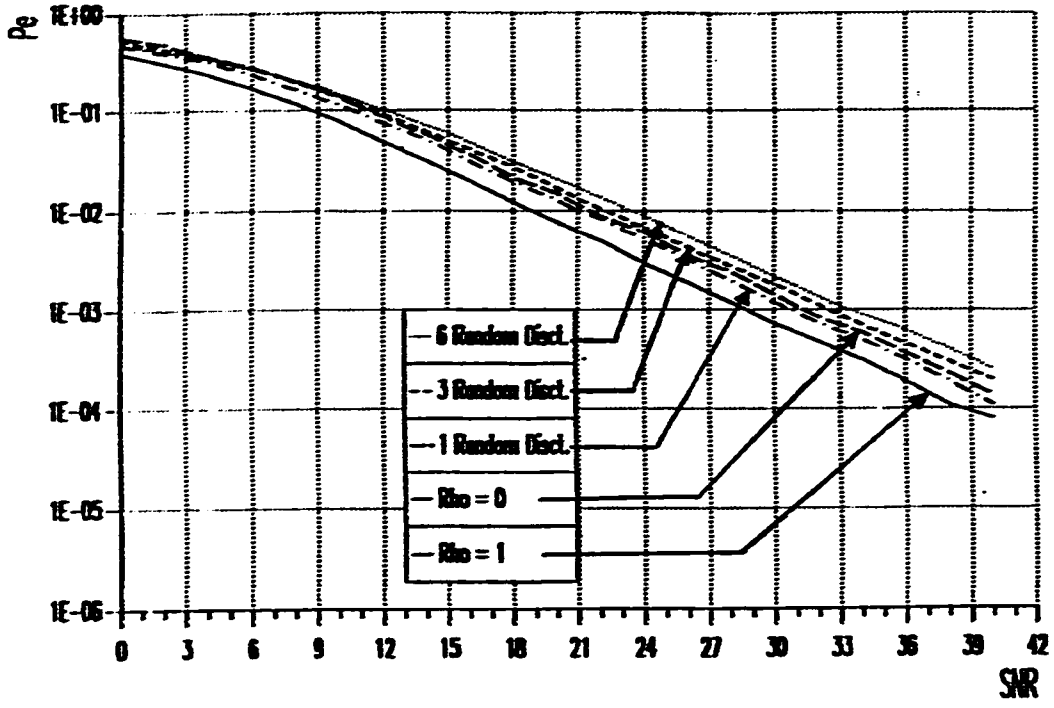


*Fig 2.17*: SQR Performance for M = 4, Under All Five Test Cases.

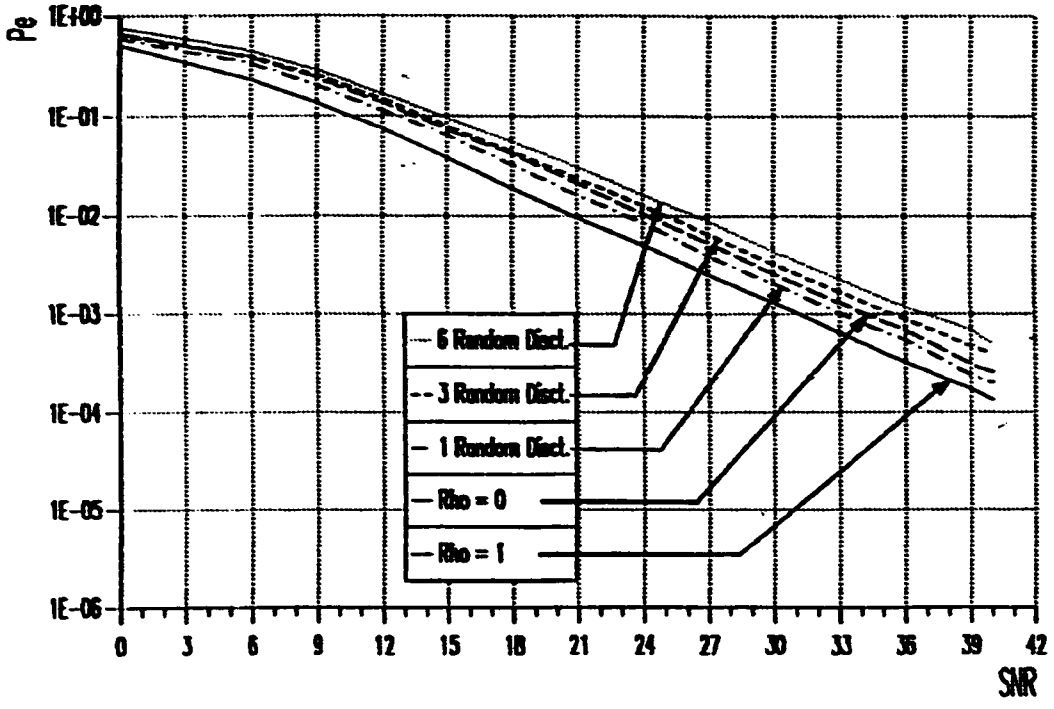


*Fig 2.18*: SQR Performance for M = 8, Under All Five Test Cases.

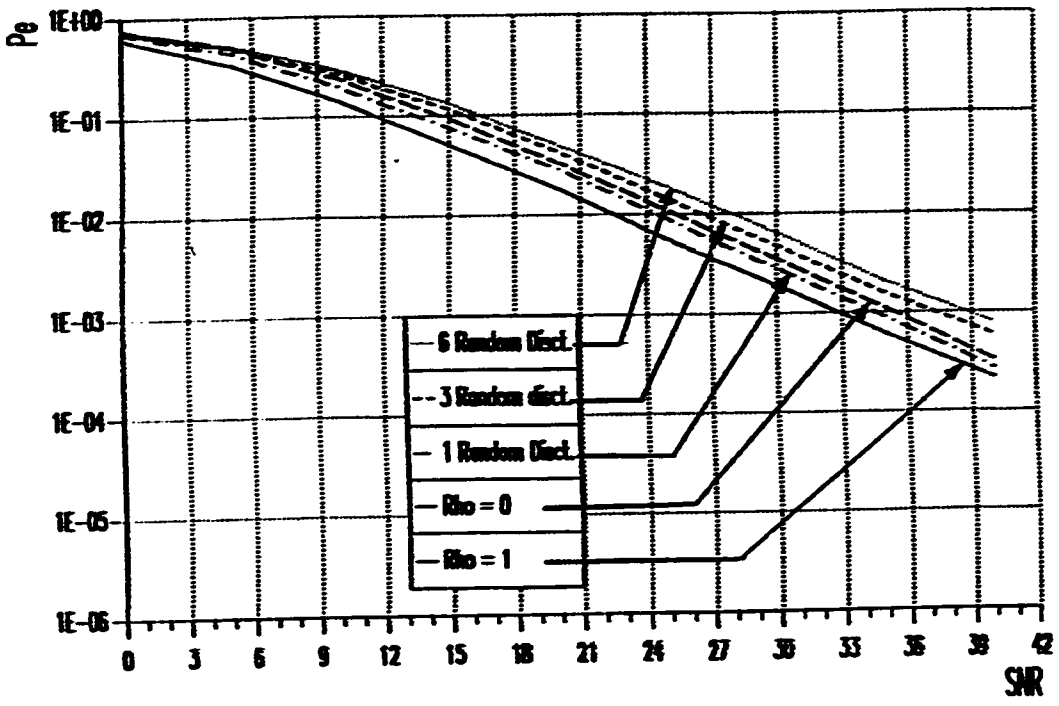


*Fig 2.19*: SQR Performance for M = 16, Under All Five Test Cases.

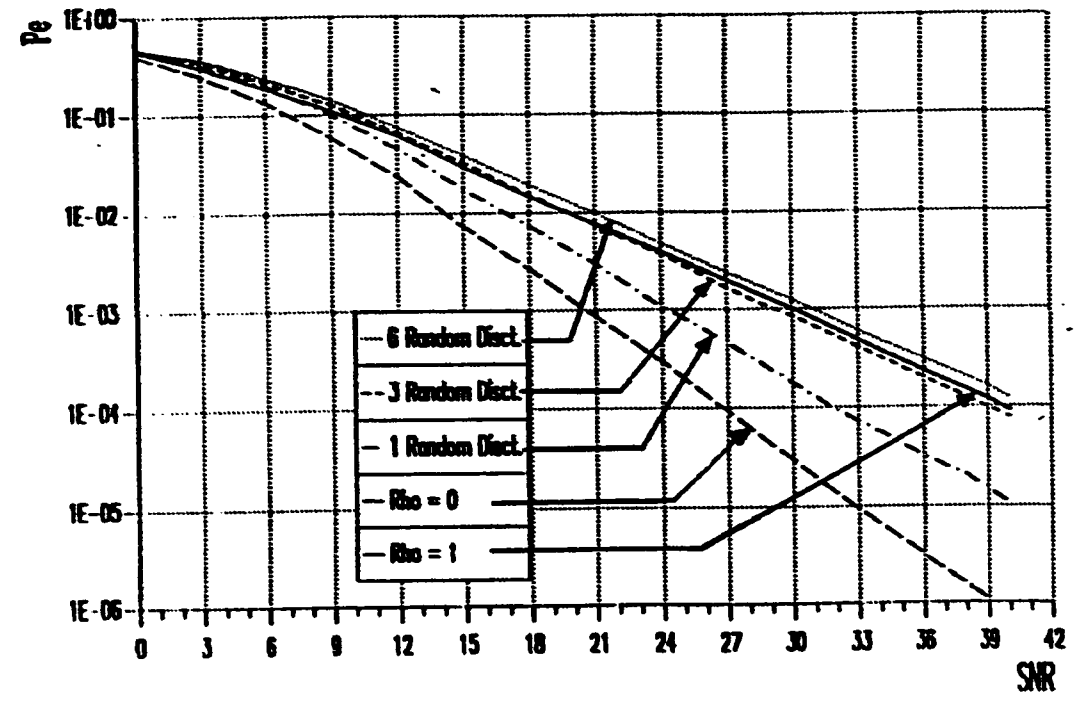


*Fig 2.20*: PQR Performance for M = 4, Under All Five Test Cases.

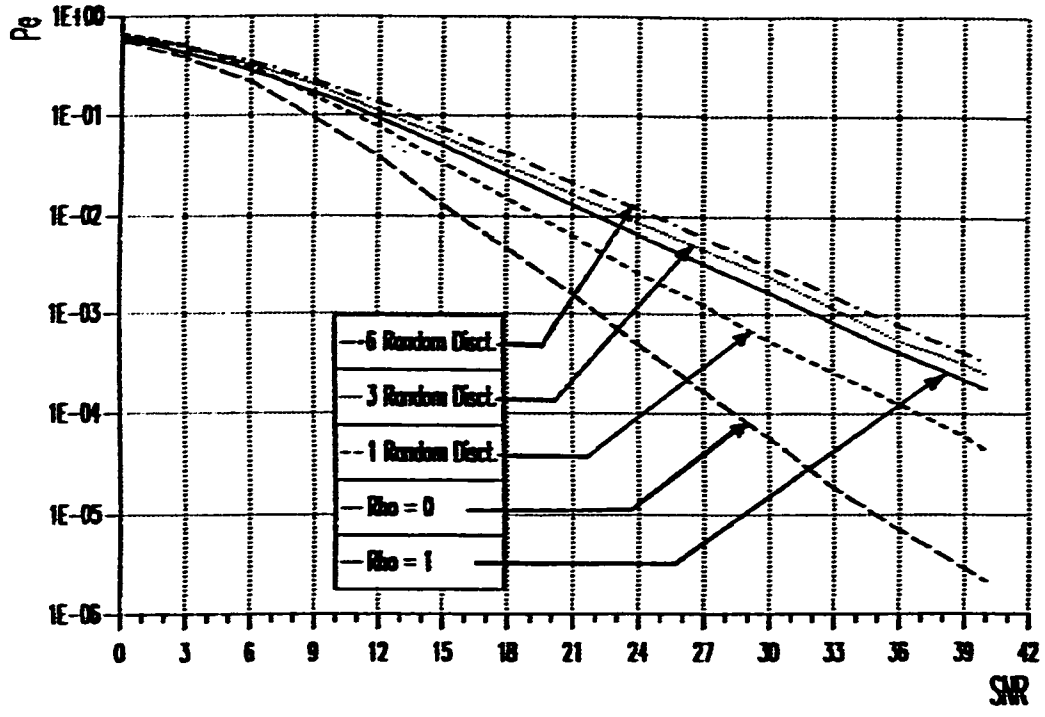


*Fig 2.21*: PQR Performance for M = 8, Under All Five Test Cases.

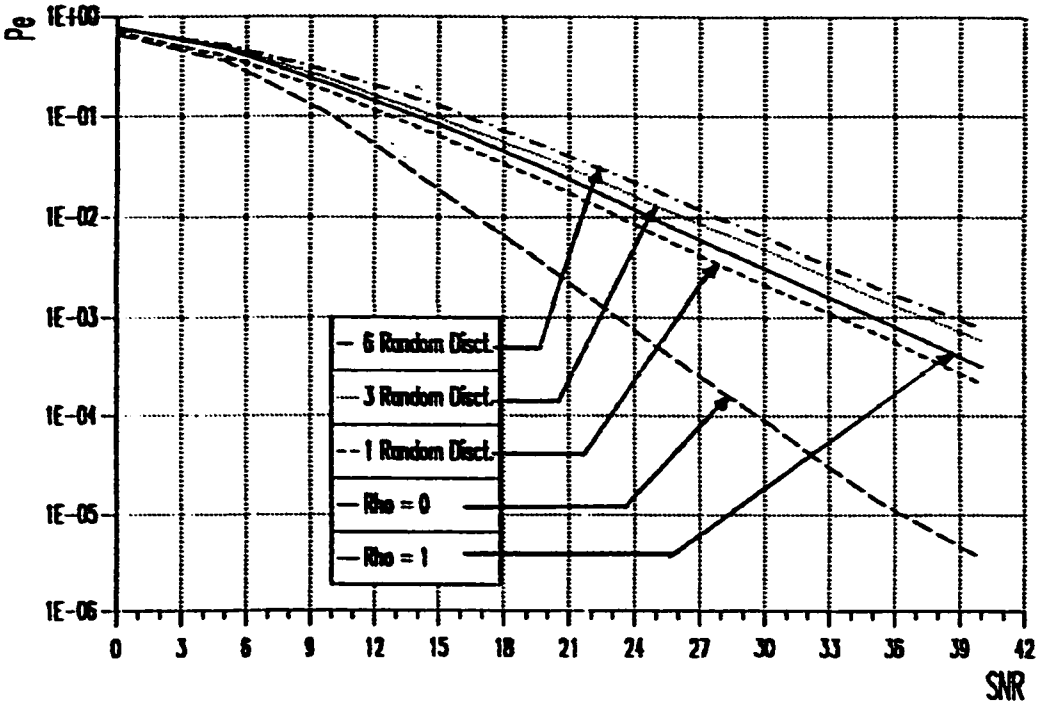


*Fig 2.22*: PQR Performance for M = 16, Under All Five Test Cases.

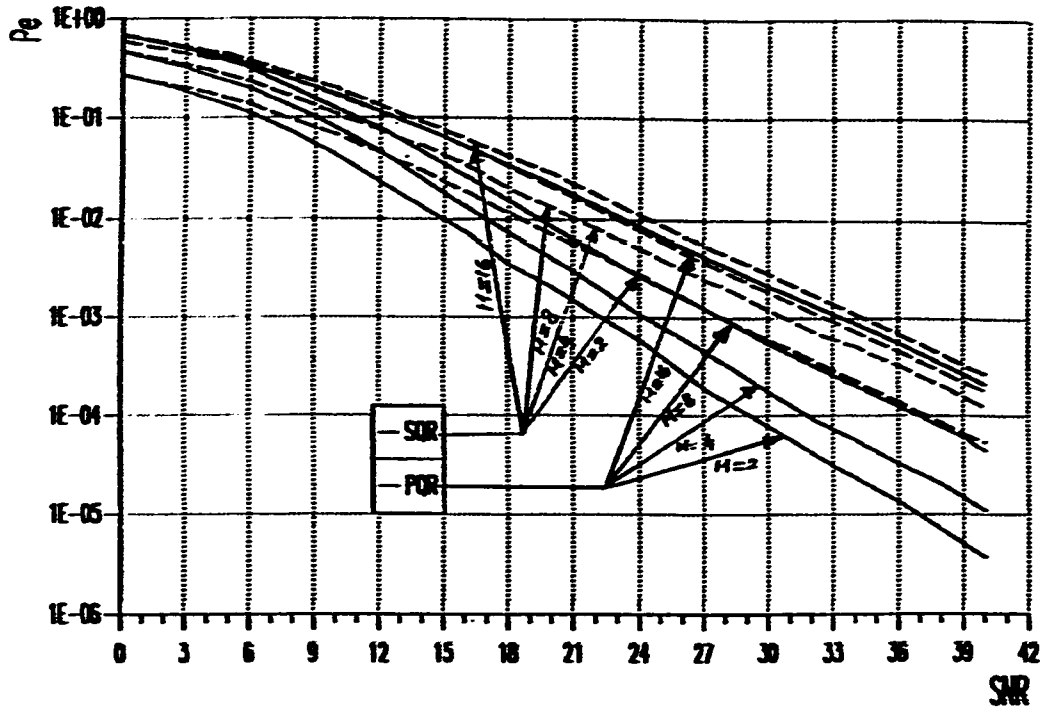


*Fig 2.23*: SQR Versus PQR Performance for the Case of One Random Discontinuity.

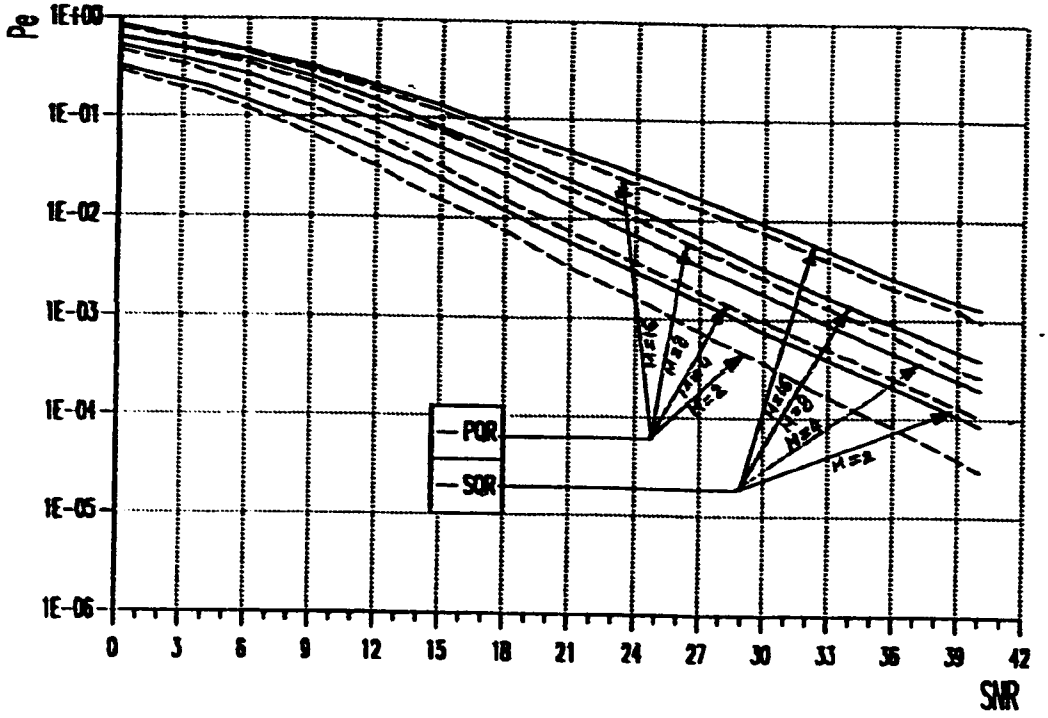


*Fig 2.24*: SQR Versus PQR Performance for the Case of Three Random Discontinuities.

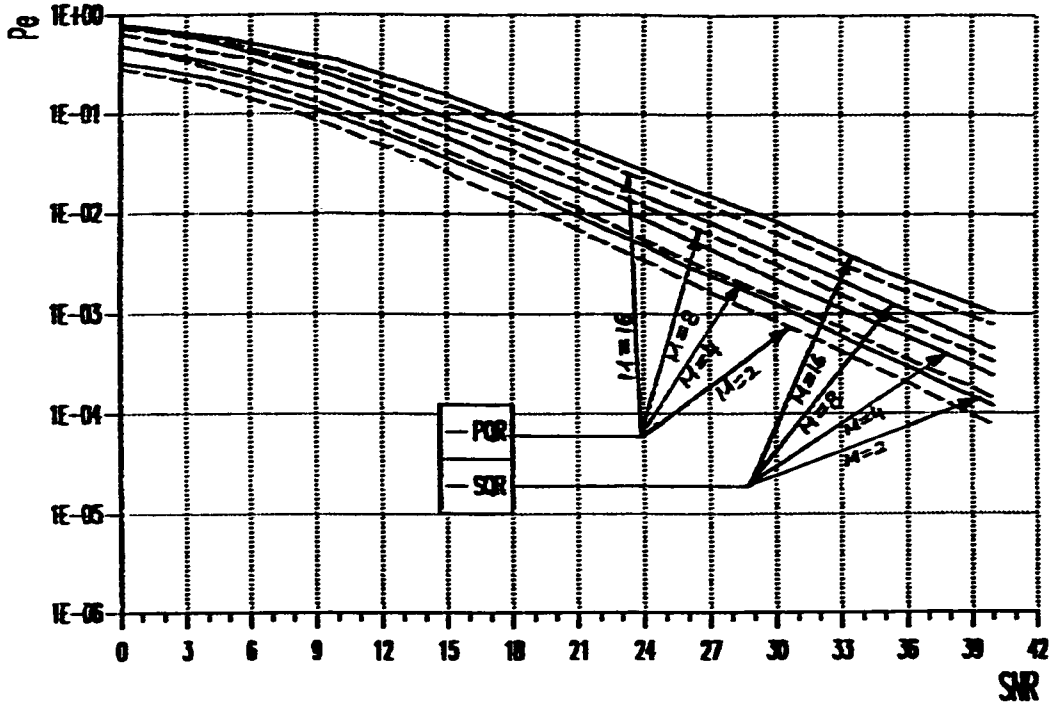


*Fig 2.25*: SQR Versus PQR Performance for the Case of Six Random Discontinuities.

nals. It proved to be working very nicely. Moreover, he has tested the DFLL for FSK signals. He has compared the loop's probability of error curves against those of the calculated values of the conventional single quadrature FSK receiver. This comparison was restricted to testing the performance of both the SQR and the DFLL, for the case of receiving an input signal that is corrupted with AWGN, and has a constant amplitude, and a constant phase throughout the symbol duration. However, the phase information of the received signal sequence was uniformly distributed with between zero and $2\pi$. This means that each received symbol has a different phase, but a constant amplitude. This is not exactly the case tested as $\rho = 1$, in this thesis, and in Higgins work [2,6]. In the case of $\rho = 1$, the phase of the different symbols was uniformly distributed, as a result of a non-resolvable multipath reception. As a result, these two cases are different.

The theory of operation of the DFLL receiver is discussed in Chapter 3 along with its performance evaluation. The DFLL receiver and the basics of the new receiver proposed in this thesis have the same origin. They are both based on the result obtained in [9,10], where parametric methods of spectrum estimation are used with low orders. The use of this technique for the implementation of the DFLL, and the new receiver, proposed in Chapter 4 of this thesis, will be discussed. In addition, a study of the performance of the DFLL, as well as a comparison to the SQR, and PQR conventional receivers, will be depicted.

## 2.8 Summary

The conventional SQR and PQR receivers are reviewed in this chapter. The limitations associated with the operation of these receivers in non-resolvable fast multipath fading channels are discussed, and new test cases are proposed to simulate the behavior of a non-resolvable fast multipath fading signals. The performance of the two conventional receivers is investigated and then results are compared to each other, for the different test cases. Both receivers were tested in the binary signaling space, and then tests were extended to the M-ary signal space. The performance of both receivers is seen to be sharply degraded as the new non-resolvable multipath signal tests were applied. However, the PQR performed always better than the SQR, under the new test cases.

In the next chapter, the DFLL receiver will be applied to non- resolvable fast multipath fading reception. It will be tested under the same multipath cases, under which the SQR and PQR were tested. And, the performance of the DFLL receiver will be compared to that of the SQR, and PQR receivers.

# Chapter III
# PERFORMANCE OF THE DFLL RECEIVER IN FAST MULTIPATH FADING CHANNELS

## 3.1 Introduction

In chapter 2 of this thesis, the behavior of the conventional SQR and PQR receivers was studied under different multipath cases. These receivers demonstrated some degradation as they were tested in fast multipath fading channel situations. This was a motive to search for other ways to improve on the detectability of the transmitted symbols, and to search for a better probability of error performance for the same signal to noise ratio.

In a quest for a better digital FM receiver, Al-Jamaan [8], has proposed a new closed-loop receiver, which he called: the Digital Frequency-Locked Loop (DFLL). This receiver operates in a manner that is similar to the one used in the conventional Phase-Locked Loops (PLLs). It is based on parametric methods of spectrum estimation, with low orders.

The DFLL was investigated thoroughly by Al-Jamaan in [8], for the demodulation of FM signals. In addition, he included a brief study of the DFLL use,

in random phase FSK detection. In this chapter, the DFLL will be employed for the detection of signals passing through fast multipath fading channels. The DFLL performance will be simulated for the same cases under which the conventional SQR and PQR receivers were tested (case 1 through 5, in Chapter 2). Then, the behavior of the DFLL under these test cases will be compared to the SQR and PQR behavior. Finally, a ground for the new multisampler receiver, which is proposed in this thesis, will be formed. However, in order to understand properly the DFLL, and to prepare for the introduction of the principle of operation of the new multisampler receiver, a brief overview of the spectral estimation methods will be included.

The Digital Frequency-Locked Loop (DFLL) operates in a manner similar to the Phase-Locked Loops (PLLs). In PLLs (both analog and digital), the baseband signals are reconstructed through the phase of the received signals. This means that the loop will first lock onto the phase of the incoming signal (by minimizing the difference between the input and the output phases). Then, it will follow the variations in the phase of the incoming signal.

In the DFLL, however, Al-Jamaan proposed that the information signal is reconstructed directly through the frequency of the incoming signal rather than the phase. In order to be able to follow the variation in the frequency of the received signal, a device is required to estimate the instantaneous frequency of the received signal. Al-Jamaan [8], has employed a new approach to estimate the instantaneous frequency of the received signal using parametric methods of spectrum estimation. He used a result that was published by El-Hennawey and Carter in [11], to locate accurately, and quickly, the poles (and consequently

spectrum peaks) of the time series model of the incoming signal, using the Maximum Entropy Method (MEM) Model [12].

In order to give a brief idea about the principle of operation of the DFLL, the following subsections will provide an overview of the parametric methods of spectral estimation. After that, the DFLL theory of operation will be reviewed.

## 3.2 Parametric Methods of Spectral Estimation

Ever since Gauss introduced the method of least squares, the estimation procedure has been a classical problem. Later, when Weiner [13], established the fact that the power spectral density (PSD) and the autocorrelation function of a process form a Fourier transform pair, spectral estimation has been of concern.

There are two types of methods that are used in spectral estimation, namely parametric methods and non-parametric methods. Parametric methods of spectral estimation consist of choosing an appropriate model, estimating the parameters of the model, and then substituting these estimated values into the theoretical PSD expressions. For signal-to-noise ratio's (SNR's) greater than 0 dB, the autoregressive (AR) PSD estimate has a better frequency resolution than that of the conventional periodogram estimates [14]. Many of the random processes that are encountered in practice can be approximated to a great extent by *time series* or *rational transfer function*. Since the variance of the wideband uncorrelated noise sequence is constant (and is equal to $\sigma_w^2$), it follows that the spectrum of the output will have the same shape as the spectrum of the model [15]. There-

fore, the spectrum of the model is viewed as an estimate of the given data. This can be seen in Fig. 3.1.

The transfer function H(z) between the input $u_n$ and the output $x_n$, for an auto-regressive moving average (ARMA) process, is the rational function.

$$H(z) = \frac{B(z)}{A(z)} \tag{3.1}$$

where

$$\text{A(z)} = \text{the Z-transform of the AR part} = \sum_{k=1}^{p} a_k \cdot z^{-k}.$$

and

$$\text{B(z)} = \text{the Z-transform of the MA part} = \sum_{k=0}^{p} h_k \cdot z^{-k}.$$

It is assumed that A(z) has all its zeros within the unit circle of the z-plane, which guarantees that H(z) is a stable and causal filter. If this is not the case, then the observed data sequence $x_n$ would not be a valid description of a wide sense stationary (WSS) random process.

It is well known that the power spectral density of a process that is output from a certain filter is equal to the power spectral density of the input process multiplied by the squared magnitude of the filter's transfer function [16]. Thus, the z-transform relationship between the input power spectral density $P_u(z)$ and the output power spectral density $P_x(z)$ would be as follows:

$$\begin{aligned} P_x(z) &= H(z) \cdot H^*(1/z^*) \cdot P_u(z) \\ &= \frac{B(z) \cdot B^*(1/z^*)}{A(z) \cdot A^*(1/z^*)} P_u(z). \end{aligned} \tag{3.2}$$

where "*" denotes the complex conjugate function.

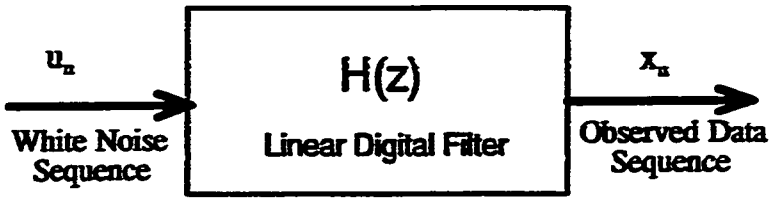


*Figure 3.1:* Transmission of a time series through a linear filter

The model may have one of several forms:

1. an autoregressive [$AR(p)$] mode represented by an all-pole rational function with $p$ poles;
2. a moving average [$MA(q)$] model represented by an all-zero rational function with $q$ zeros;
3. or a mixed autoregressive moving average [$ARMA(p,q)$] model represented by a rational function with $q$ zeros and $p$ poles.

Fig. 3.2-a shows the AR model, while Fig. 3.2-b shows the MA model. The driving noise of the model $u_n$ is different from any observation noise. The AR, MA or ARMA model noise is not an additive or an observation noise. Rather, $u_n$ is an innate part of the model, and gives rise to the random nature of the observed process $x_n$ [17]. This means that any observation noise can be modeled within the certain process by modifying its parameters.

## 3.2.1 MEM Method Of Spectral Estimation

In 1967, Burg [18], developed an estimator that is based on maximizing the entropy of the process, to overcome the periodogram problems. This method was coined the name "maximum entropy method (MEM)". It has the following advantages: [9]:

a. smoothed spectrum, and

b. the applicability to short data records.

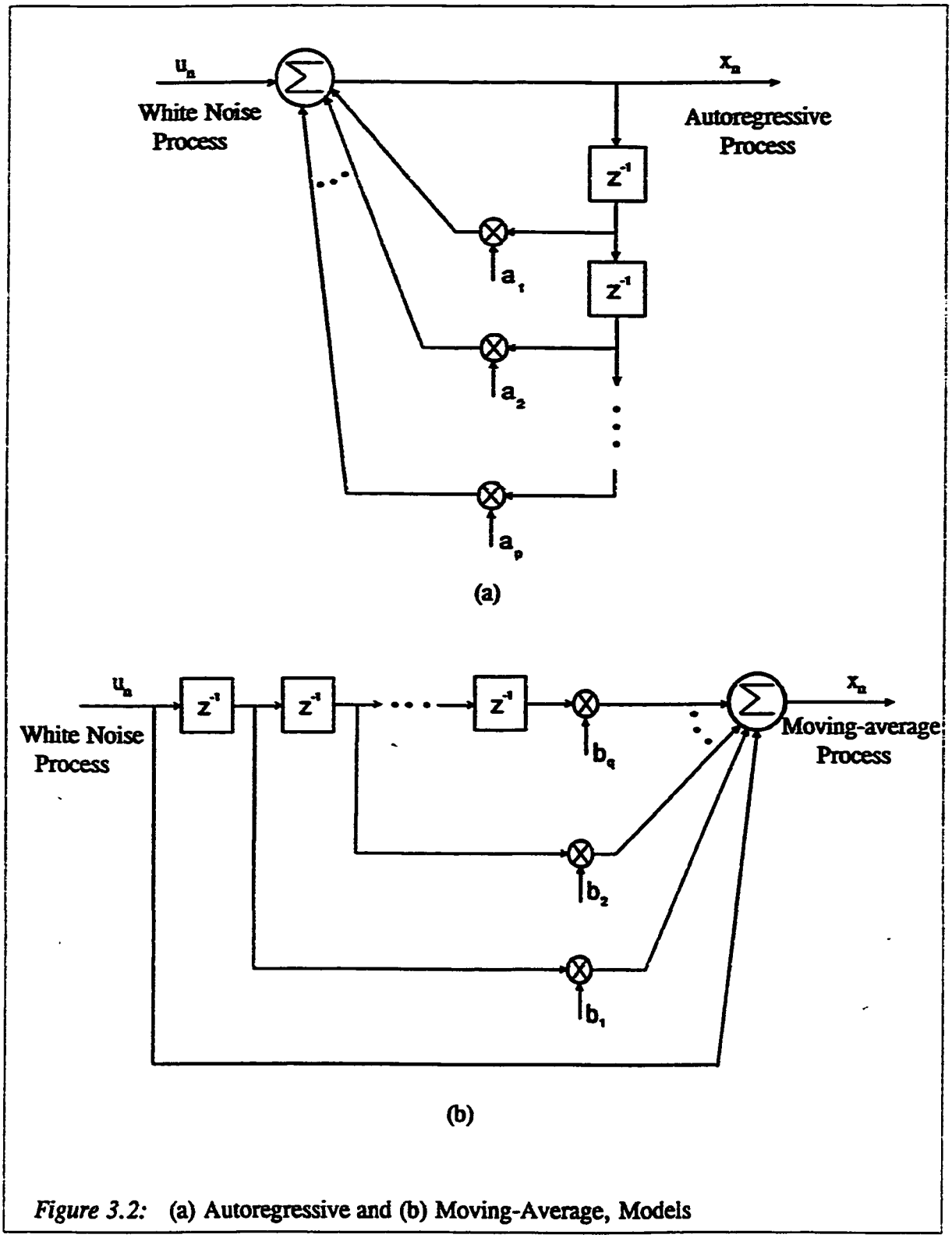


*Figure 3.2:* (a) Autoregressive and (b) Moving-Average, Models

The MEM method has the feature of being parametrically natured. This means that the spectrum can be calculated using the parameters of the prediction error filter (PEF) [17]. Later, Prazen [19], showed that both the MEM and the autoregressive model are exactly equivalent. This, in turn, has directed the attention to the field of time series analysis and modelling [20]. For short data records, the AR method yields reasonable spectral estimates. The method used to estimate the autoregressive model parameters is the key to the performance of the AR technique. If M+1 lags of the autocorrelation function for a process are known, the M autoregressive parameters can be obtained by solving the normal Yule-Walker equations. For high model orders, the Levinson recursion algorithm is used very often to solve the Yule-Walker equations [21].

The use of an autoregressive spectral estimate tacitly assumes that the underlying model for the sampled process is an autoregression, as shown in Fig. 3.2-a. The observed complex sequence $x_1, x_2, \ldots, x_n$ is an output from a $p^{th}$ order AR model driven by a white noise process $u_n$. Mathematically, the current output sample $x_n$ is a weighted sum of p past output samples plus a noise term:

$$x_n = -\sum_{k=1}^{p} a_k \cdot x_{n-k} + u_n \tag{3.3}$$

where $a_k$ is an AR parameter of a $p^{th}$ order AR process.

The parameters of the AR model can be obtained by solving the Normal Yule-Walker equations [9]. They can be written in the matrix form as:

$$\mathbf{R} \cdot \mathbf{A} = \mathbf{P} \tag{3.4}$$

where **R** is the autocorrelation matrix, **A** is the parameters' vector of an AR model (or the PEF coefficients vector), and **P** is the noise power spectral density.

Usually, only N data samples are available, rather than the actual auto-correlation function lags. In this case, the biased lag estimates

$$\hat{R}_m = \frac{1}{N}\sum_{n=0}^{N-m} x_n \cdot x^*_{n+m} \quad \text{,for } m = 0, 1, \ldots, p \tag{3.5}$$

are typically computed when selecting the Yule-Walker approach for the AR parameter estimation. The use of Eqn. (3.6) guarantees a positive-definite auto-correlation matrix. This method is termed the autocorrelation method of spectral estimation. However, since we are estimating the frequency received in the form of one carrier sinusoid, we do not need to get more than the autocorrelation function matrix values until the second lag. That is, we need to get the auto-correlation values at lag zero, one, and two. The MEM model parameters can be calculated using one of many algorithms. In Al-Jamaan work [8], as well as in this thesis, the algorithm given by Marple in [12], is used to calculate the MEM model parameters.

## 3.2.2 ARMA Method of Estimation

Different data records, need different models to describe them. Some sequences can be modeled using an AR Model, while others might be estimated more accurately using an ARMA model. For any given data with unknown statistics (unknown model), AR or MA modelling may fit the data well. However, an infinite order of each may be required. It is clear that the ARMA model is the most general one. In addition, it has been shown by Jenkins and Watt [22] that if a pure continuous autoregressive process is sampled to give discrete data, then

the resultant time series will be an ARMA process. Moreover, Cadzow [23] has shown the adequency of ARMA models in describing sinusoids with additive noise.

The normal Yule-Walker equation is used to estimate the pole parameters of the received AR model, and the extended Yule-Walker equation is used to estimate the parameters of the ARMA model. In general, the extended Yule-Walker Equation (EYW), for an ARMA(p,q) process is written as [10]:

$$R_x(m) = -\sum_{i=0}^{p} \varphi_i R_y(m-i) \quad , \quad m > q \quad . \tag{3.6}$$

As mentioned earlier, a second order ARMA model (ARMA(2,2)), will be sufficient to describe the input samples of a received FSK signal. This is because a signal consisting of n sinusoids, with additive white noise is closely represented by an ARMA(2n,2n) model [23]. In our case of a single sinusiod, n = 1.

However, according to Eqn. (3.6), the values of the autocorrelation matrix up to the fourth lag need to be determined. It can be seen when Eqn. (3.6) is expanded, the noise power term does not appear in the expression. This is one of the reasons of the more accurate representation of the FSK signals by an ARMA model. This will be seen clearly in the simulation.

## 3.3 Locating Spectrum Peaks:

The main drawback of the parametric methods of spectral estimation, is their computational complexity. This is due to the fact that the estimation process is a two-step procedure. First, the data is processed to obtain a set of parameters, then the spectrum is calculated. In addition, the appropriate model order selection might add one more step sometimes.

In many cases, however, only few points on the spectrum are of concern. Particularly, the location of the spectrum peaks might be the only concern, with the relative magnitudes, being of less or no importance, as in the FSK and SARSAT signals [9]. Hence, it is highly desirable to eliminate, or at least reduce to the minimum, the spectrum calculation process.

An equation to locate the spectrum peaks directly from the model parameters was derived by El-Hennawey in [10]. In addition to the significant reduction in computational complexity, it provides a higher accuracy in the peak frequency measurements. Spectrum peaks are mainly characterized by the model poles of an ARMA model, while the zeros might resemble spectrum notches [23,24]. In our case, the peaks of the spectrum are our only concern. This will lead to focusing our attention on the MEM, and ARMA models only (where the AR part of the ARMA model will be of concern to us). Thus, spectrum calculation for these two models will be similar in this case particularly.

The power spectral density of the MEM or of the AR part of an ARMA model can be described with the equation:

$$S_y(f) = \frac{1}{\left|1 + \sum_{i=1}^{p} a_i \exp(-j2\pi f T_s)^i\right|^2}$$

$$S_y(f) = \frac{1}{\prod_{i=1}^{p} |1 - g_i z^{-1}|^2_{z=\exp(j2\pi f T_s)}} \quad . \tag{3.7}$$

where $a_i$'s are the AR parameters, $g_i$'s are the corresponding poles in the z-plane, and $T_s$ is the sampling period.

Although the above equation can be used for peak detection of both MEM and ARMA models, the corresponding set of parameters (poles) need not be the same, in general.

If the observed signal data to be analyzed, are real valued, then all of the model parameters are real [10]. In certain applications, such as those using FSK signals, one frequency is received at a certain time. This means that a second order model will be sufficient enough to describe it. In a continuous-time system, a spectrum peak will occur if it is associated with a complex conjugate pole pair. Thus, let us consider the following transfer function:

$$H(z) = \frac{1}{1 + a_1 z^{-1} + a_2 z^{-2}} \quad , \tag{3.8}$$

where $a_1$ and $a_2$ are the model coefficients. The system will contribute a spectrum peak, if it has a complex conjugate pair, i.e.

$$H(z) = \frac{1}{(1 - g z^{-1})(1 - g^* z^{-1})} \quad . \tag{3.9}$$

where g and $g^*$ are the z-plane poles, and "*"denotes the complex conjugate. The pole g can be represented in polar coordinates as follows:

$$g = r \cdot \exp(j\beta) \quad . \tag{3.10}$$

Using this expression in the above equation, and applying some algebra and calculus manipulations, the peak frequency can be calculated as follows [10]:

$$f_p=(1/2\pi T_s)\ Cos^{-1}[0.5(r+1/r)Cos(\beta)] \quad . \tag{3.11}$$

where $f_p$ is the peak frequency, and $T_s$ is the sampling period. A necessary and sufficient condition for $f_p$ to exist, is that:

$$|Cos(\beta)| < 2r/(1+r^2) \quad . \tag{3.12}$$

A simulation of the above equation was carried out by El- Hennawey, in [10]. It was found that if the estimated peak frequency is one fourth of the sampling frequency (i.e. $f_p=f_s/4$), then, the estimation error is zero, regardless of the SNR value [11]. Simulations of the above equation were carried out again, in the course of study of this thesis for convenience. Fig 3.3. depicts these simulations. It can be seen that the relation between the sampling frequency and the error of estimation is almost linear in a certain interval. This interval increases as the SNR increases.

The above result forms the main principle upon which the DFLL is built. It also, will be used to propose and develop the new multisampler FSK receiver, that will be studied in the proceeding chapter, and will be compared to the conventional SQR, and PQR receivers.

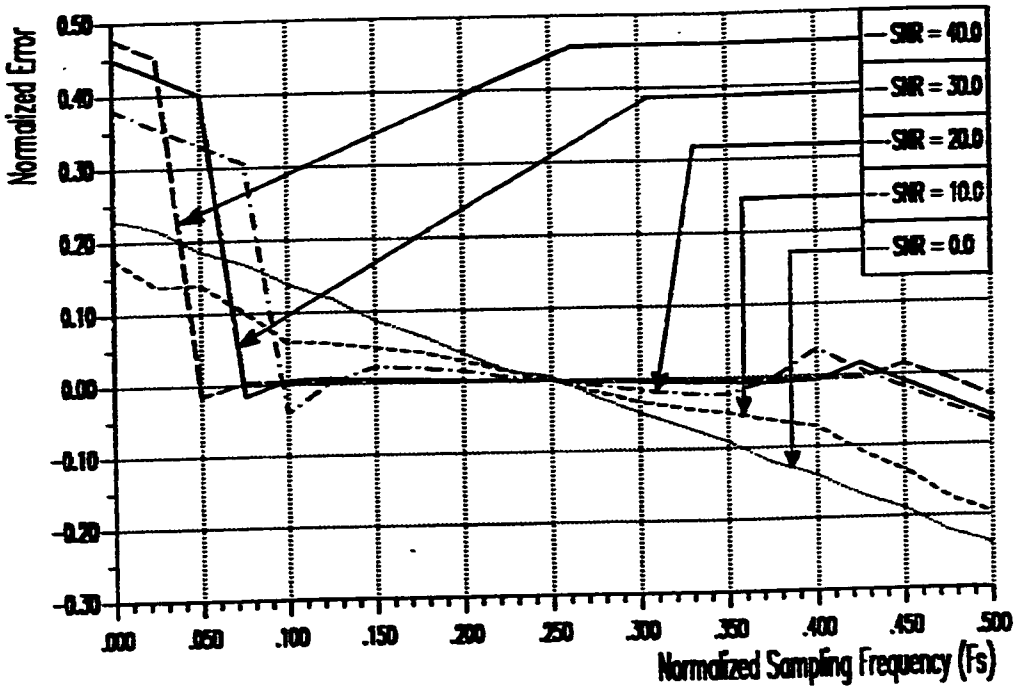


*Figure 3.3:* Error in Estimation Vs. the Sampling Frequency for an ARMA Model.

## 3.4 The DFLL Structure

As mentioned earlier, the DFLL was proposed to have a structure that is similar to that of PLLs. However, the frequency is to be estimated, instead of the phase of the incoming signal. Based on the discussion in the previous subsection (Locating Spectrum Peaks), Al-Jamaan has proposed the DFLL receiver in [8].

The block diagram of the DFLL is shown in Fig. 3.4. It consists of five major parts: a multiplier, a low-pass filter, a frequency estimator . a loop filter, and a numerically controlled oscillator (NCO).

The lowpass filter eliminates the high frequency components of the multiplier. The frequency estimator is a device used to estimate the peak frequency of the signal. It uses the frequency estimation equation (Eqn 3.11) derived in the previous section. The numerically controlled oscillator (NCO) is a first order positive feedback system which can be represented by the equation:

$$X(z) = \frac{1}{(1-z^{-1})} \tag{3.13}$$

When the DFLL locks into the frequency of the incoming signal, the frequency estimator will be in the linear region, and a linearized DFLL diagram may be considered as shown in Fig. 3.5a. Al-Jamaan has reduced this diagram further [8], to give another diagram of the linearized DFLL, as can be seen in Fig. 3.5-b. From the above figures, he formulated the equation relating the input freqnency $f_i$ to the output frequency $f_o$. The DFLL was simulated in [8], using a Fortran computer Program. Certain conclusions, regarding the operation of the DFLL, from the simulation were made. These conclusions are enlisted here for convenience:

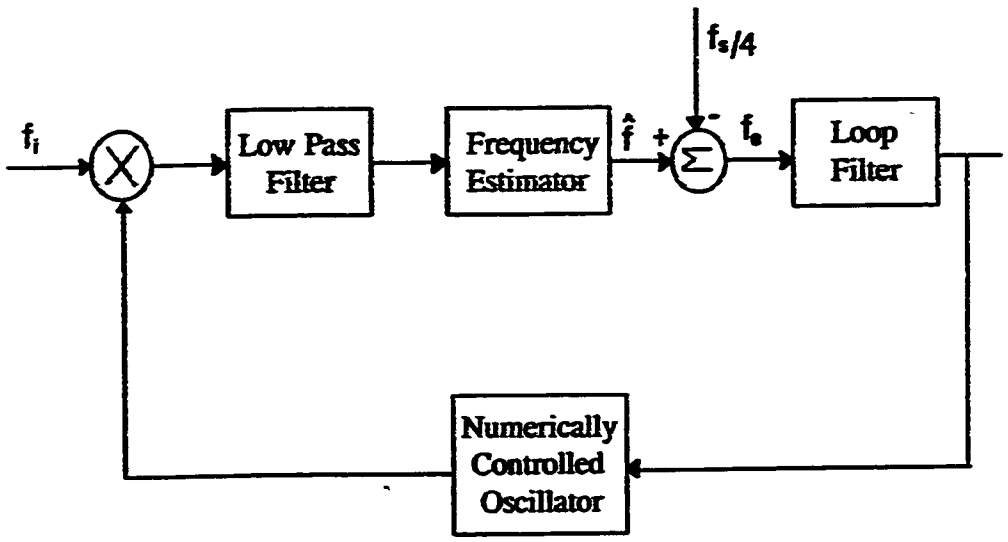


*Figure 3.4:* The Digital Frequency-Locked Loop Receiver

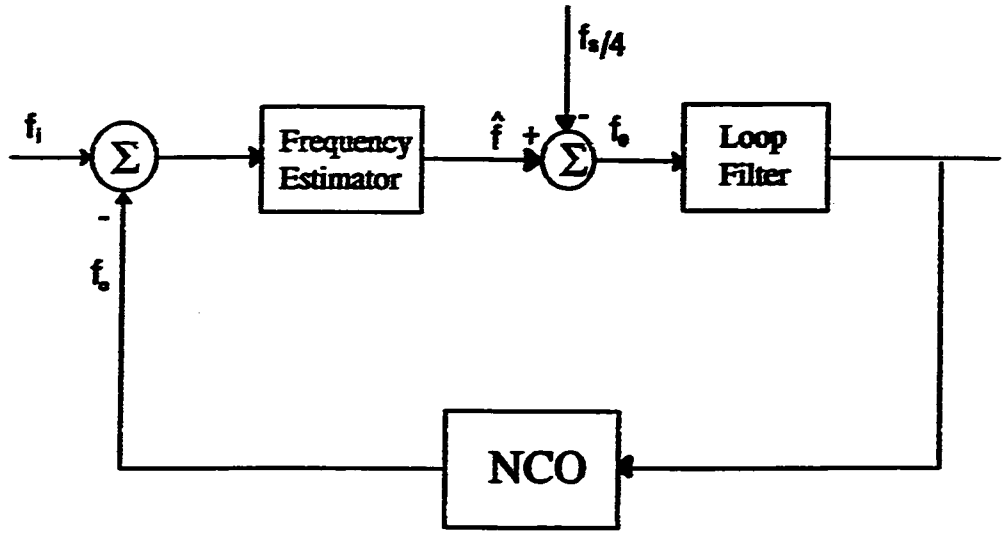


(a)

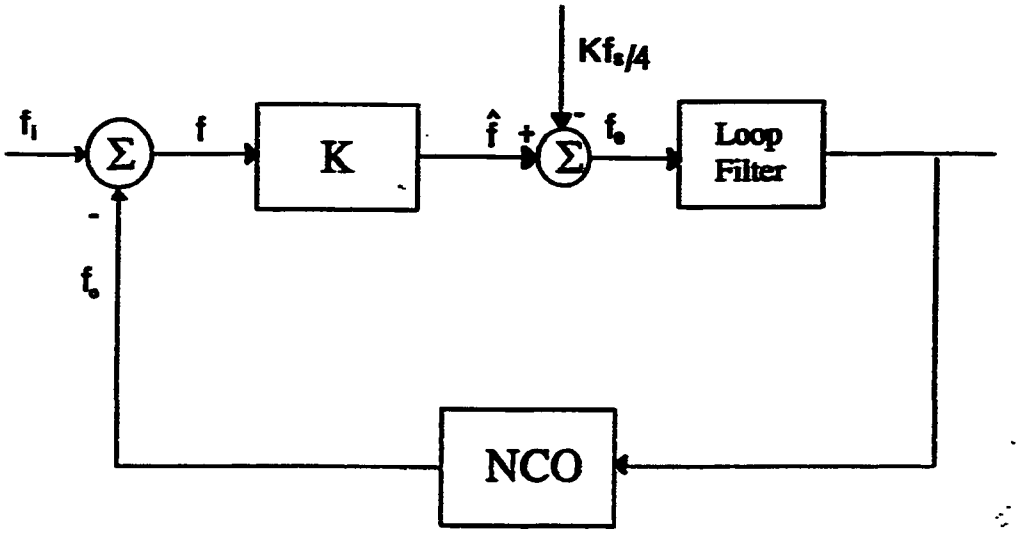


(b)

*Figure 3.5:* Linearized DFLL Receivers.

1. the DFLL locks onto the incoming signal frequency faster if the input samples are completely overlapped with the samples that are fedback from the NCO;
2. there is an optimum loop filter gain factors set which results in a faster convergence of the loop;
3. higher SNRs improve on the convergence time of the DFLL;
4. as in the case of PLLs, a second order loop filter performs better than a first order loop filter.

These results were used to write the simulation program of the DFLL receiver here, for testing purposes. Al-Jamaan has studied the DFLL in [8], for FM demodulation. In addition, a brief study of the DFLL use in random phase continuous-wave FSK detection was included. In his simulation, the performance of the DFLL was better than the noncoherent envelope detector receiver for low signal to noise ratios. However, as the SNR values were increased to reach better probability of error levels, the DFLL performance was poorer than that of the conventional envelope detector receiver.

In the following sections, the DFLL will be simulated again, using a Fortran computer program. The results enlisted from Al-Jamaan Thesis [8], will be used in the implementation and simulation of the DFLL. This simulation, and its results will be used to study the behavior of the DFLL under the fast multipath fading cases, under which the conventional SQR and PQR receivers were studied in Chapter 2 of this thesis. After that, these results will be compared to those of the two conventional SQR and PQR receivers.

## 3.5 Simulation of the DFLL Receiver in Multipath Reception

In this section, the behavior of the DFLL under multipath fast fading FSK detection situations will be investigated. The results of the simulation under the five cases under which the SQR and PQR were investigated, will be shown. Furthermore, these results will be compared to those of the SQR and PQR receivers to determine the suitability of the DFLL receiver for non coherent detection of multipath fast fading FSK transmissions. The results enlisted in the last sub-section, are used to achieve the best behavior of the DFLL. A second order DFLL was used in the simulation.

A Fortran computer program was developed to simulate the DFLL on an IBM 370/3090 digital computer. The main steps of the program can be listed as follows:

1. The same procedure that was used for signal generation and the same channel effects that were applied to the SQR, and PQR receivers is applied here. The same seeds and conditions are used to produce the same received signal at the receiver end.
2. The signal is then received and entered to the DFLL. The DFLL will operate according to Fig. 3.4. First, a number of samples of the received signal are input to the loop and are mixed with the same number of samples from the NCO branch of the DFLL. The mixer is simply a multiplier. Then, the high frequency components of the mixed signal are filtered out through the low pass filter (LPF). Next, the peak frequency of the output vector from the LPF is estimated. After that, the error in

frequency estimation, is calculated, by subtracting one fourth the sampling frequency ($f_s/4$) from the estimated frequency $f_e$. Finally, the frequency error is passed through the loop filter and the output from the loop filter is used to update the NCO vector. The NCO updated vector is mixed with the input vector from the received signal. This way, the DFLL keeps tracking the frequency changes of the received signal.

3. As the frequency is estimated, the frequency estimation values are summed over the symbol period. This addition process takes place after the convergence is achieved. Then, the average value of the frequency estimation values is calculated. Finally, the estimated average frequency of a certain symbol $f_a$, is compared to the transmitted frequency to find about the correctness of the estimate. This, process is repeated for a large number of symbols, and the probability of error versus SNR is calculated.

A simulation of the DFLL according to the previous procedure was carried out, for the five cases of fast multipath fading channels that were proposed in Chapter Two of this thesis.

### 3.5.1 Performance of the DFLL for Binary Signaling

The DFLL is simulated under different fast multipath fading channel cases. In this section, the behavior of the DFLL under different cases will be shown to give a brief idea about the way the DFLL will act under such situations. Then, the $P_e$ versus SNR curves will be shown for each of the five studied cases.

A random sequence of binary symbols was applied to the DFLL to demonstrate the effect of different multipath situations on the behavior of the loop. The effect of different loop filter gains on the behavior of the loop is shown in Fig. 3.6. The signal to noise ratio was chosen to be SNR = 40 dB, and the sequence was applied with no discontinuities to the loop (i.e. $\rho = 1$). As the loop filter gains were varied from: G1 = 0.01, G2 = 0.05, in Fig.3.6-a, to the values: G1 = 0.07, G2 = 0.05, in Fig.3.6-b, the behavior of the loop changed dramatically. In Fig.3-6-a the loop converged very smoothly and quickly to the correct values, and followed the symbol changes accurately. Once, a different set of loop gains was used, Fig. 3.6-b demonstrates how the loop takes a longer time before it locks onto the frequency of the received signal. The number of discontinuities resulting from a fast multipath fading channel reception, affects the behavior of the loop. Fig.3.7 demonstrates this effect. Fig.3.7-a shows the behavior of the loop with the SNR = 40 dB, and with the input sequence having no discontinuities associated with the input symbols. On the other hand, Fig. 3.7-b shows the behavior of the loop at the same SNR and with the same loop gains, but with one fixed discontinuity in the middle of each symbol ($\rho = 0$). In addition, Fig. 3.7-c, illustrates the behavior of the loop at the same SNR, and for the same loop gains, but with a maximum of three random discontinuities being applied in the input symbols. As can be seen in these three figures, the loop locking deteriorates as discontinuities are applied in the input symbols. Similarly, Fig. 3.8 compares the behavior of the loop with a maximum of three random discontinuities being applied in the input symbols of the test sequence, to the same sequence, but with a maximum of six random discontinuities being applied to

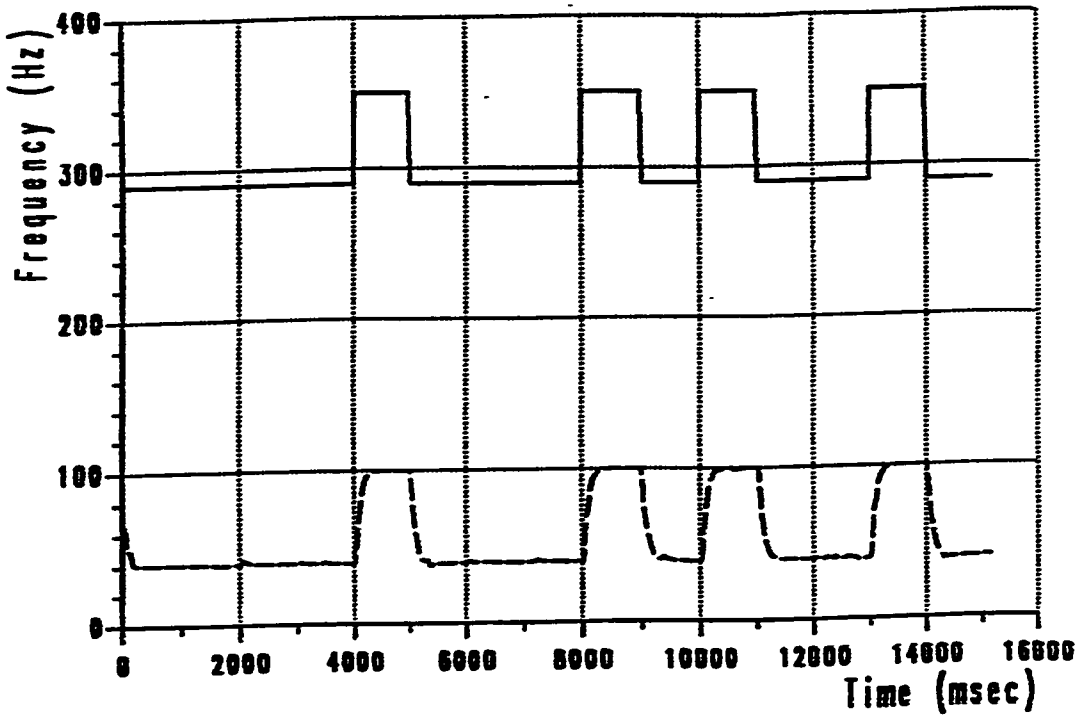


(a) $G_1 = 0.01$, $G_2 = 0.05$

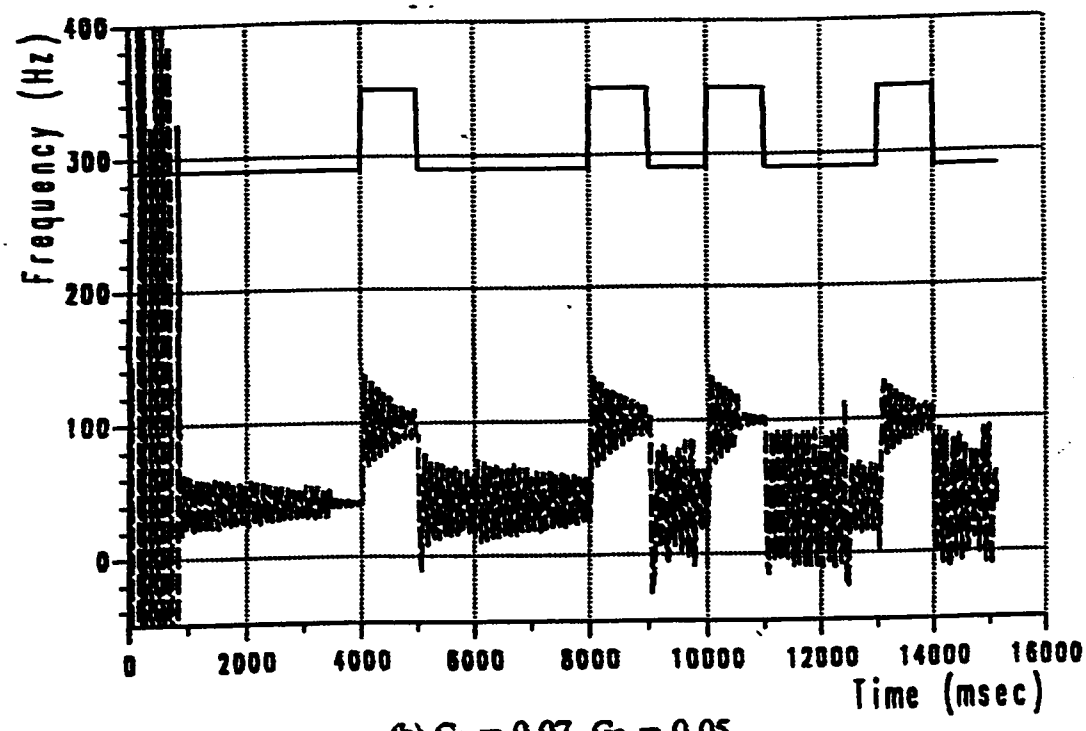


(b) $G_1 = 0.07$, $G_2 = 0.05$

*Figure 3.6*: The effect of loop filter gains on the behavior of the DFLL Receiver.

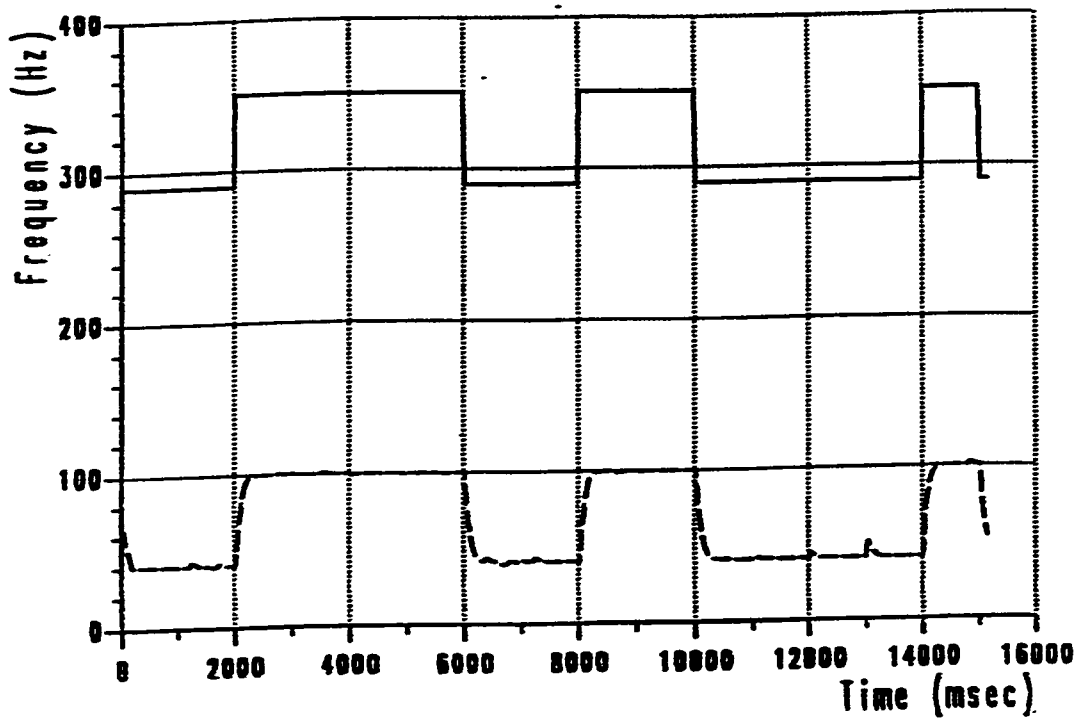


(a) No Phase Discontinuities ($\rho = 1$)

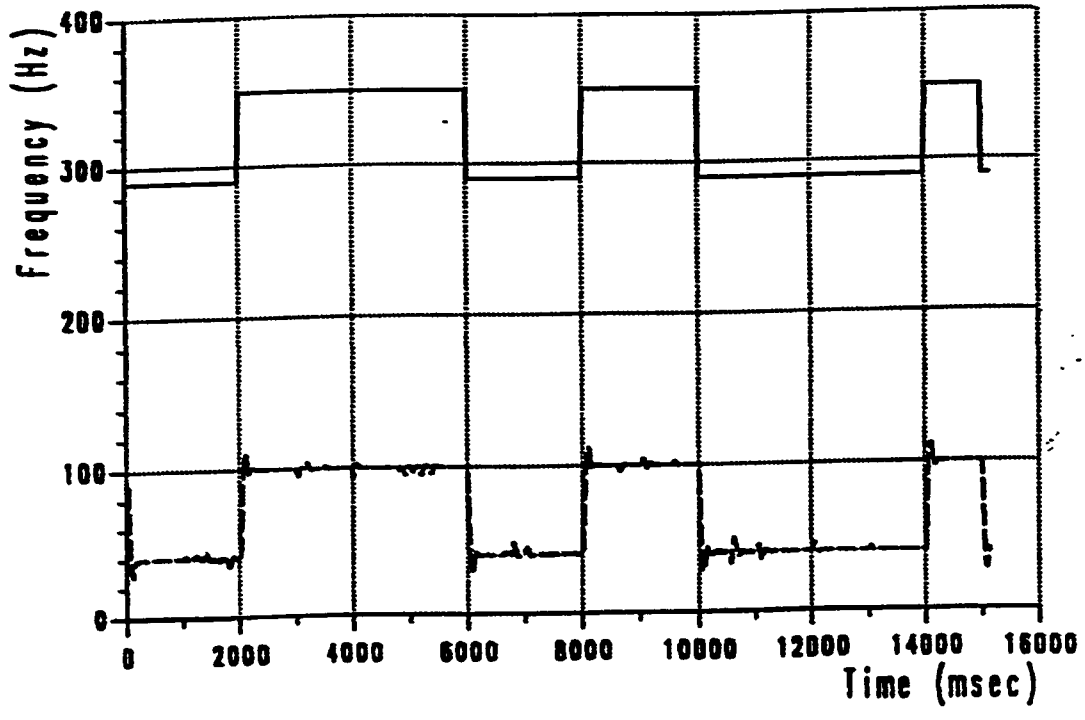


(b) One Fixed Phase Discontinuity ($\rho = 0$)

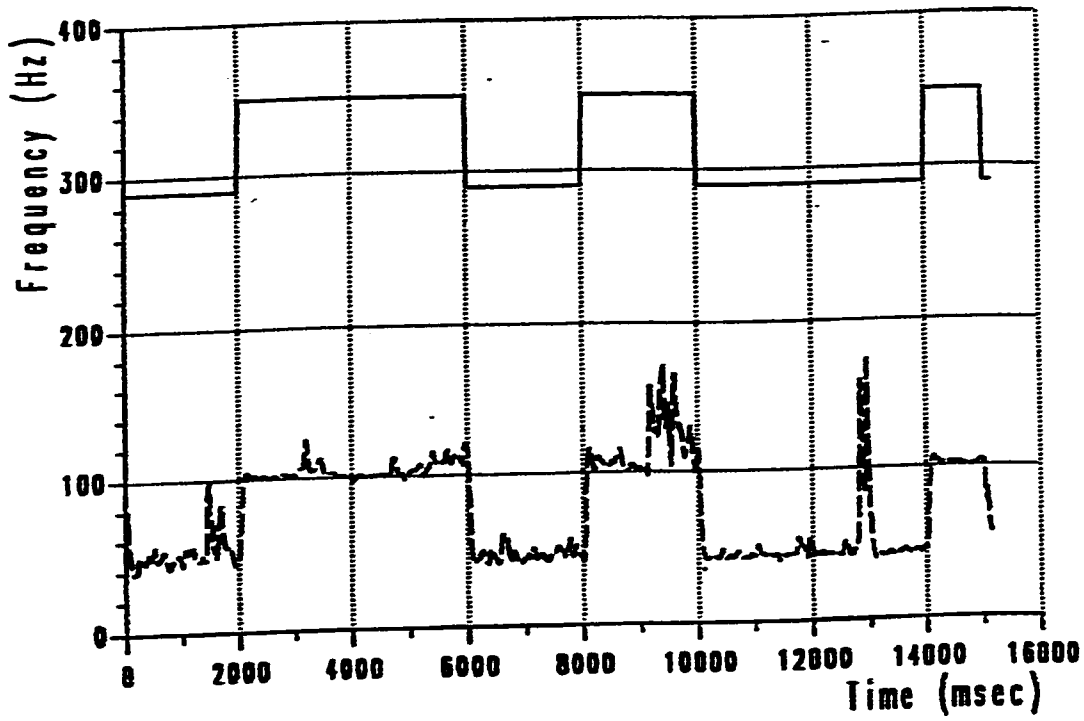


(c) One Random Phase Discontinuity

*Figure 3.7*: The effect of introducing phase discontinuities in the symbol duration, on the behavior of the DFLL.

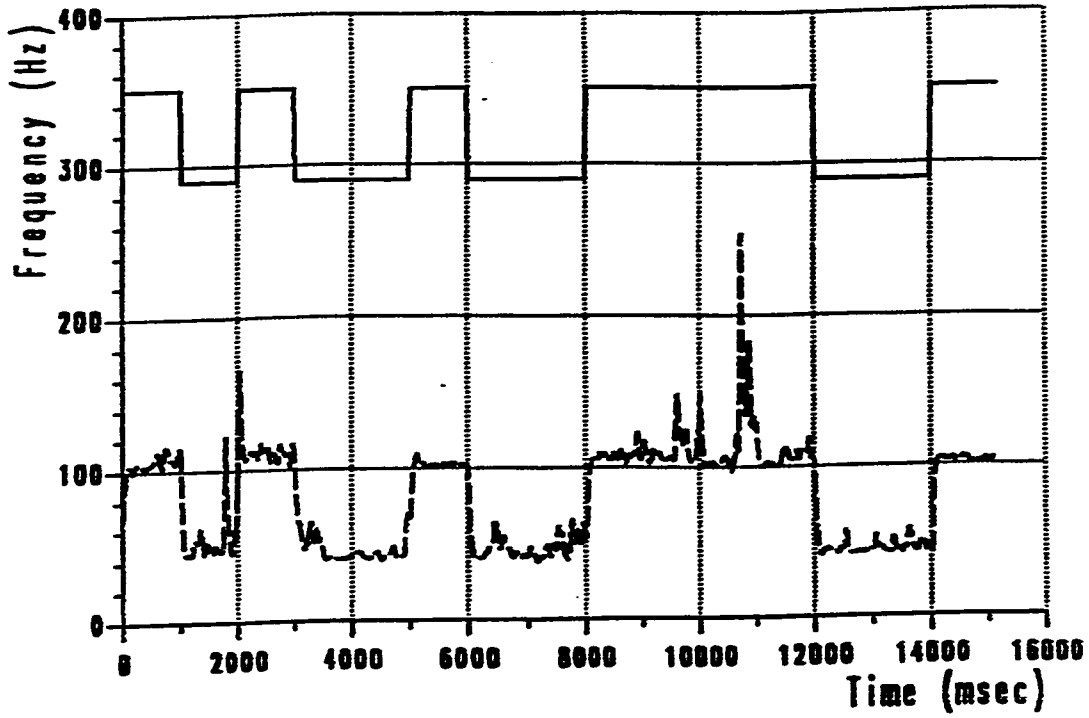


(a) Maximum of three phase discontinuities

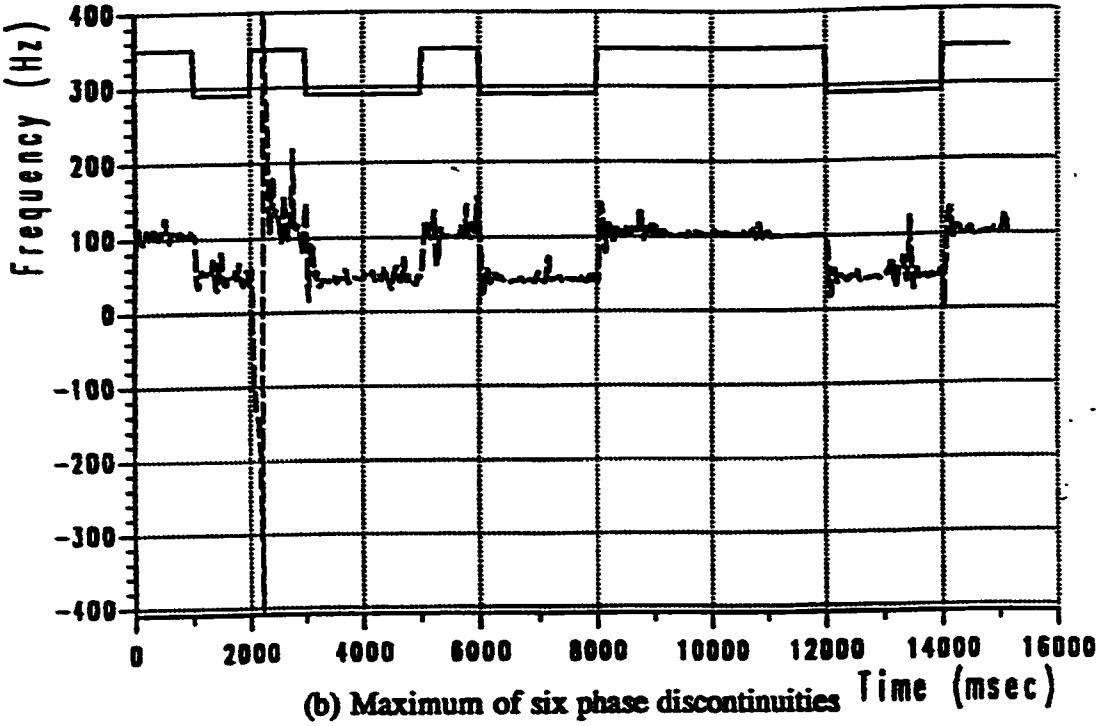


(b) Maximum of six phase discontinuities

*Figure 3.8*: The effect of increasing the number of phase discontinuities, from (a) a maximum of three, to (b) a maximum of six phase dicontinuities, within the symbol duration.

the input sequence. Once again, the loop filter gains were fixed to the same value, and SNR = 40 dB. One can draw the same conclusion about this figure: as the number of discontinuities increases, the loop's locking becomes less stable. These results will help in understanding the probability of error ($P_e$) performance of the loop.

The DFLL receiver was simulated according to the computer program steps listed previously. Fig. 3.9 shows the behavior of the DFLL, for these cases of $\rho = 0$, and $\rho = 1$. As can be seen, the DFLL behavior is exactly the same for both cases. This can be explained as follows. As disturbances take place, and the loop unlocks temporarily, it establishes locking again. And, as the frequency estimated in the loop is averaged over the symbol's period, the average value tends to match in both cases of $\rho = 1$ and $\rho = 0$. This yields the same probability of error. The same behavior is expected to take place when one random discontinuity is applied to the input sequence. Fig. 3.10, demonstrates the behavior of the DFLL receiver for the case of the first three fast multipath fading cases are applied. As one random discontinuity is applied to the input sequence, the DFLL receiver performance is better than the case of having a maximum of three random discontinuities applied in the input sequence, which in turn, is better than the case of having a maximum of six random discontinuities being applied to the input sequence. However, this difference in performance is not so big. This again can be tributed to the fact that the loop's unlocking effect, will be reduced by the averaging of the estimated frequency values over the symbols period. Moreover, Fig. 3.11 shows the behavior of the DFLL under the five cases. As was expected, the performance of the DFLL receiver is the same for the

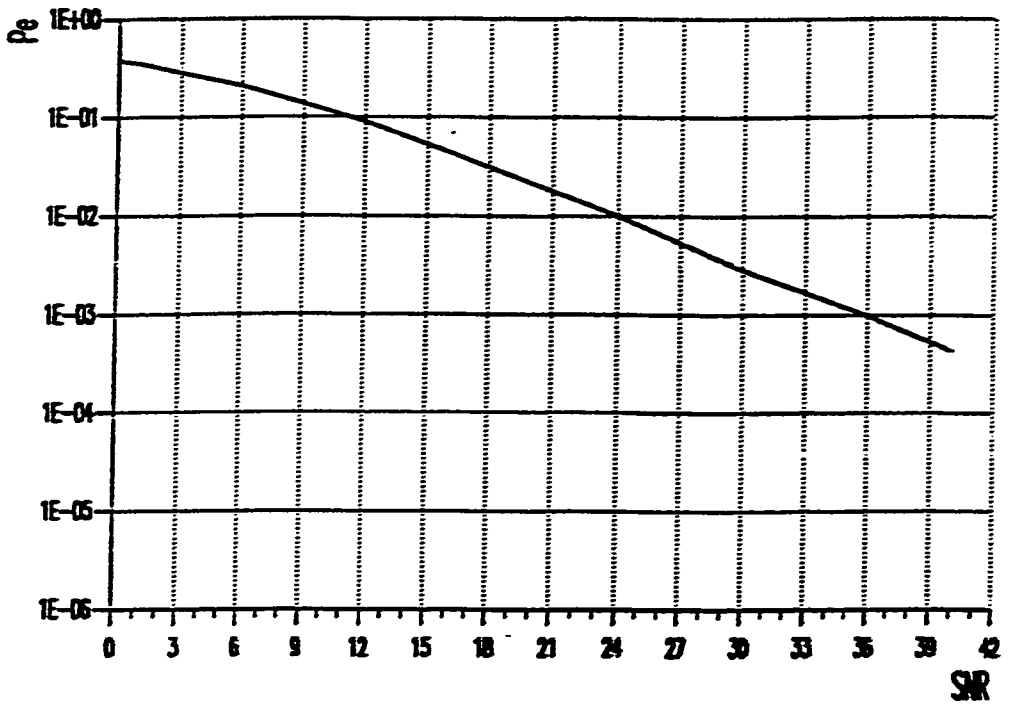


*Figure 3.9*: DFLL Performance for M = 2, in the case of $\rho = 1$, and $\rho = 0$.

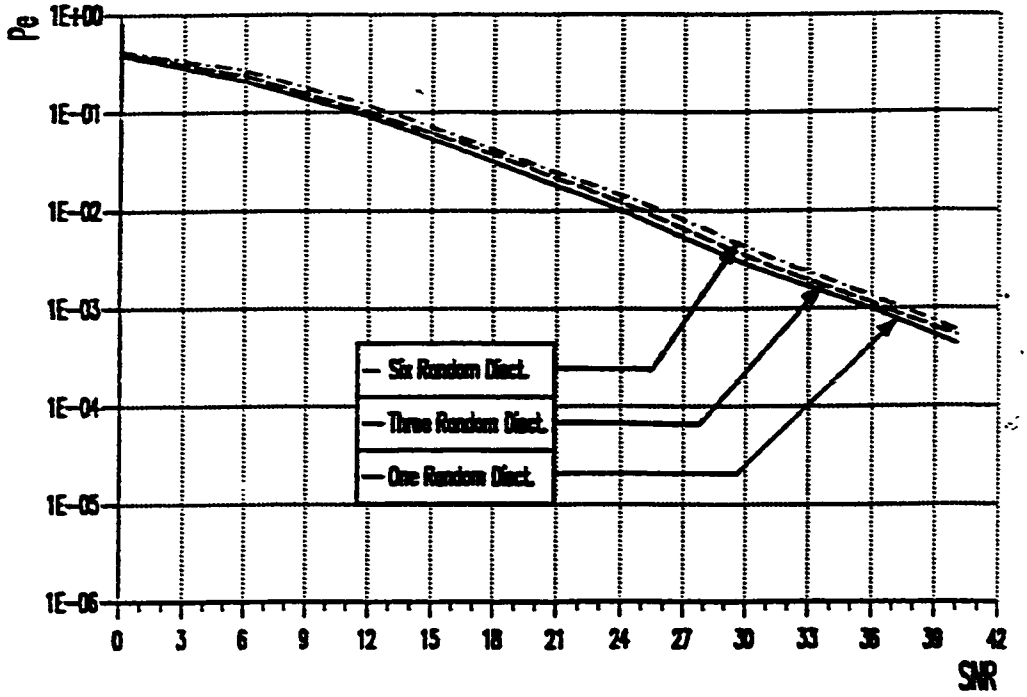


*Figure 3.10*: DFLL Performance for the cases of one, maximum of three and maximum of six, random phase discontinuities, for M = 2.

three cases of $\rho = 0$, $\rho = 1$, and the case of one random discontinuity that is existent in the duration of the received input symbols. However, the performance of the DFLL receiver is aggravated more by the increase and randomness of occurrence of discontinuities in the symbols' duration.

### 3.5.2 The DFLL Receiver Versus the Conventional SQR and PQR Receivers

In order to be able to judge the suitability of the DFLL receiver to work in fast multipath fading situations, it has to be compared to the conventional SQR and PQR receivers operating under the same conditions.

Figure 3.12 compares the performance of the DFLL receiver to this of the SQR and PQR for the cases of $\rho = 1$, $\rho = 0$ and the case of one random discontinuity in the duration of the input symbols. It can be seen clearly that the SQR and PQR outperform the DFLL receiver. Similarly, the PQR and SQR receivers outperform the DFLL receiver for the cases of maximum of three and maximum of six random discontinuities. This is depicted in Fig. 3.13. Finally, Fig. 3.14 compares the behavior of the DFLL with that of the SQR for the five test cases. It can be seen clearly, that the SQR outperforms the DFLL receiver with a good margin. As the SNR increases, so does the gap between the curves of the SQR and the DFLL receiver. The same result can be expected when comparing the behavior of the PQR to that of the DFLL receiver, since the PQR's performance is even better than that of the SQR as already shown in Chapter Two.

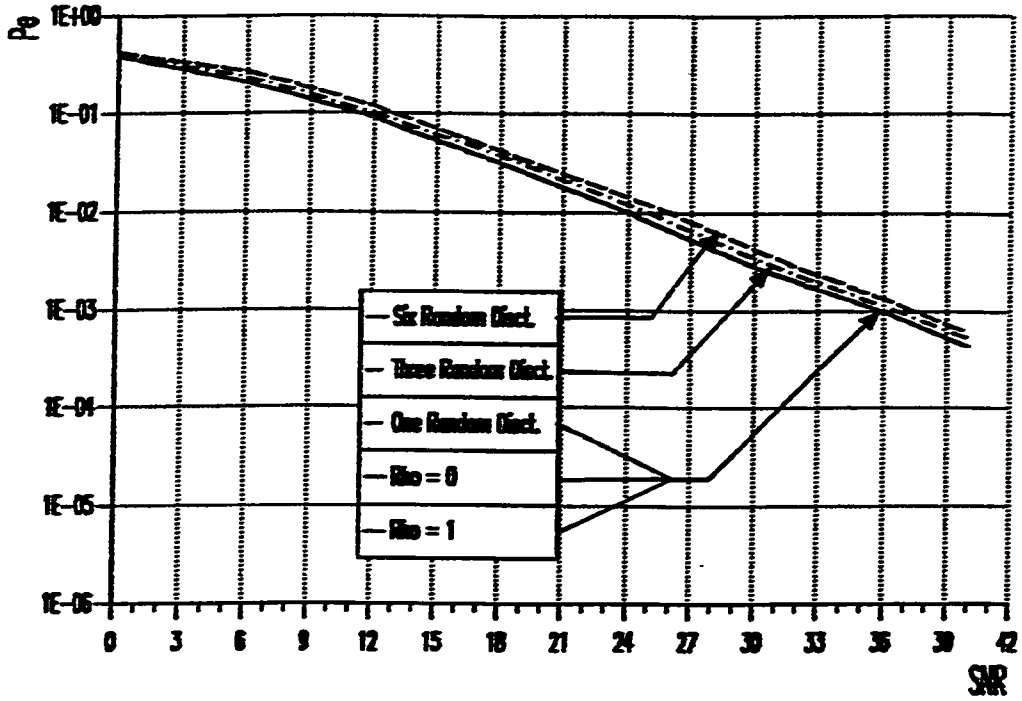


*Figure 3.11*: DFLL Performance for the cases of $\rho = 1$, $\rho = 0$, one, maximum of three and maximum of six, random phase discontinuities, for $M = 2$.

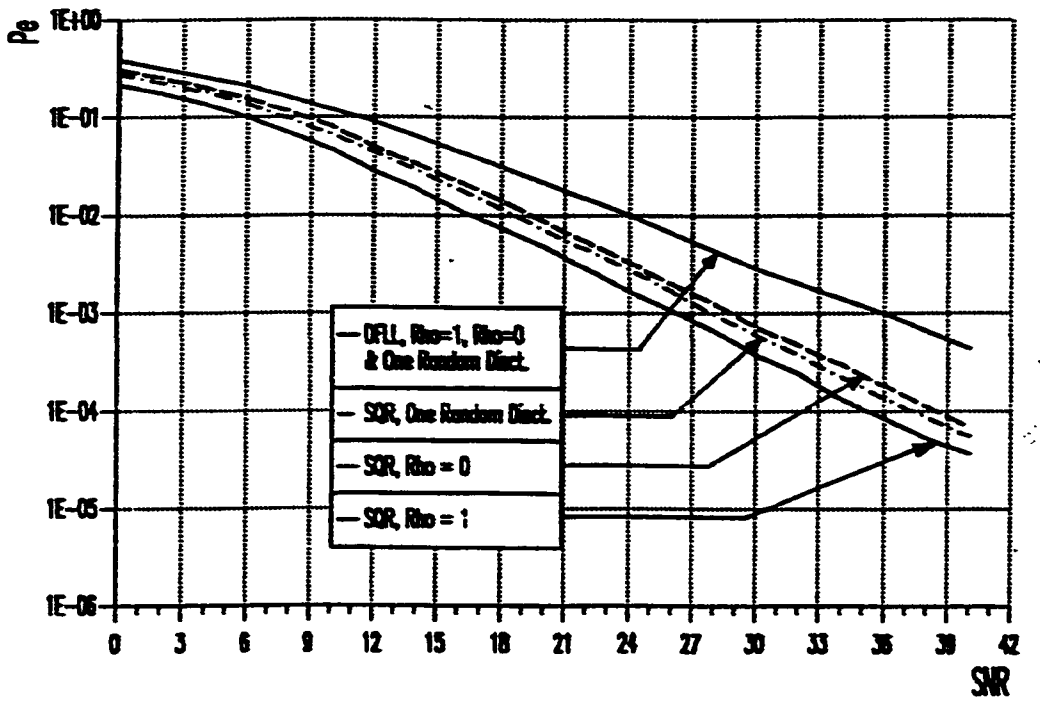


*Figure 3.12:* DFLL Versus SQR Performance for $M = 2$.

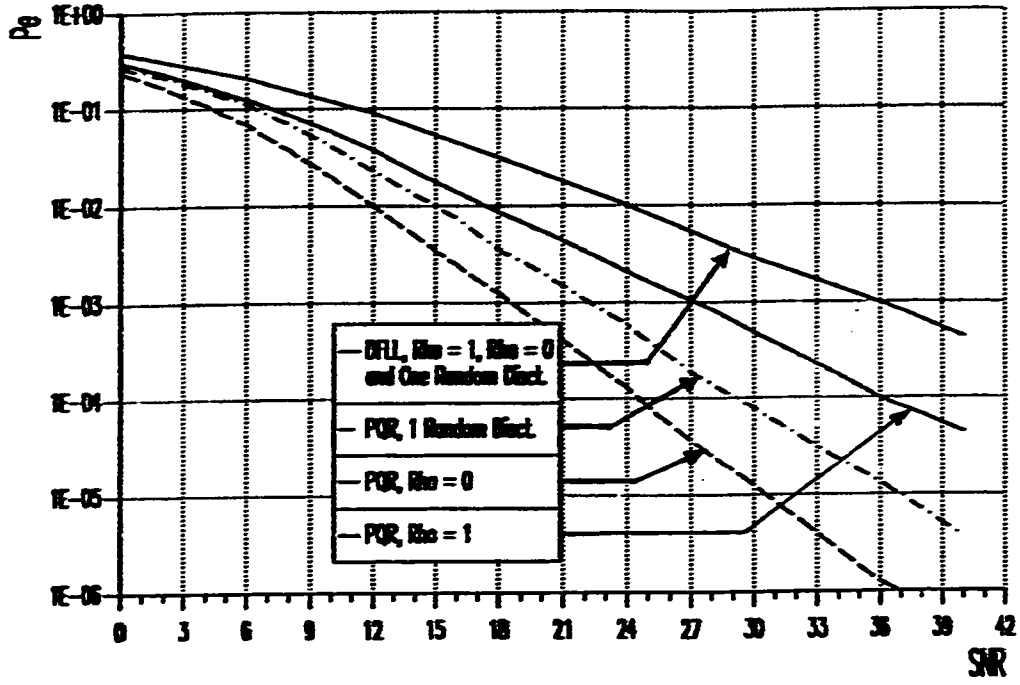


*Figure 3.13*: DFLL Versus PQR Performance for $\rho = 1$, $\rho = 0$, and one random discontinuity, for $M = 2$.

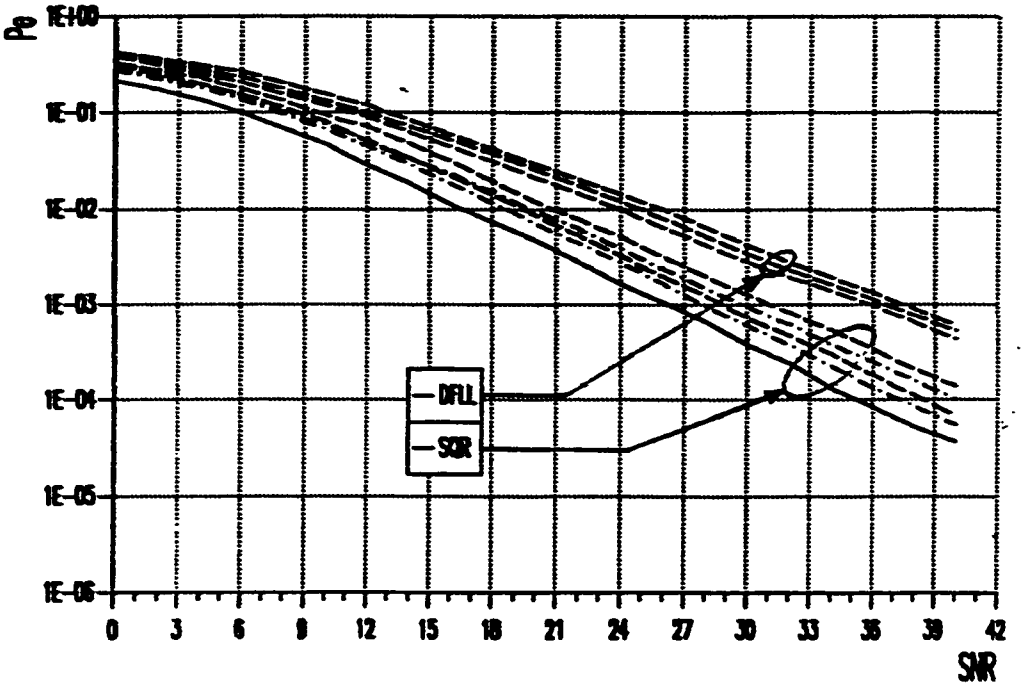


*Figure 3.14*: DFLL Versus SQR Performance, under all the five test cases for $M = 2$.

This poor performance of the DFLL receiver as opposed to the performance of the SQR and PQR receivers, can be explained as follows. The DFLL receiver is much less sensitive to the occurrence of discontinuities in the duration of the received symbols, than the SQR and PQR. However, as the discontinuities take place within the symbol duration, the different loop settings that are suitable for the case of $\rho = 1$ well, might not suit the case of a three or five discontinuities as well. For example, the set of loop gains that is optimum for a certain case, might not be optimum for another case or they might be completely unsuitable for a third case. This is an important factor that must be taken in the design of the DFLL receiver. The loop filter gains have to be adapted to fit different cases. However, since the occurrence of these cases is completely random, the use of certain adaptive algorithms to control the loop filter gains is necessary to improve on the performance of the DFLL receiver. The use of adaptive MEM algorithms in the estimator block of the DFLL receiver might help, also, in improving the performance further. However, this is beyond the scope of this thesis.

One more drawback of the DFLL receiver is the computational complexity. This is because the frequency estimation process, and the updates of different values of the DFLL components, have to take place for every sample of the received signal. This increases the computational complexity to a great extent, and significantly slows down the receiver operation. And, if adaptive MEM and adaptive loop filter gains' algorithms are used, the DFLL receiver will be slowed down even further.

The above observations and results make the current form of the DFLL receiver a poor selection for fast multipath fading channels' reception. Unless the performance of the receiver is enhanced, and the computational complexity is reduced dramatically this receiver cannot be used in practice. Thus, the DFLL receiver was not investigated further for operation in the M-ray signal space.

In all receivers considered (SQR, PQR and DFLL), the sampling rate is fixed. In the DFLL, it is the frequency that is adapted to try track the transmitted frequency. However, we can use the result of [11]. That is if the sampling frequency is four times the estimated frequency, then the error in estimation should be reduced to zero. Thus, it can be sampled at four times its expected value and then be estimated. This way, one can get the best estimate of the frequency. In the next chapter, the effect of varying the sampling rate will be discussed. This will give grounds to proposing the new multisampler receiver.

## 3.6 Summary

In this chapter, the Digital Frequency-Locked Loop (DFLL) receiver was tested under the different fast multipath fading channel cases, that were introduced in chapter two of this thesis. The performance of the DFLL receiver was then compared to that of both the conventional SQR and PQR receivers. The DFLL receiver's performance was poorer than that of the other two receivers. In addition, this receiver is slower in operation, than the other two. These two observations make the DFLL receiver inferior to the SQR and PQR.

In the next chapter, the concept of changing the sampling frequency, instead of adapting to lock to the incoming frequency, will be used to propose a new receiver. The new receiver will be tested under the different fast multipath fading channel cases under which the other receivers were tested. And, the performance of the new receiver will be evaluated and compared with that of the other receivers.

# Chapter IV
# THE NEW MULTISAMPLING-BASED RECEIVER: STUDY AND COMPARISON

## 4.1 Introduction

As processing power is increased, and as signal processing techniques are becoming more advanced and more powerful, new methods for solving and implementing new solutions, are emerging. In this chapter, the results and methods of spectral estimation techniques that were discussed in the previous chapter will be applied to develop a new receiver structure. This new receiver will be focused on overcoming the deficiencies existent in both the Single and Parallel Quadrature receivers, with emphasis on the probability of error, when used in fast multipath fading environments.

As mentioned earlier, the PQR cures the SQR problems with phase discontinuities. However, the solution is limited to the case of known location of occurrence of phase discontinuity. When the discontinuities resulting from a multipath reception take place at locations that are unknown *a priori* to the receiver, the probability of error, $P_e$ curves of the PQR, becomes much higher than in the

case of known locations of occurrence of discontinuities. This deterioration in the performance of the receivers might not be tolerable in many cases.

The main principle which was used to propose and implement both the SQR and PQR receivers is matching. That is if the locations of discontinuities are known, then by matching the correlation and integration times of these receivers, to the times of occurrence of these discontinuities the receivers will give optimum detection results. However, if these times are unknown, both receivers perform poorly.

On the contrary, using methods of spectral estimation techniques, the spectrum is calculated, and the peaks are located from the incoming signal samples. Once the peaks are located, the frequencies are determined and a decision of which frequency, and thus which message was transmitted, is made. However, due to many factors, these decisions are not always accurate. Some of these factors are proper model selection, sampling frequency, and many others.

In orthogonal FSK schemes, only one frequency is transmitted in a symbol duration. And, if we are searching for one pair of spectrum poles (corresponding to one spectrum peak) only, then an MEM, or an ARMA model will be suitable for this purpose. In fact, a second order mode l will be sufficient.

In [10, 11], an equation was formulated, to allow for the calculation of the spectrum peak location, of a second order MEM or ARMA models, without the need to calculate the spectrum throughout the entire frequency band. In addition, it was concluded that if the the sampling frequency of the incoming signal is four times the incoming frequency, then the error in estimating the peaks, is reduced to a minimum, regardless of the of the value of the Signal to Noise

Ratio (SNR). This represents the key issue for the new receiver structure proposed in this thesis. More discussion follows.

## 4.2 Theory of Operation

A new multisampling-based receiver is proposed in this section. It is based on the results found by El-Hennawey and Carter in [11], which were discussed in the previous chapter. It forms the basis to this new receiver.

As discussed earlier, if the received frequency is sampled at four times its magnitude (i.e. $f_s = f_i/4$), and is then estimated using one of the parametric methods (MEM or ARMA) of estimation, then the error in frequency estimation is supposed to be zero. However, due to the limited number of observations, the incoming sampled signal frequency might not be estimated free of error.

Based on the aforementioned facts, the theory of operation of the new Multisampling Based receiver can be stated as follows. If the incoming signal is sampled at four times its true frequency, then the error in estimation will be of less magnitude than if it is sampled at any other rate. Using this difference in error magnitude, the new multisampler receiver is proposed.

Prior to explaining the principle of operation of the multisampler receiver, the error in frequency estimation is modeled, to give a better understanding to the behaviour of the receiver. A binary signaling scheme is used for this error model analysis.

## 4.2.1 Error Model

In the linear region of the curve of Fig. 3.3. of the error in frequency estimation versus the normalized sampling frequency, the error can be described using the following function:

$$f_e = A - kf \quad . \tag{4.1}$$

where $f_e$ is the error in frequency estimation, and $f$ is the frequency being estimated. At $f = f_s/4$, the estimation error is zero ($f_e = 0$). Thus,

$$0 = A - k f_s/4 \quad .$$

which means that,

$$A = k f_s/4 \quad .$$

Thus, the estimation error can be modeled as:

$$f_e = k f_s/4 - kf \quad .$$

in the linear region.

## 4.2.2 Error Analysis

In the following, an analysis of the behavior of the multisampler receiver is included for a binary multisampler receiver. The same analysis can be followed in the case of an M-ary multisampler receiver. Two cases will be discussed for the two branches of the binary NCFSK receiver, which expects to receive one frequency $f_1$ or $f_2$ during one symbol (bit).

***Case 1: A transmitted signal, with $f_r = f_1$***

Assuming that $f_r$ is the received frequency, in Fig. 4.1, we have two samplers $f_{sa}$ and $f_{sb}$, such that

$$f_{sa} = 4f_1$$

$$f_{sb} = 4f_2$$

and,

$$f_1 < f_2$$

where $f_{sa}$ is the sampling frequency in branch "a", and, where $f_{sb}$ is the sampling frequency in branch "b".

In the following, we will analyze the error of the receiver in the two branches, which will be called "a", an "b", to distinguish them from each other.

***Branch "a":***

Since the received frequency is assumed to be $f_1$, then let

$$f_{ra} = f_1,$$

thus,

$$|f_{ea}| = 0.$$

where $f_{ra}$ is the estimated frequency in branch "a", and $|f_{ea}|$ is the magnitude, of the error in branch "a".

***Branch "b":***

$$f_{rb} = f_1 + f_e \quad .$$

thus,

$$|f_{eb}| = f_2 - f_1 + f_e \quad . \tag{4.2}$$

Since,

$$f_e = kf_2 - kf_1$$

$$= k(f_2 - f_1) \quad . \tag{4.3}$$

then,

$$f_{rb} = f_1 + k(f_2 - f_1) \quad .$$

$$= kf_2 + (1 - k)f_1 \quad . \tag{4.4}$$

and since,

$$f_{eb} = f_2 + f_{rb} \quad .$$

then, using Eqn. (4.4), we get:

$$f_{eb} = f_2 - kf_2 - (1 - k)f_1 \quad .$$

$$= (1 - k)f_2 - (1 - k)f_1 \quad .$$

Thus,

$$f_{eb} = (1 - k)(f_2 - f_1) \quad . \tag{4.5}$$

or,

$$|f_{eb}| = (1 - k)f_d \quad . \tag{4.6}$$

where,

$$f_d = |f_2 - f_1| \tag{4.7}$$

Next we will consider the reception of the other frequency.

***Case 2: A transmitted signal, with $f_r = f_2$,***

In Fig. 4.2. the following assumptions hold:

$$f_{sa} = 4f_1,$$

$$f_{sb} = 4f_2,$$

and,

$$f_1 < f_2 \quad ,$$

where $f_{sa}$ is the sampling frequency in branch "a", and $f_{sb}$ is the sampling frequency in branch "b".

Then, analyzing the two branches:

***Branch "a":***

$$f_{ra} = f_2 + f_e',$$

thus,

$$|f_{ea}| = |f_2 - f_1 + f_e| \tag{4.8}$$

where $f_{ea}$ is the estimated frequency in branch "a".

***Branch "b":***

$$f_{rb} = f_2$$

$$|f_{eb}| = 0 \quad .$$

Analyzing the error in the first branch, we get:

$$f_e = kf_1 - kf_2 = k(f_1 - f_2) \quad , \tag{4.9}$$

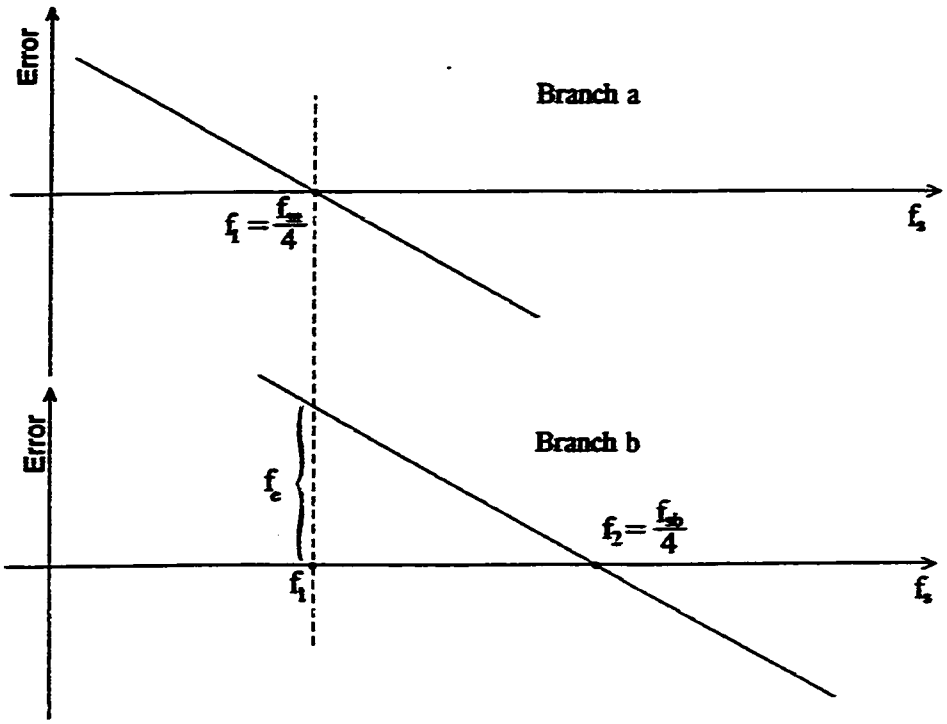


*Figure 4.1*: Case 1: Transmitted Signal with $f_r = f_1$

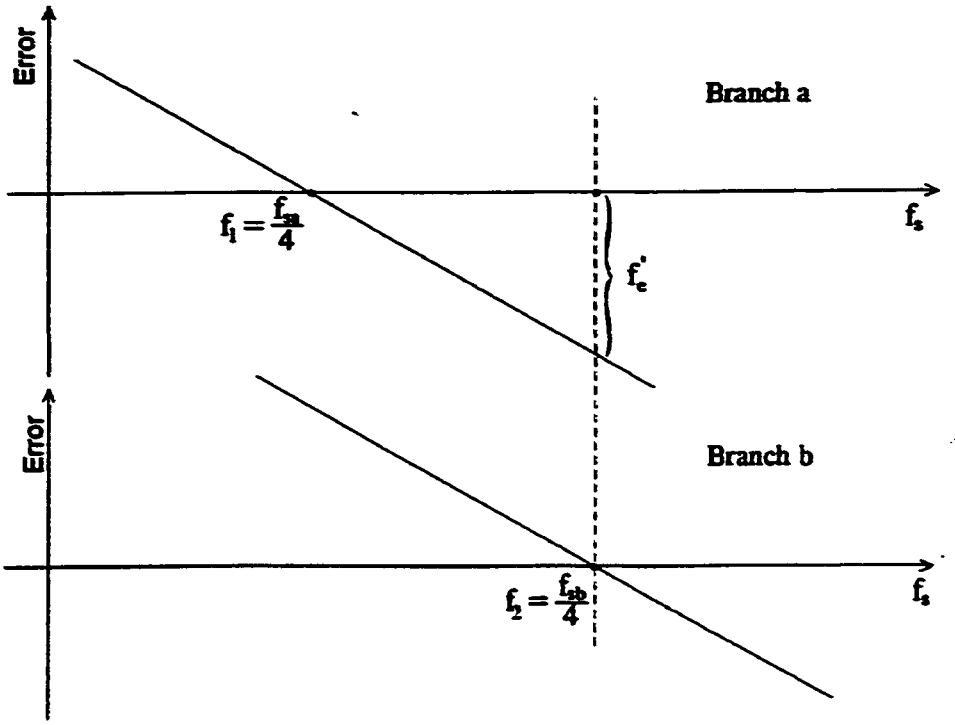


*Figure 4.2*: Case 2: Transmitted Signal with $f_r = f_2$

Form Fig. 4.2, and using Eqn. 4.8, we can conclude that:

$$f_{ra} = f_2 + k(f_1 - f_2) \quad ,$$

$$= (1-k)f_2 + kf_1 \quad . \tag{4.10}$$

Since,

$$f_{ea} = f_1 - f_2 \quad ,$$

then, using Eqn. 4.9, the error in branch "a" can be written as:

$$f_{ea} = f_1 - (1-k)(f_2 - kf_1)$$

$$= (1-k)f_1 - (1-k)f_2$$

$$= (1-k)(f_1 - f_2) \quad , \tag{4.11}$$

or,

$$f_{ea} = -(1-k)(f_2 - f_1) \quad .$$

Thus,

$$|f_{ea}| = (1-k)|f_2 - f_1| \quad .$$

$$= (1-k)f_d \quad . \tag{4.12}$$

From Eqn. 4.6 and Eqn 4.12, it can be seen that the error magnitude in both cases is comparable as the multisampler receiver is used. In summary we can conclude that upon receiving one of the possible two frequencies $f_1$ and $f_2$, the estimation error in one of the branches (a and b), of the receiver will be zero and the other branch will give an estimation error of a value equal to (1-k) $f_d$.

If a signal is received, it is sampled before its spectrum is calculated. As the frequencies used in transmission are supposed to be known *a priori*, the sampling rates can be set to certain values in advance. This means that for each

branch of the receiver, we will have a distinct sampling rate. In conventional receivers, the sampling rate used to be fixed for all the branches in the receiver, where the incoming signal is sampled first, then it is entered in parallel to different branches in the receiver. However, in this new receiver, the incoming signal is entered to the different branches of the receiver at the same time, and is sampled at different rates, in parallel, in each branch. A binary Multisampling-Based parametric receiver, is shown in Fig. 4.3. As can be seen from the figure, the signal is first sampled at a distinct rate in each branch. In the second step, the samples are entered into the parametric estimation block (ARMA). This block is supposed to give an estimate of the frequency content of the incoming signal. This frequency estimate is expected to have a certain error. To be able to decide on the magnitude of error, the estimated frequency is subtracted from the expected frequency of that certain branch (which is equal to one fourth the corresponding sampling frequency). It is this error magnitude that will help the receiver to determine which frequency is transmitted. Ideally, the error magnitude associated with the branch that is sampling the received signal at four times its transmitted frequency is supposed to be zero. However, due to the different practical reasons, associated with a practical receiver, the error will have a certain magnitude that is not equal to zero. It is this error magnitude that will affect the performance of the receiver. The sign of this error is not of importance to the receiver. In order to be able to compare the error magnitudes to each other, we need to first take the absolute value of the differences resulting from the subtracters. Finally, the error magnitudes are entered into a decision device which will decide in favor of the branch that has the smallest error magnitude.

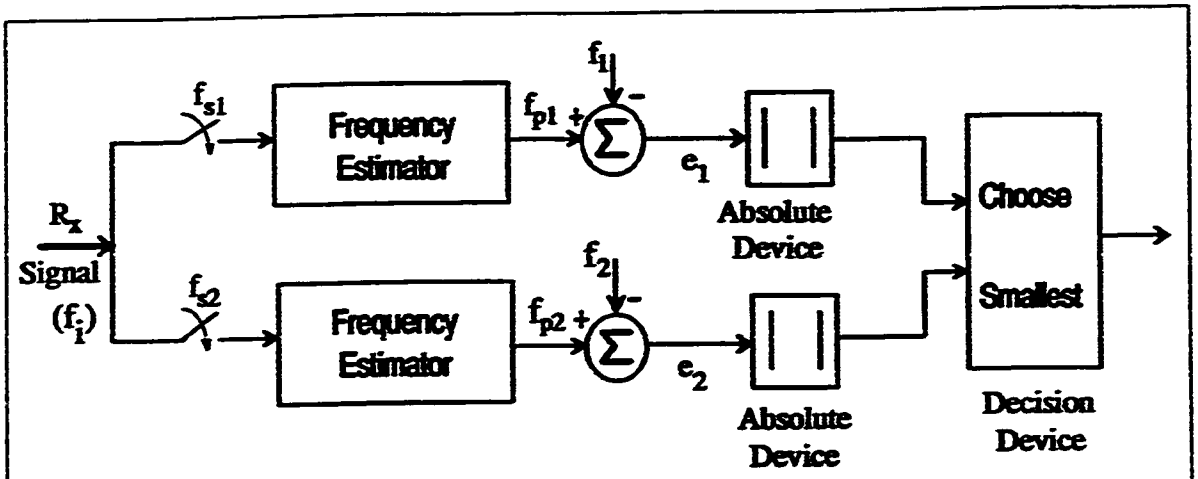


*Figure 4.3:* The New Multisampler Receiver for Binary Transmission.

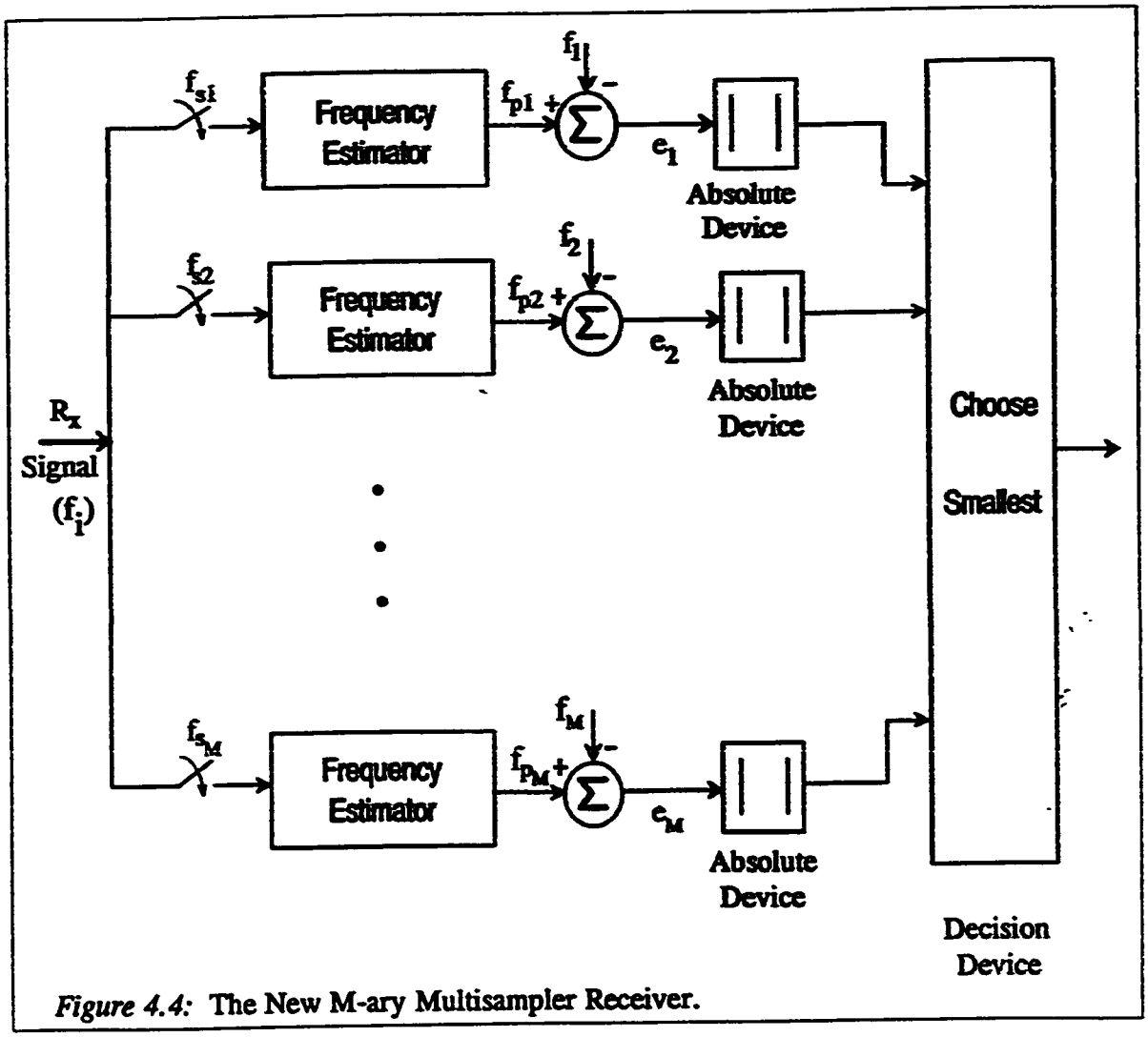


*Figure 4.4:* The New M-ary Multisampler Receiver.

The receiver can be extended to accommodate M-ary FSK Signaling for higher transmission rates. An M-ary Multisampling-Based receiver is shown in Fig. 4.4. Again, the same principle is applied in this figure. The number of branches that are existent in the receiver, is equal to the number of messages (frequencies) in the transmitted signal space.

## 4.3 Simulation of the New Receiver

In this section, a simulation of the new multisampler receiver, is carried out. Then, a study of its performance under the same cases mentioned in Chapter two, is presented.

### 4.3.1 Simulation Steps:

In order to evaluate the performance of the new multisampler receiver, and to find out how it compares to the conventional SQR, and PQR receivers, a computer simulation was performed for the binary signaling scheme. It was then extended to cover the M-ary signaling scheme.

A FORTRAN computer program was developed to simulate the behavior of the new multisampler FSK receiver proposed in this thesis. The simulation program was carried on the same IBM 3090 digital mainframe computer system that the earlier simulations for the conventional receivers, were carried on. In the following are the steps of the program (see Appendix A):

1. Generate the frequencies that are to be used in the simulation. This is a frequency shift keying receiver which means that the dimension of the signal space will be equal to the number of messages that are in the signal space; that is:

$$M = N$$

where M is the number of messages in the signal space of transmission and N is the dimension of the signal space. The same frequencies and the same center frequency that were used to simulate the behavior of the SQR, and PQR, are used here. That is, the center frequency $f_c$ was set to 75 Hz, and the bandwidth $2\delta f$ was set to 6 Hz.

2. A pseudo random message sequence is generated using a pseudo random sequence generator (V.32). This message sequence is exactly the same sequence that was used with the SQR, and the PQR receivers' testing program.

3. Generate a Rayleigh distributed amplitude sequence that serves as the amplitude of the received signal as a result of the multipath signal reception. This sequence is also the same sequence used in the simulation of the behavior of the SQR and PQR receivers.

4. Then, a phase discontinuities sequence is generated to be applied with a uniformly random distribution to the messages, to simulate a multipath reception. The number of discontinuities per symbol duration is applied randomly, and the phase shift is randomly distributed.

5. Next, the messages are corrupted with noise. They are sampled at a certain sampling rate (that depends on the specific branch in which they

are entered; i.e. $4f_1$, $4f_2$, $4f_3$, ... etc.). The noise is Gaussian distributed with zero mean and a power spectral density of $N_o/2$. The power spectral density is dependent on the signal to noise ratio (SNR), that is applied at that certain instance. Again, the noise sequence is exactly the same as that was applied to the SQR, and PQR receivers, earlier.

6. At this stage, the channel response has been simulated, and the received signal is being obtained. The signal's samples are generated, the noise values are added, and the phase shifts with their respective amplitudes are added randomly, according to the sequences at an earlier stage. This gives the received signal its final sample values, according to the specific branch of the receiver, in which they are entered.

7. The frequency of the incoming signal is estimated in each branch. The signal samples in each branch are entered in the parametric estimator block, at this point. The peak frequency is calculated, in this block, using Eqn. 3.11 which was developed by El-Hennawey, and Carter in [10, 11]. The estimated-peak frequency ($f_{r1}$ and $f_{r2}$ ... etc.), are the actual values, and not the normalized ones.

8. After that, the expected branch's frequency ( $f_c = f_s/4$), is subtracted from the estimated peak frequency that was output from the parametric (ARMA) estimator block. This is done in order to find the error in frequency estimation of that branch.

9. Since the error magnitude is the important factor that will decide which branch has the correct estimation, the difference of each branch is entered into an absolute value block. Ideally, the branch that has sam-

pled the incoming signal at four times its true transmitted frequency, is supposed to have an error magnitude of zero. However, due to the existence of the Rayliegh distributed amplitudes, of the different segments in the symbol duration, and the other factors of a practical receiver, the error magnitude of the branch that is sampling the incoming signal at four times its true frequency should have the lowest error magnitude.

10. Using the critereon of the previous step, the differences in magnitude of error of all the branches of the receiver are entered in the decision device. The frequency of the branch that has the lowest error magnitude will be chosen as the transmitted frequency. This decision is then compared with the true transmitted frequency, to determine the rectitude of the receiver's decision. This process is repeated for a large number of times (about 100,000 times per SNR) to be able to draw an idea about the probability of error of this receiver for a certain signal space, and the behavior of the receiver under such circumstances.

This new receiver was simulated following the previous steps. A binary signaling scheme was used first to simulate Fig. 4.3. A center frequency of 75 Hz was used, with a bandwidth of 6 Hz. The same sequence generators that were used to test the SQR and PQR are used here. This is done in order to use, exactly, the same input to test all the receivers. This is done for comparison purposes, between the SQR, PQR, and the new multisampler receiver.

Figure 4.5, shows the behavior of the new multisampler receiver, for binary signaling scheme. The two cases of no discontinuity ( $\rho = 1$), and one fixed dis-

continuity in the middle ( $\rho = 0$), are simulated. As can be seen from Fig. 4.6, the new receiver behaves much better in the case of one fixed discontinuity in the middle than in the case of no discontinuity. It can be noticed that this is the same behavior as the PQR receiver.

### 4.3.2 A Study of the New Multisampler Receiver

The new multisampler receiver will be studied under different circumstances. These circumstances will be exactly those under which both the SQR, and the PQR receivers were tested. As a matter of fact, and for the sake of comparison purposes, the same samples that were used with the SQR, and the PQR will be used with the new multisampler receiver. Moreover, the testing will be extended to cover the M-ary signaling scheme.

Following the same steps that were listed in the last subsection, the study is applied to the new M-ary multisampler receiver. Fig. 4.6, shows the behavior of the new receiver in the M-ary case, as the signals are applied to receiver with no discontinuities (i.e. $\rho = 1$). It can be seen that as M increases, the probability of error $P_e$ increases. Similarly, Fig. 4.7, depicts the performance of the new receiver for the case of one phase discontinuity positioned in the middle of the symbol duration. As with the earlier case, $P_e$ increases as M increases. This is an expected result. However, it can be noticed that for M = 16, the $P_e$ increases at a higher rate than with the case of M = 2, 4, or 8.

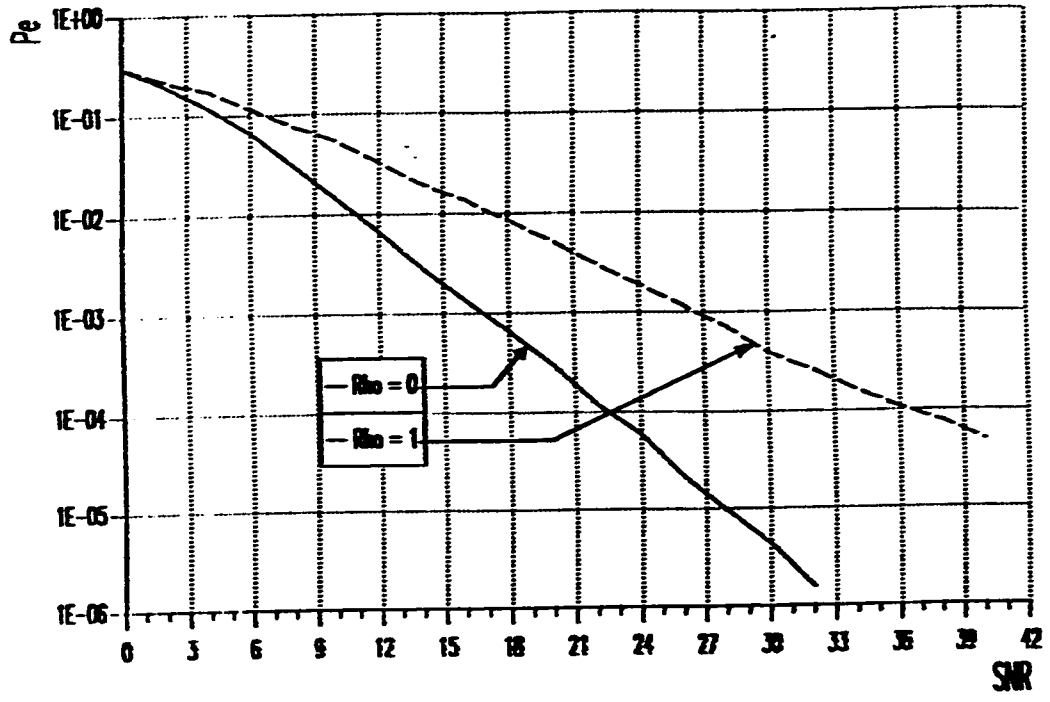


*Figure 4.5*: The Multisampler Receiver Performance for M = 2, for ρ = 1, and ρ = 0.

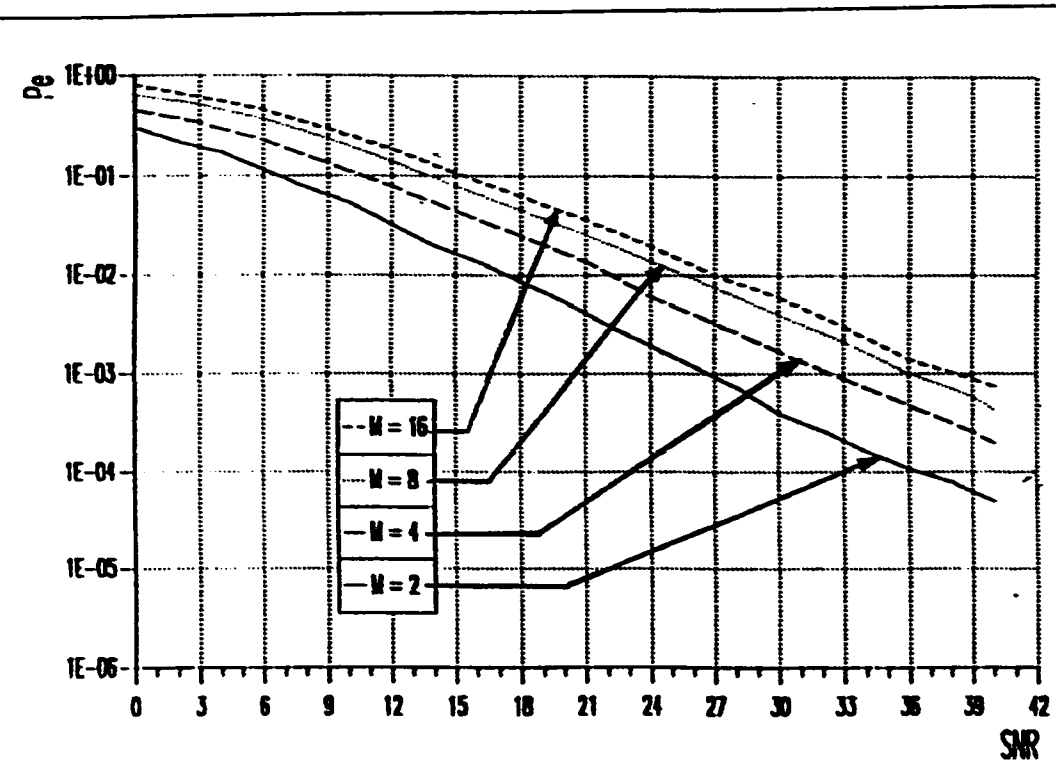


*Figure 4.6*: The Multisampler Receiver Performance for M = 2, 4, 8, 16, for ρ = 1.

In order to be able to compare the behavior of the new receiver in the M-ary signaling space to each other, for both cases $\rho=0$ and $\rho=1$, the $P_e$ curves are joined. This is shown in Fig. 4.8. As one can see, the behavior of the new receiver, for the case of one fixed phase discontinuity being embedded in the middle of the symbol duration in the received signal ( $\rho=0$), is much better than the case of no phase discontinuities ( $\rho=1$). Nevertheless, it can be seen that both curves of the two cases (for the same M) begin at the same values for SNR = 0. Then, the gap between the two respective curves, begins to widen as the SNR increases.

As mentioned in Chapter One, the case of one phase discontinuity taking place in the middle of the symbol duration exactly, is somewhat very rare. On the other hand, it is more likely that the discontinuity will take place at random locations within the symbol duration. Moreover, it is more likely that a varying number of phase discontinuities will take place in the symbol duration or nothing at all might happen in the symbol duration. That is the frequency of occurrence of the phase discontinuities is random. These situations are tested for the new receiver. Again, the same samples that were used earlier to test the SQR, and the PQR are used to test the new receiver.

In figures 4.9 to 4.12, the results of the three additional tests are shown as well as the results from the two original tests ( $\rho=0$, and $\rho=1$). These three additional tests are for the following cases: one randomly located phase discontinuity within the symbol duration, a maximum of three randomly located phase discontinuities, within the symbol duration, and a maximum of six randomly located phase discontinuities within the symbol duration. In the last two cases,

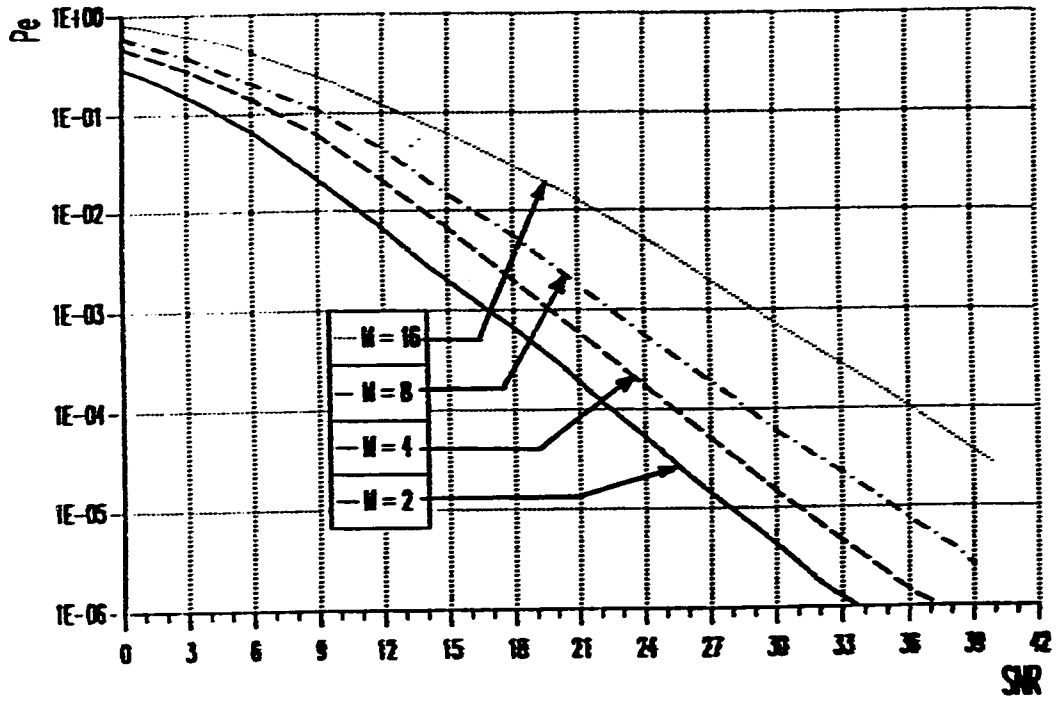


*Figure 4.7*: The Multisampler Receiver Performance for M = 2, 4, 8, 16, for ρ = 0.

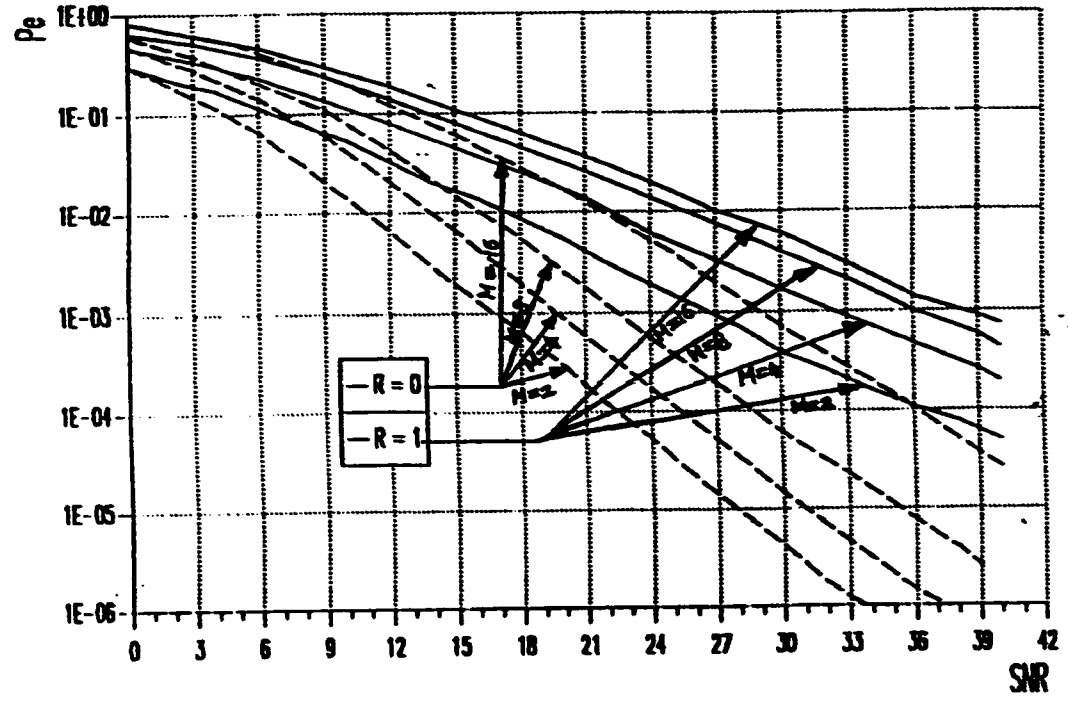


*Figure 4.8*: The Multisampler Receiver Performance for ρ = 1 Versus ρ =0.

the number of discontinuities is varied in the successive symbols, according to a random distribution. These cases are the same as those ones introduced in Chapter 2 of this thesis.

Fig. 4.9, depicts the behavior of the new receiver for binary signaling scheme (M = 2), for the five cases. The receiver is seen to behave the best for the case of the occurrence of one phase discontinuity, which is confined to take place at the middle of the symbol duration. Moreover, it can be seen that when the phase discontinuity takes place at a random location within the symbol duration (and not necessarily in the middle), the performance of the receiver is degraded. Nevertheless, it is still better than the performance when there is no phase discontinuity ( $\rho = 1$). The $P_e$ curve is higher in the case of a maximum of three random discontinuities, than in the case of one (fixed and random) discontinuity. It is even higher in the case of a maximum of six random discontinuities, than in the case of a a maximum of three random discontinuities. However, one can see that the highest of these curves, is that of the case of no phase discontinuities within the symbol duration ($\rho = 1$).

Similarly, Fig. 4.10, Fig. 4.11 and Fig. 4.12 show the behavior of the new receiver for the same (five) cases, for M = 4, M = 8, and M = 16, respectively. It can be seen in Fig. 4.10, that when M = 4, the best behavior of the five cases takes place also when there is one fixed discontinuity in the middle of the symbol duration $\rho = 0$. The performance is degraded when the discontinuity is not fixed to the middle of the symbol duration. It is even more degraded as the frequency of random occurrences of discontinuities in the symbol duration is increased, to a maximum of three or six. The performance of the receiver, is the

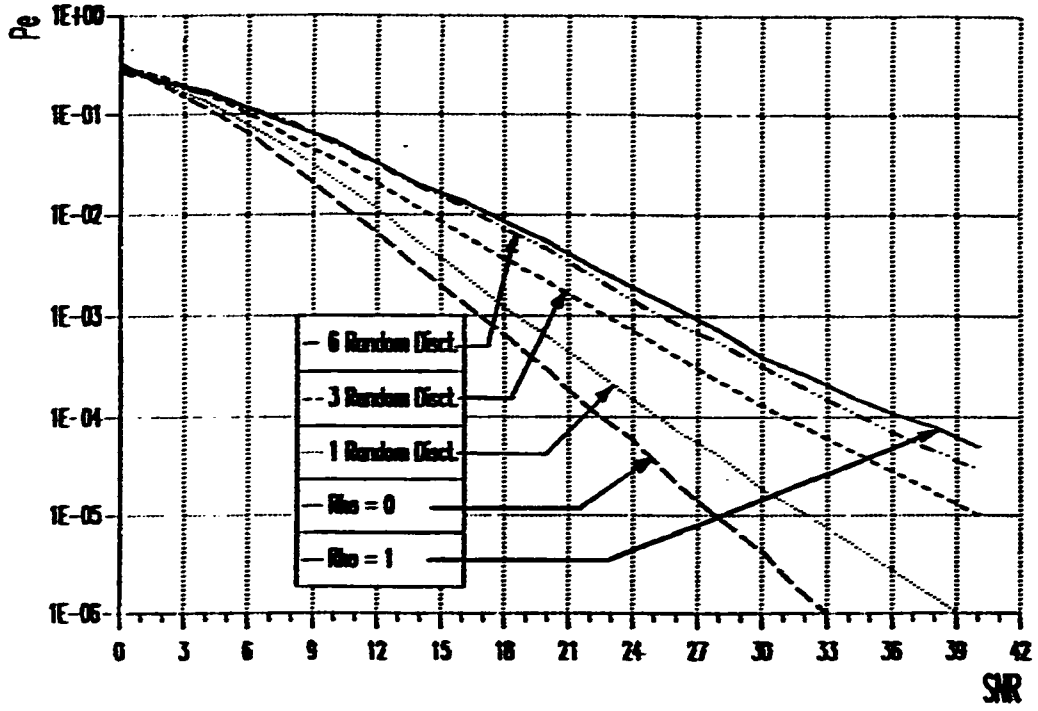


*Figure 4.9*: The Multisampler Receiver Performance for the five test cases for M = 2.

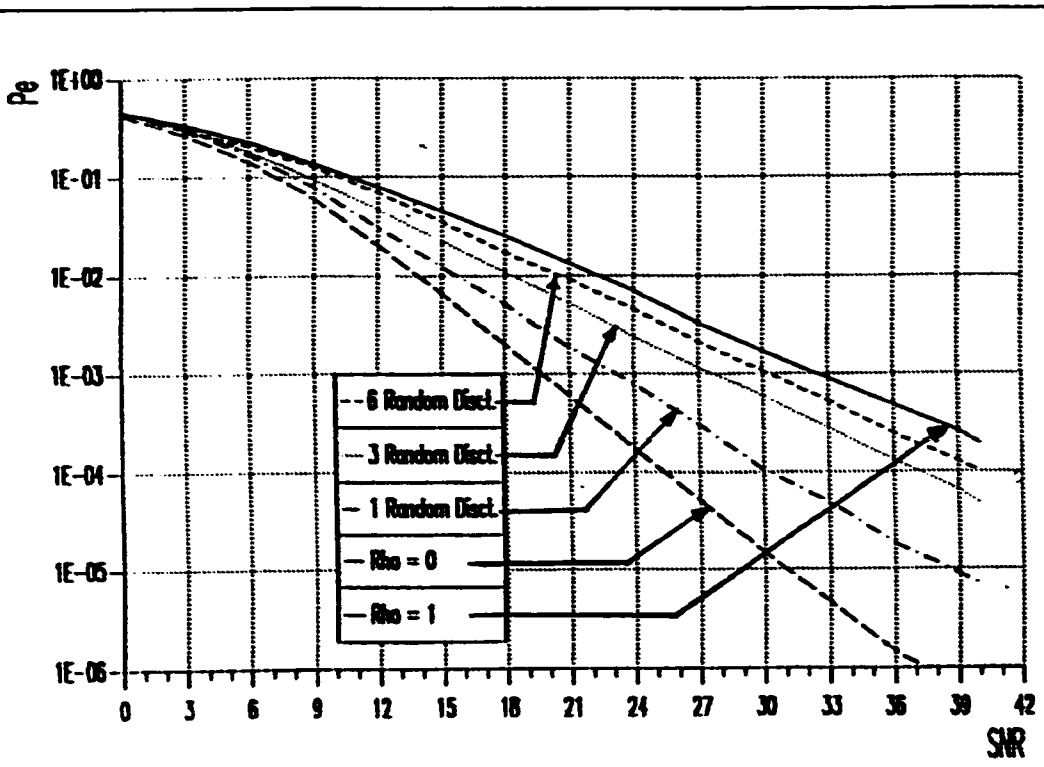


*Figure 4.10*: The Multisampler Receiver Performance for the five test cases for M = 4.

worst in the case of no occurrence of any discontinuities in the symbol duration which is even worse than the case of occurrence of a maximum of six discontinuities within the symbol duration.

The performance of the receiver is degraded further for M = 8, and M = 16, as can be seen in Fig. 4.11, and Fig. 4.12. respectively. Although the performance of the receiver remains, basically, in the same order as in the two previous signal schemes, one can notice that the performance of the receiver is worse in the case of maximum of six discontinuities than in the case of no discontinuity ($\rho = 1$), for M = 8 and also for M = 16.

From the above figures, and results, one can deduce that the performance of the receiver, is not only degraded as M is increased, but also, as the number of random phase discontinuities in the symbol duration is increased.

## 4.4 Comparison of the New Receiver with the Conventional SQR and PQR Receivers

As the new multisampler receiver is based on parametric methods of spectral estimation, it is expected to be less affected by phase discontinuities [10], than the conventional recivers. However, the fact that different segments within the symbol duration, have different amplitudes, implies that the accuracy of estimation might not be as good as the estimation of a constant amplitude series of samples (corrupted with noise).

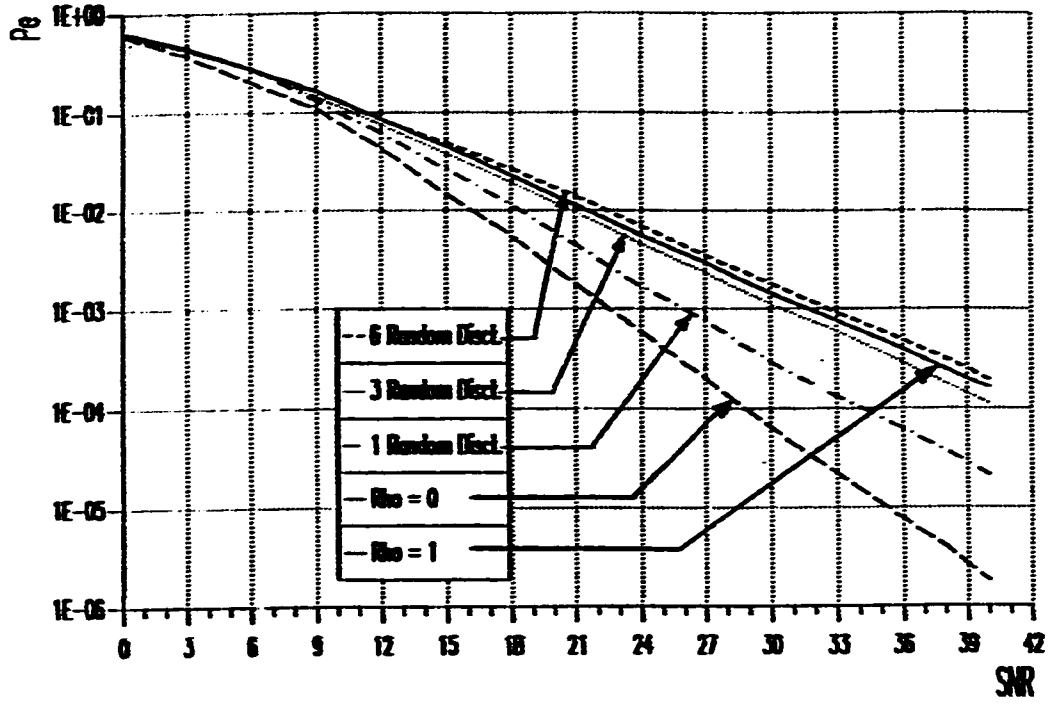


*Figure 4.11*: The Multisampler Receiver Performance for the five test cases for M = 8.

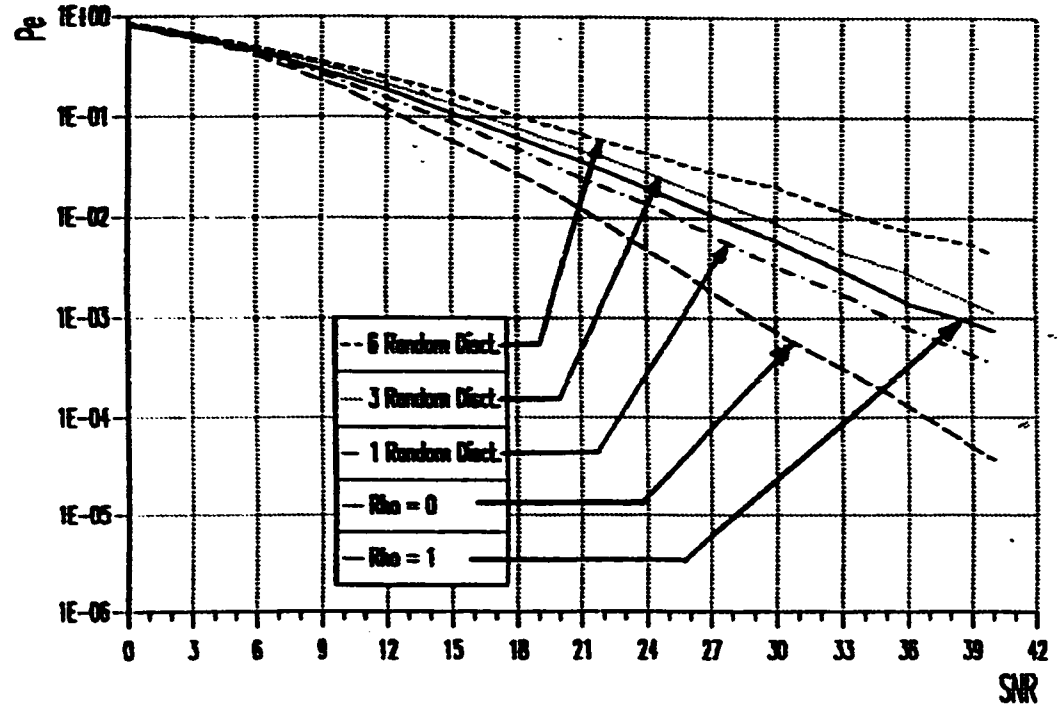


*Figure 4.12*: The Multisampler Receiver Performance for the five test cases for M = 16.

For performance evaluation, and for comparison purposes, the tests done on the new receiver for the five cases are compared to the results and performance figures that were depicted in Chapter Two of this thesis.

Figure 4.13, shows a comparison between the SQR receiver, and the new multisampler receiver, for the binary signaling scheme (M=2), with no pahse discontinuities existent in the symbol duration ( $\rho=1$). It can be seen that the single quadrature receiver behaves slightly better than the new receiver, for this case. The difference can be estimated to be 1 dB, at any SNR. Fig. 4.14, shows a comparison between the SQR, and the new receiver for the case of one fixed phase discontinuity in the middle of the symbol duration ( $\rho=0$), for binary signaling space (M=2). For this case, the new receiver behaves significantly better than the SQR. As a matter of fact, for $P_e = 10^{-4}$, there is a 14 dB enhancement in performance, between the two receivers.

Fig. 4.15, combines the SQR, PQR, and the new receiver perfomances, in the binary signaling space (M=2). This is done for both cases of $\rho=1$ and $\rho=0$, again. It can be seen that the SQR outperforms both receivers with a small margin for the $\rho=1$ case. This is an expected result, since the SQR is optimized for this particular situation. Nevertheless, it can be noticed that the difference in performance for the three receivers is insignificant.

Once a phase discontinuity resulting from a multipath reception is applied, the performance of the receivers changes completely. Fig. 4.16 shows the performance of the new receiver as opposed to the two conventional recievrs for $\rho=0$, for binary (M=2) signal space transmission. As was depicted earlier, the PQR performance is much better than the SQR. And, the new receiver is, also,

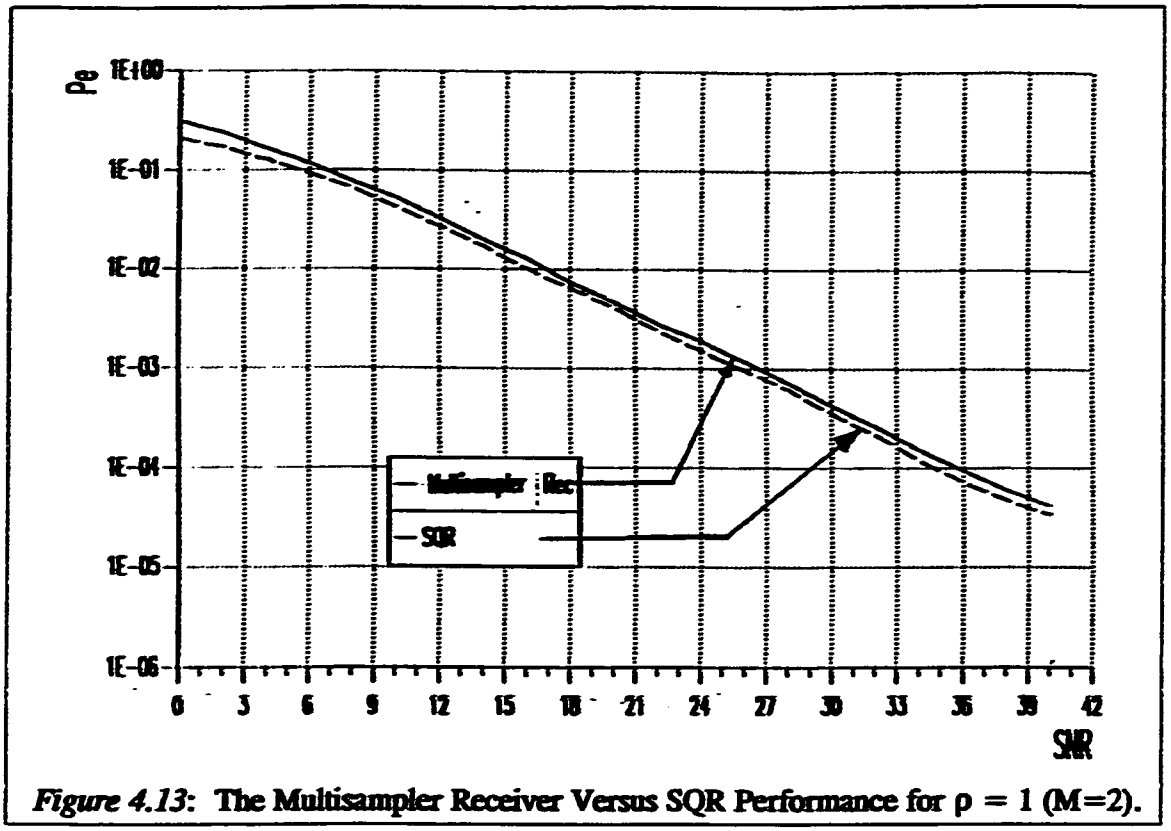


*Figure 4.13*: The Multisampler Receiver Versus SQR Performance for $\rho = 1$ (M=2).

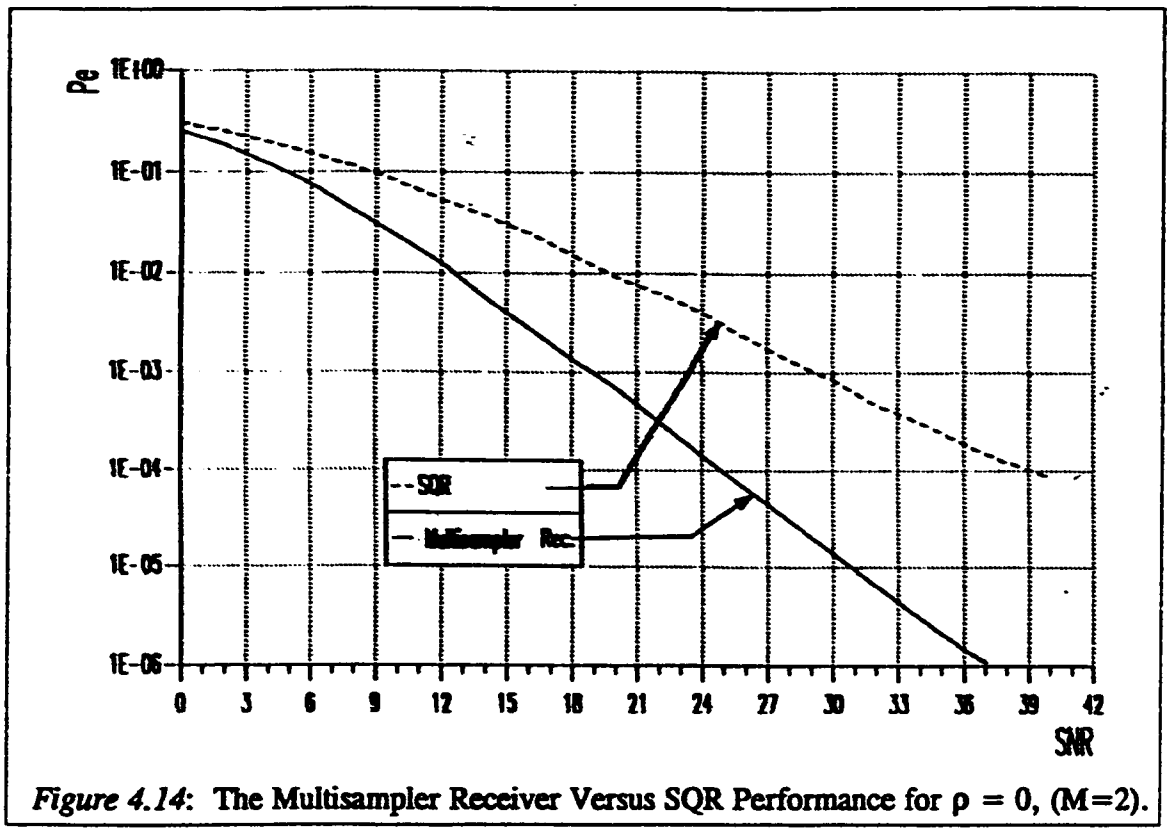


*Figure 4.14*: The Multisampler Receiver Versus SQR Performance for $\rho = 0$, (M=2).

better than the SQR for this situation. However, the PQR is still the best performer for this kind of test. The performance of the PQR is slightly (1 dB) better than the new receiver in such a test. This result, again, is expected, since the PQR is optimized for this particular case.

The previous tests were extended to the M-ary case. The same conclusions drawn when comparing the new receiver with the SQR and PQR for binary signaling (M=2) are also obtained for the M-ary signaling. This is quite illustrated in Figures 4.17 through 4.20.

As the receivers are tested under different cases, their behaviors change. The performance of the two conventional receivers and the new multisampler receiver are next compared to each other for the three new realistic cases proposed in this thesis.

As the performance of the three receivers is compared, one can see the superiority of the new receiver to the two conventional receivers tested earlier, under these new circumstances. As can be seen in Fig. 4.21, the new receiver outperforms significantly both the SQR, and the PQR, for the case of one random phase discontinuity in the symbol duration, in the binary signaling space (M = 2). In this particular case, the new receiver has an advantage of about 12 dB and 6 dB over the SQR and PQR, respectively, for $P_e = 10^{-4}$. In addition, the new receiver outperforms significantly the two conventional receivers, for the two cases of a maximum of three and six random discontinuities, as can be seen in Fig. 4.22, and Fig. 4.23, respectively, for M = 2. As can be noticed from Fig. 4.21, Fig. 4.22, and Fig. 4.23, the enhancement in performance is reduced as the number of discontinuities within the symbol duration, is increased from one to

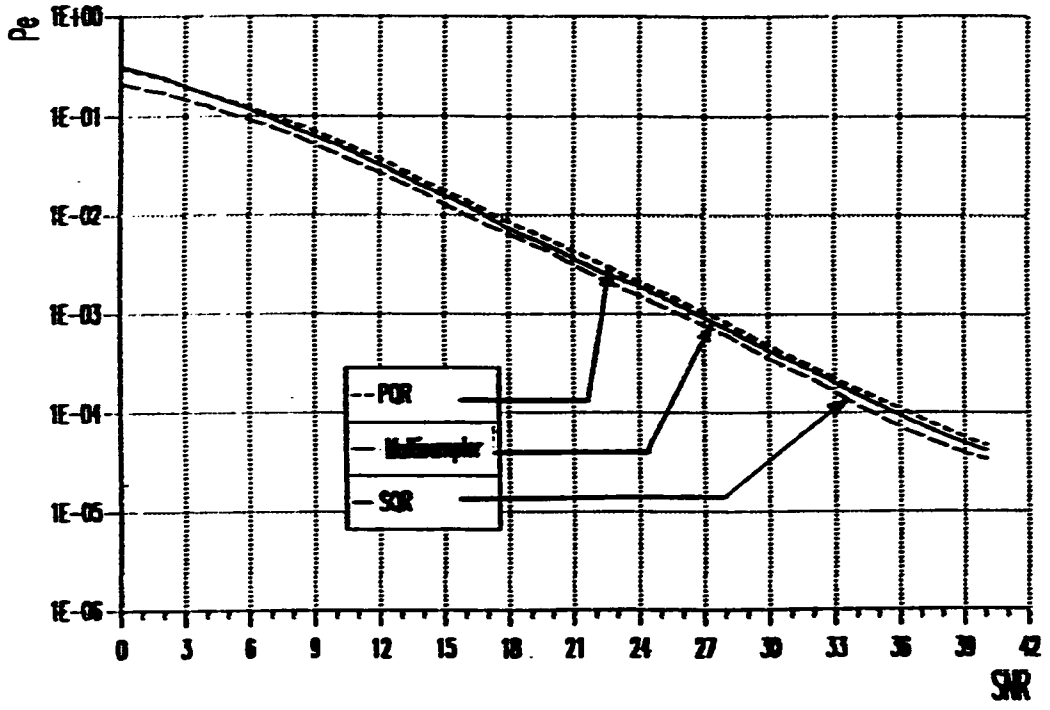


*Figure 4.15*: The Multisampler Receiver Versus SQR and PQR Performance for $\rho = 1$ (M=2).

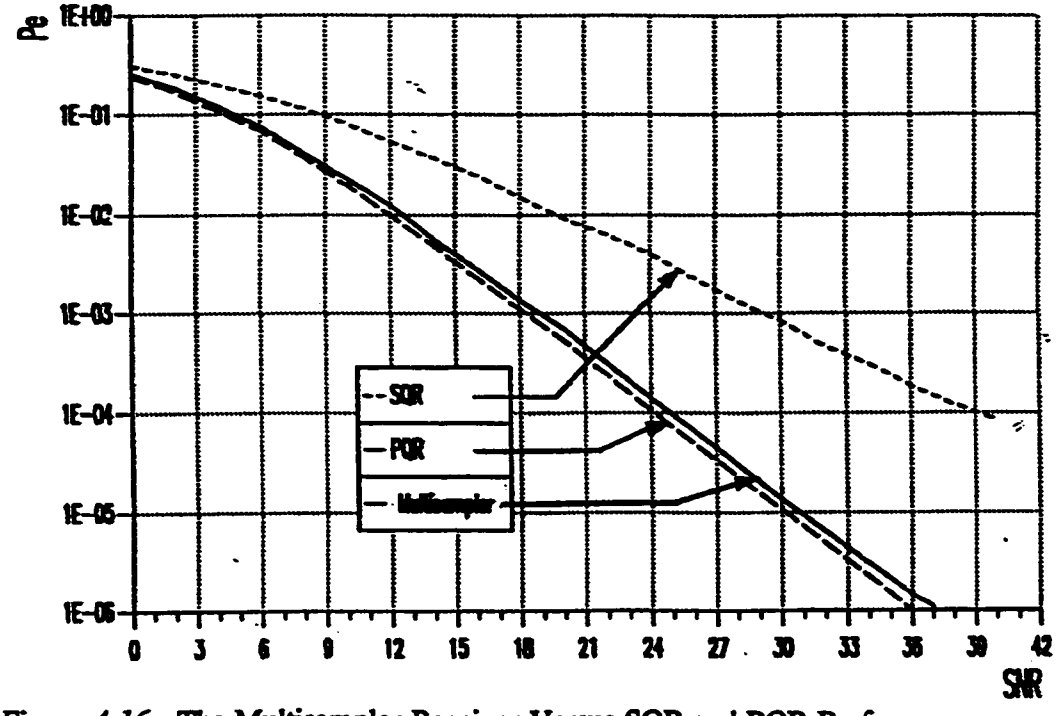


*Figure 4.16*: The Multisampler Receiver Versus SQR and PQR Performance for $\rho = 0$, (M=2).

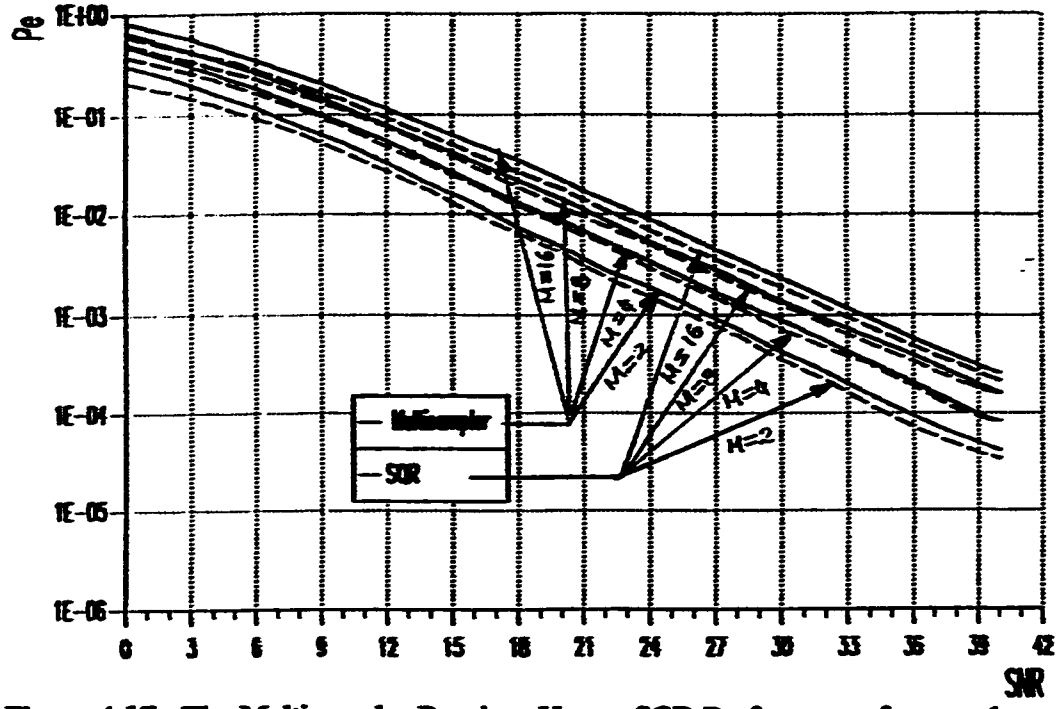


*Figure 4.17*: The Multisampler Receiver Versus SQR Performance for $\rho = 1$ (M=2, 4, 8, 16).

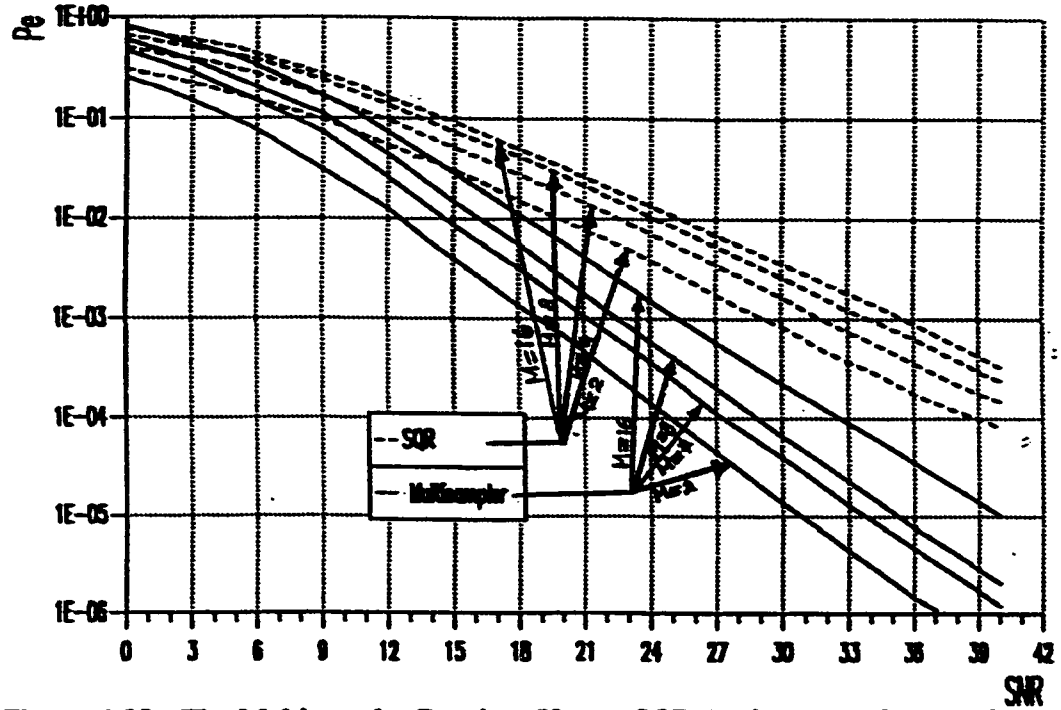


*Figure 4.18*: The Multisampler Receiver Versus SQR Performance for $\rho = 0$ (M=2, 4, 8, 16).

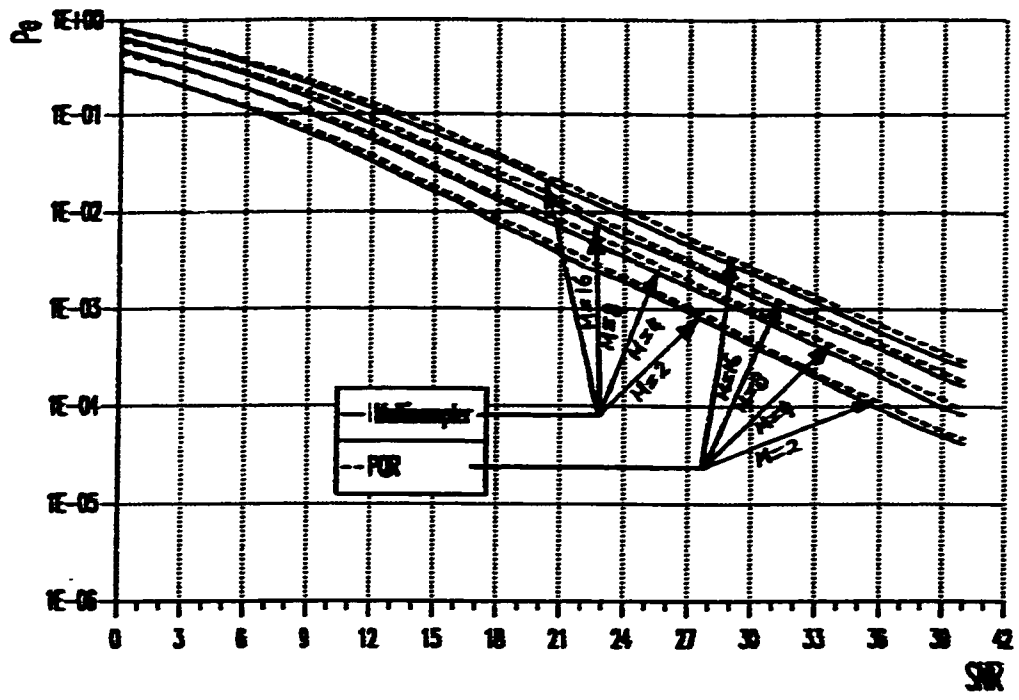


*Figure 4.19*: The Multisampler Receiver Versus PQR Performance for $\rho = 1$ (M=2, 4, 8, 16).

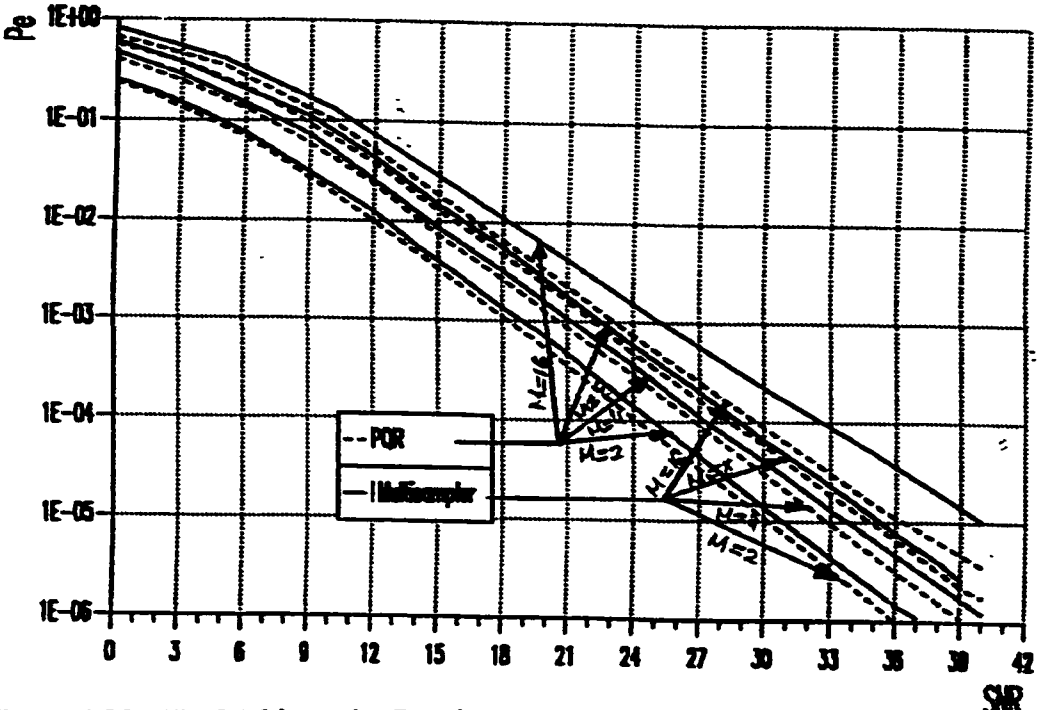


*Figure 4.20*: The Multisampler Receiver Versus PQR Performance for $\rho = 0$ (M=2, 4, 8, 16).

six. This can be related to the fact that for a certain ratio of the total number of symbols in the transmitted sequence, in the last two tests (maximum of three and six discontinuities in the symbol duration), the tests will reduce to the first two tests ($\rho=1$, and $\rho=0$). This is because the distribution of the number of discontinuities was implemented with a uniform distribution. This means that about 14% to 30% of the total number of received symbols, in these two tests, will be one of the first two tests ($\rho=1$, or $\rho=0$).

Fig. 4.24 through Fig. 4.29 generalize the comparison between the new receiver, the SQR and the PQR receivers to the M-ary signal space for the three new cases. As with the binary case, the new receiver outperformed, significantly, both the SQR and the PQR.

Quantitative comparisons between the new multisampler receiver, the SQR and the PQR are presented in Tables 4.1 through 4.4. In these tables, the probabilty of error value is fixed to $P_e=10^{-4}$, and the SNR values are compared, for each of the three receivers. While Table 4.1 compares the new multisampler receiver to ver to t the SQR and PQR for M = 2, Table 4.2 compares the same receivers to each other but M = 4. Similarly, Tables 4.3 and 4.4 compare the same receivers to each other for M = 8, and M = 16, respectively. These tables confirm what has been mentioned before about the behavior of these receivers.

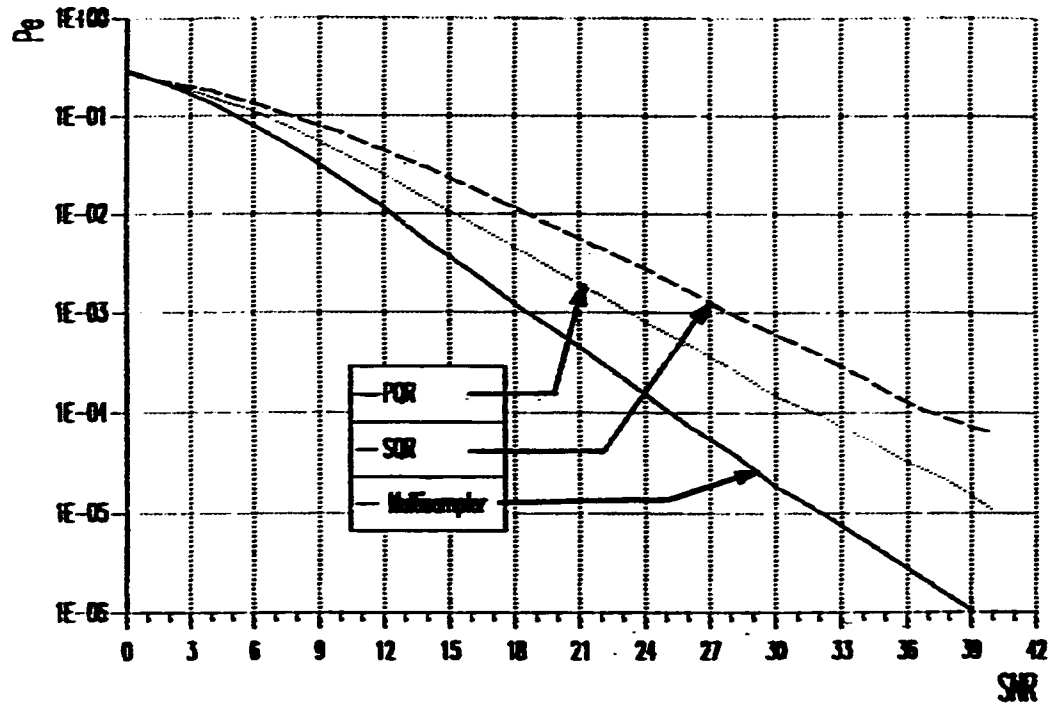


*Figure 4.21*: The Multisampler Receiver Versus SQR and PQR Performance for the case of one random discontinuity, (M=2).

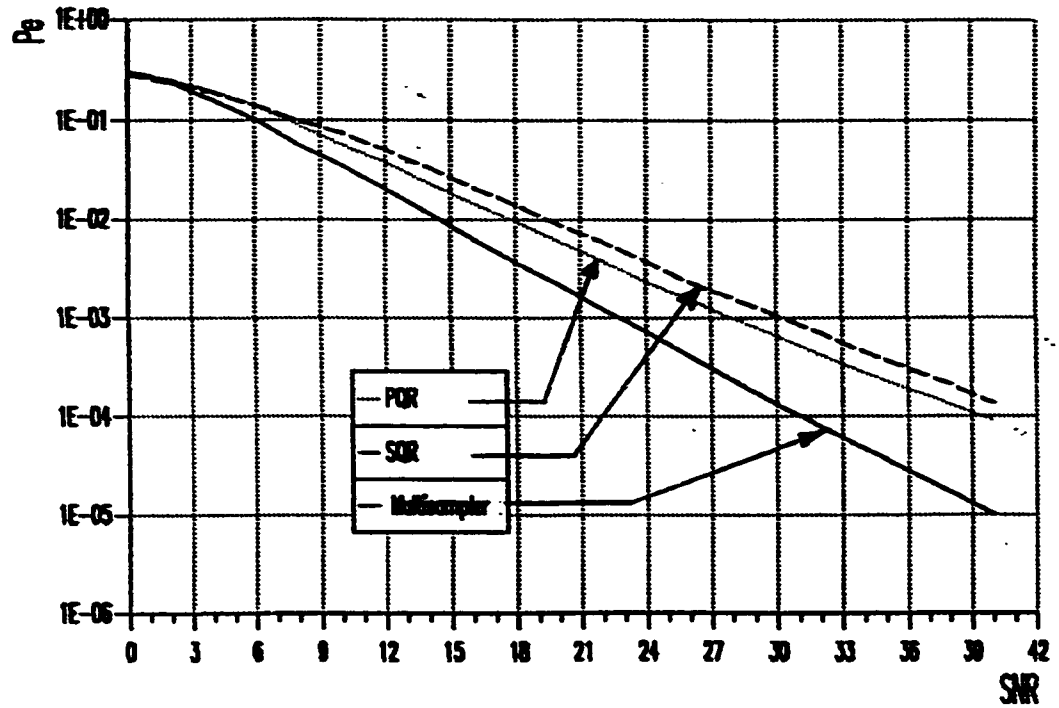


*Figure 4.22*: The Multisampler Receiver Versus SQR and PQR Performance for the case of maximum of three random discontinuities, (M=2).

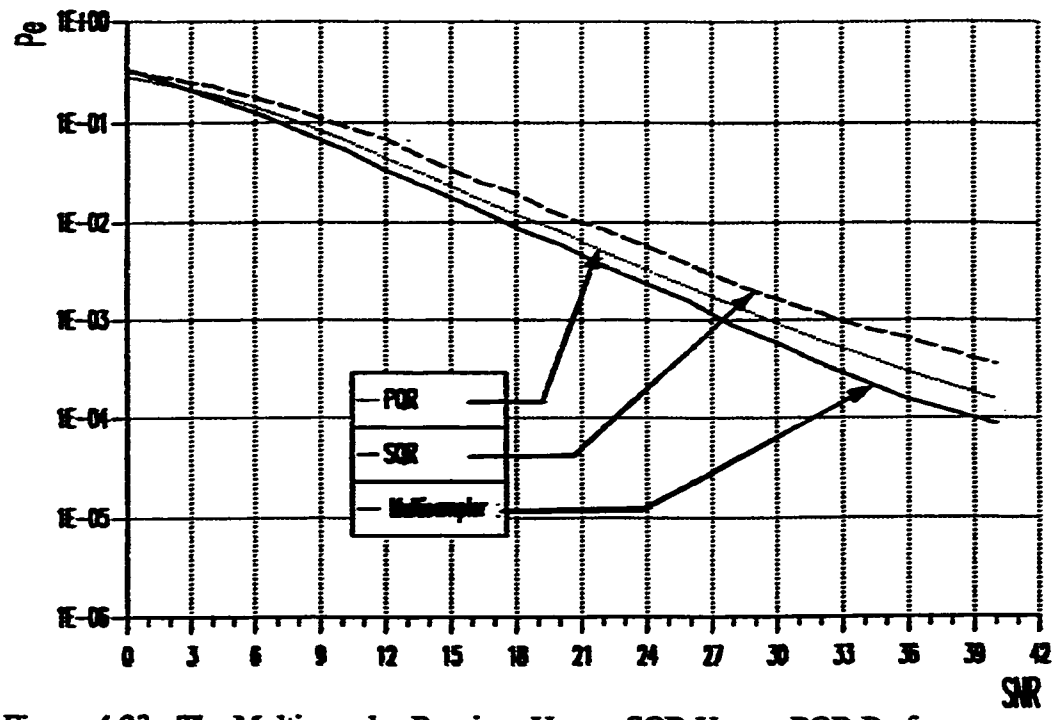


*Figure 4.23*: The Multisampler Receiver Versus SQR Versus PQR Performance for the case of maximum of six random discontinuities, (M=2).

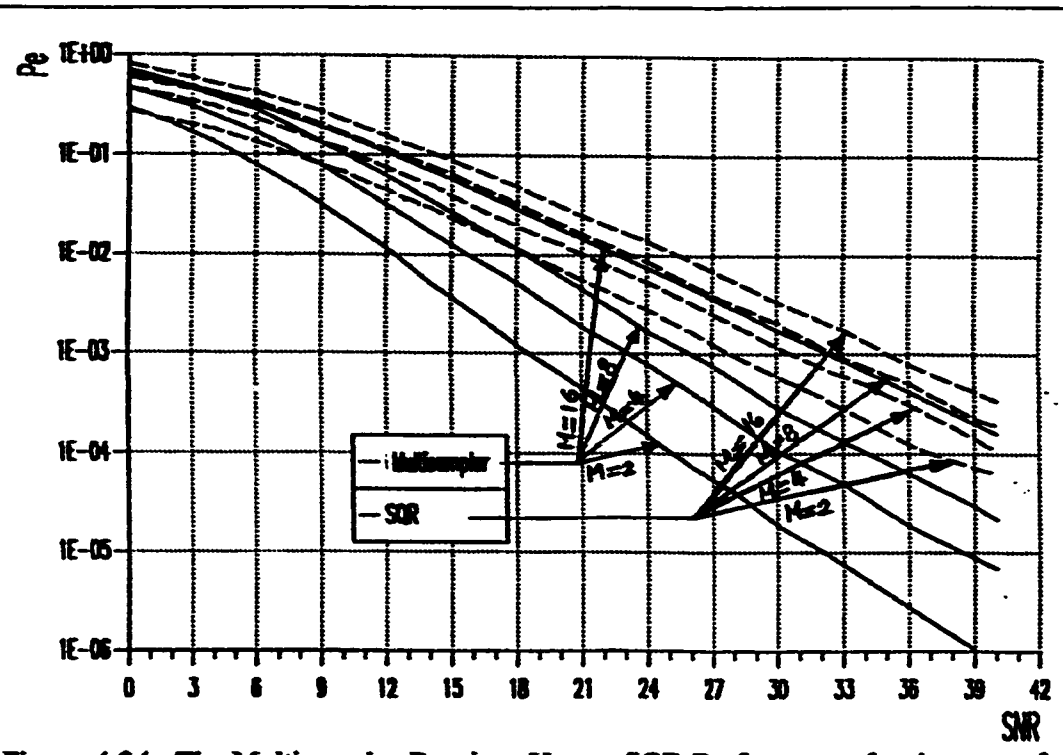


*Figure 4.24*: The Multisampler Receiver Versus SQR Performance for the case of one random discontinuity, (M=2, 4, 8, 16).

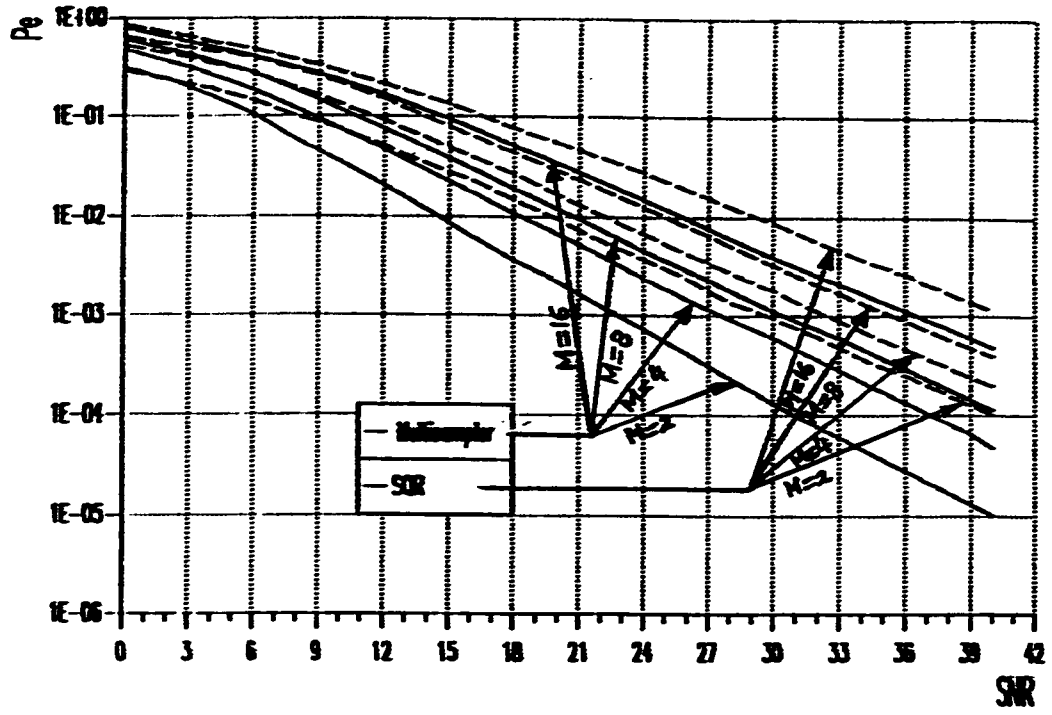


*Figure 4.25*: The Multisampler Receiver Versus SQR Performance for the case of maximum of three random discontinuities, (M=2, 4, 8, 16).

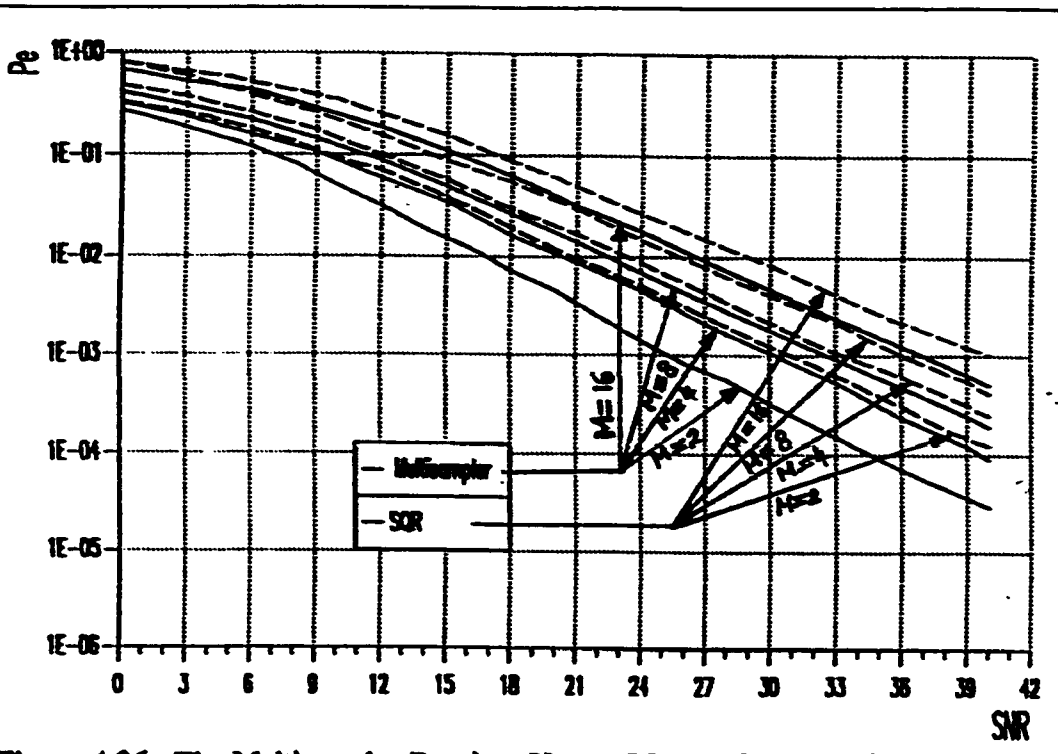


*Figure 4.26*: The Multisampler Receiver Versus SQR Performance for the case of maximum of six random discontinuities, (M=2, 4, 8, 16).

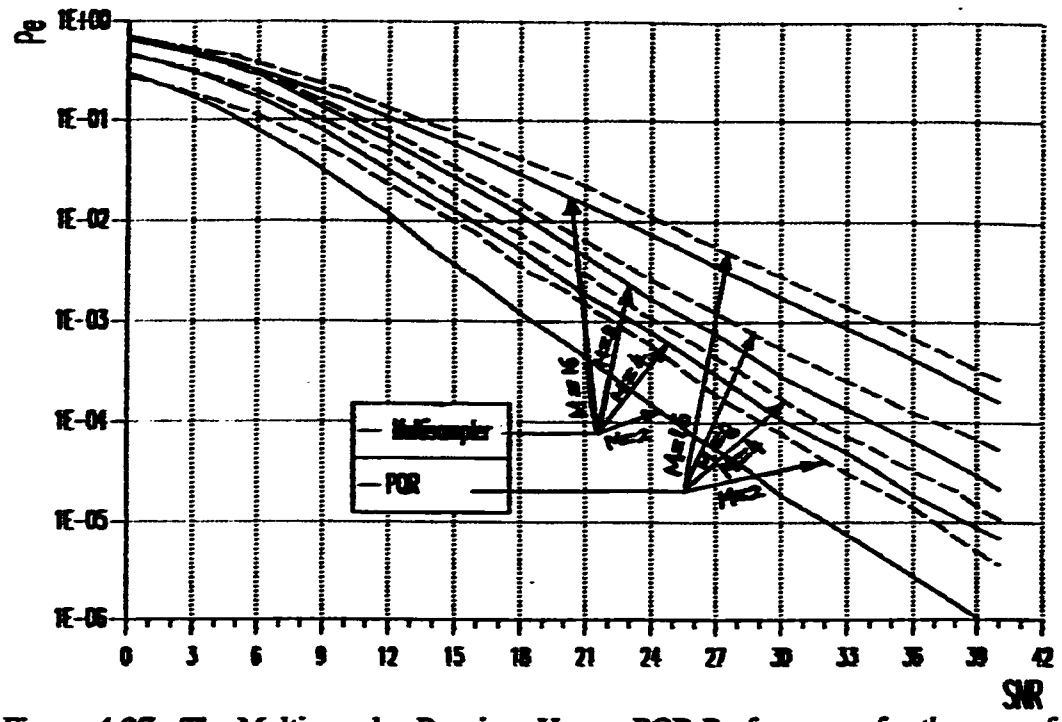


*Figure 4.27*: The Multisampler Receiver Versus PQR Performance for the case of one random discontinuity, (M=2, 4, 8, 16).

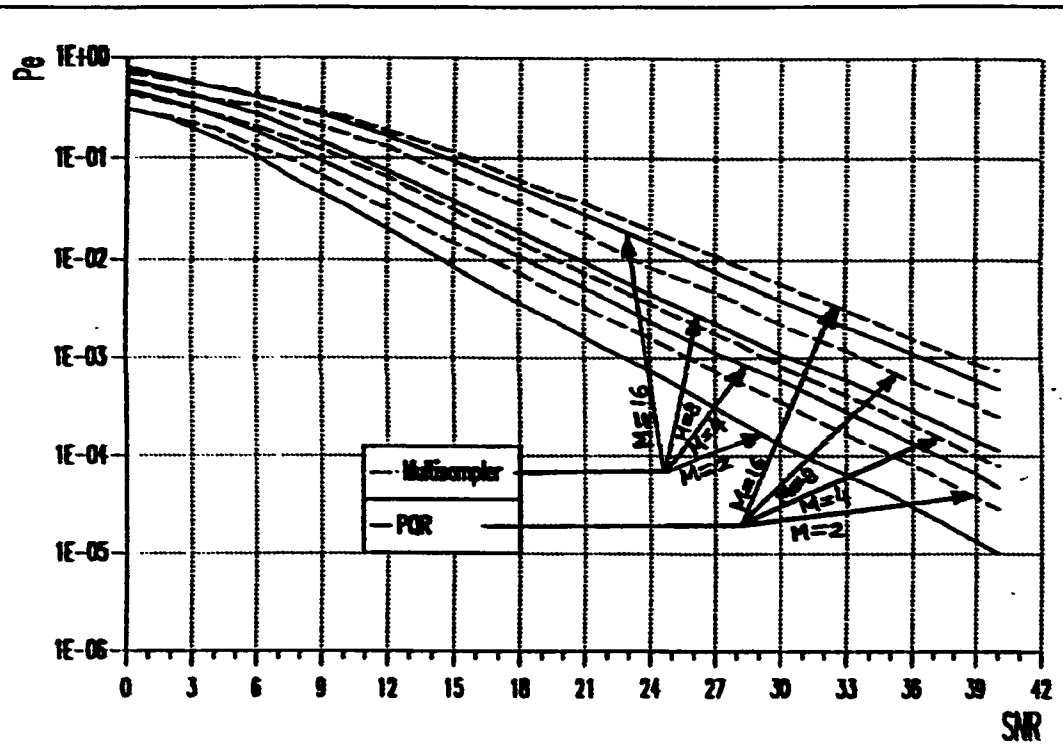


*Figure 4.28*: The Multisampler Receiver Versus PQR Performance for the case of maximum of three random discontinuities, (M=2, 4, 8, 16).

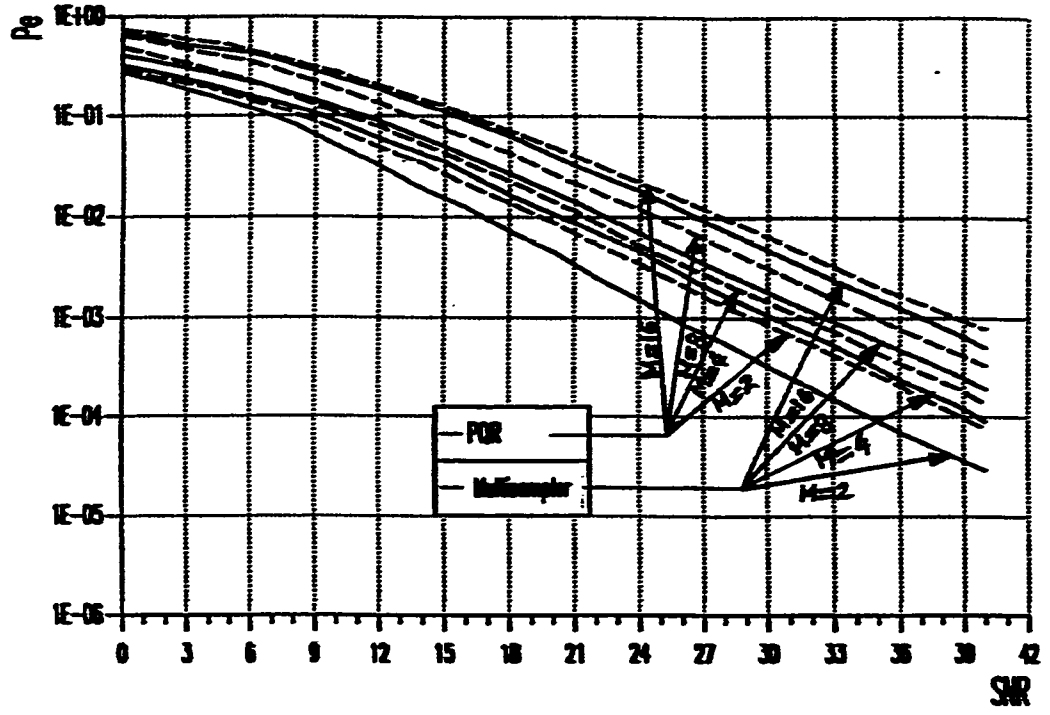


*Figure 4.29*: The Multisampler Receiver Versus PQR Performance for the case of maximum of six random discontinuities, (M=2, 4, 8, 16).

| | SQR | PQR | Multisampler Receiver |
|---|---|---|---|
| Case 1 | 35.5 | 36.5 | 36.0 |
| Case 2 | 38.5 | 24.0 | 25.5 |
| Case 3 | 37.0 | 32.0 | 28.0 |
| Case 4 | 41.5 | 37.0 | 31.5 |
| Case 5 | 43.0 | 42.0 | 39.0 |

*Table 4.1*: SNR Values for the SQR, PQR, and the Multisampler Receiver at $P_e = 10^{-4}$, for M = 2.

| | SQR | PQR | Multisampler Receiver |
|---|---|---|---|
| Case 1 | 38.0 | 40.0 | 39.0 |
| Case 2 | 41.0 | 26.5 | 27.5 |
| Case 3 | 41.0 | 33.0 | 30.0 |
| Case 4 | 42.5 | 39.5 | 37.0 |
| Case 5 | 45.0 | 43.5 | 40.5 |

*Table 4.2*: SNR Values for the SQR, PQR, and the Multisampler Receiver at $P_e = 10^{-4}$, for M = 4.

| | SQR | PQR | Multisampler Receiver |
|---|---|---|---|
| Case 1 | 41.0 | 43.0 | 42.0 |
| Case 2 | 43.0 | 28.0 | 29.0 |
| Case 3 | 44.5 | 37.0 | 34.5 |
| Case 4 | 45.5 | 44.0 | 41.0 |
| Case 5 | 46.5 | 45.5 | 43.0 |

*Table 4.3*: SNR Values for the SQR, PQR, and the Multisampler Receiver at $P_e = 10^{-4}$, for M = 8.

| | SQR | PQR | Multisampler Receiver |
|---|---|---|---|
| Case 1 | 43.0 | 45.0 | 44.0 |
| Case 2 | 46.0 | 29.5 | 32.5 |
| Case 3 | 48.5 | 44.5 | 42.0 |
| Case 4 | 50.0 | 48.0 | 46.0 |
| Case 5 | 52.0 | 51.0 | 49.0 |

*Table 4.4*: SNR Values for the SQR, PQR, and the Multisampler Receiver at $P_e = 10^{-4}$, for M = 16.

## 4.5 Summary

In this chapter, the concept of changing the sampling frequency of the receiver was applied to propose a new receiver structure, to work in fast multipath fading channels. The new receiver is called the multisampler receiver. The frequency is estimated in this receiver using a parametric frequency estimation method. Then, the receiver decides which symbol was transmitted, by comparing the errors in frequency estimation in each branch, and finding the lowest frequency estimation error.

The multisampler receiver was simulated using a Fortran computer program, and then was tested under the different cases of fast multipath fading channels, under which the SQR, PQR, and DFLL receivers were tested. For all cases, but those for which the SQR and PQR receivers are optimized for ( $\rho=1$ and $\rho=0$, respectively), the proposed multisampler receiver outperforms the other two. Even with $\rho=1$ and $\rho=0$ cases, the new receiver is comparable in performance to the corresponding optimized receiver.

# Chapter V
# CONCLUSIONS AND SUGGESTIONS FOR FURTHER WORK

A summary of what has been accomplished in this thesis is presented in this chapter. In addition, some suggestions and recommendations for further future work are included.

## 5.1 Conclusions

As communication systems are advancing and mobile communications systems are increasingly growing in many areas, the detection problem of fast multipath fading channels is gaining an increased attention.

Many non coherent FSK receivers have been proposed to work in such environments and under such circumstances. This is because the NCFSK receivers are less sensitive to phase discontinuities that are inherent in the non-resolvable fast fading multipath received signals. One of these receivers is the so called Quadrature receiver, or equivalently, the single quadrature receiver (SQR). If the received signal does not have any phase discontinuities, this receiver will achieve the optimum performance. However, in fast multipath fading channels,

the occurence of phase discontinuities is very possible. To overcome this problem, another receiver, which consists of a parallel interconnection of quadratures, was proposed. In order for this receiver to operate in the optimum way, the quadratures of the receiver have to be matched to the locations of phase discontinuities within the symbol duration. This means that the locations of the discontinuities have to be known *a priori*.

Due to the nature of multipath fast fading channels, it is impossible to know the frequency or location of phase discontinuities. This means that the PQR is not very helpful in such realistic cases.

In Chapter Two of this thesis, the abovementioned receivers were simulated using Fortran computer programs. The cases tested by Higgins in [2], have been simulated and the results were compared to those reported before. In addition, three new test cases were introduced to simulate the SQR and PQR behavior under different realistic situations. The PQR receiver was found to, give better results than the SQR in such cases with much degraded performance than in the case where the PQR is optimized for.

In chapter 3 of this thesis, the Digital Frequency Locked Loop (DFLL) was applied as a receiver for fast multipath fading channels. It was tested under the same cases under which, both the SQR and PQR were tested. However, the DFLL did not give satisfactory results. The performance of the DFLL was poorer than both the SQR and PQR for all cases. It was concluded, that the DFLL would not fit in these situations, at least with its current structure.

The DFLL uses the concept of adapting the loop frequency to the incoming one. This is based on a conclusion made by El-Hennawey and Carter in [11].

This result states that if a received signal is sampled at four times its frequency, the error in estimation, using parametric methods, will be zero, regardless of the SNR for SNR > 0 dB. In Chapter Four of this thesis, the above principle was applied to propose a new receiver structure which was coined the name: multisampler receiver. In this receiver, the sampling rate of each branch is different from the others. The sampling rate of each branch is set to four times one of the transmitted frequencies. Then the errors in the estimation are compared to each other in each branch, and a decision is made. This receiver was tested under the same cases, under which the SQR, PQR and the DFLL receivers were tested. The performance of the new multisampler receiver is slightly lower than that of the SQR and PQR for the two cases of no phase discontinuity, and of one phase discontinuity fixed in the middle of the symbol duration. This is an expected result, since the SQR is optimized for the case of no phase discontinuity, and the PQR is optimized for the case of one phase discontinuity fixed in the middle of the symbol duration. However, once the more realistic three cases of fast multipath fading channels are applied, the new receiver significantly outperforms the other receivers.

The tests were applied to the receivers in the binary signal scheme, and then were extended to the M-ary signal space. In all cases, the multisampler receiver was found to outperform the SQR and PQR receivers in fast multipath fading channels under realistic conditions.

## 5.2 Suggestions for Further Work

In the following, some suggestions for further work are listed:

1. Applying adaptive MEM, or other more efficient ARMA algorithms to in the frequency estimator block, to reduce the computational complexity, and to be able to get a more accurate frequency estimation.
2. Applying some ARMA algorithms which are less affected with phase change within the duration of the estimated symbol duration.
3. Combining some coding techniques, to achieve a better probabilty of error performance against SNRs.
4. The multisampler receiver has been tested for cases of frequency non-selective fading channels. It is suggested to test the receiver for frequency selective fast multipath fading channels.
5. The multisampler receiver has been tested for the case of Gausian fading channel. It is suggested to test the receiver under cases of Non-Gausian channels.
6. Testing the new receiver for the cases of urban area detection, where fixed reflectors exist, and the distribution of the envelope of the received signals is modeled as Rician (Rician Fading Channels), instead of the Rayleigh Fading Channels.
7. Implementation of the new multisampler receiver in real time and comparing the results to these found by simulation.

# APPENDIX A

In the following, the programs and subroutines that were developed to simulate the Single Quadrature Receiver (SQR), the Parallel Quadrature Receiver (PQR), and the new FSK Multisampler receiver, are presented. Each of these receivers is simulated in a main program. The main programs call certain subroutines to do specific functions for them such as generating the random message sequence, adding noise, adding Rayleigh distributed amplitudes, ... etc. The main program of the SQR is enlisted starting at page 127, while the PQR main program is enlisted starting at page 130. Moreover, the main program of the new FSK Multisampler receiver is enlisted starting at page 133. Finally, the subroutines are enlisted starting from at 137.

All these programs and subroutines have been run on an IBM 370/3090 Mainframe computer system.

# APPENDIX A

This program is developed to simulate the Single Quadrature Receiver on an IBM370 mainframe computer system. The principle of operation of this program was described in chapter two of this thesis.

```
**********************************************************************
                    Single Quadrature Receiver
**********************************************************************
C
C   RANDOM # OF DISCONTINUITIES WITHIN EACH BIT
C   WITH A RANDOM PLACE OF OCCURRANCE WITHIN THE
C   BIT DURATION.
C
C       ***************************************************
C       RANDOM GENERATION OF THE SIGNAL.
C       ***************************************************
C

      DIMENSION MSGMIN(300),MSG(100000),AMP(7*100000)
      DIMENSION NDSCAR(100000),AMPMG(7),RMSGI(300),RMSGQ(300)
      REAL NC,DT,PI,T,FC,F1,F2,FS,SNR,TS,MSGMIN,AMP,AMPMG
      REAL RMSGI,RMSGQ,SC(23),RSLT1,RSLT2
      REAL RESLT(16),F(16)
      INTEGER NDSCAR,MSG
C
      NMSGS  = 100000
      NRUNS =  21
C
      M = 16
      ND = 4
C
      SNR = 0.0
C
      MODE1 = 2
      MNDSCT = 1
      MD2 = 1
      MD3 = 1
C
      DF = 0.01 * REAL(NR)
      NC = 2 * DF
      TB = REAL(NC) / (2.0*DF)
      FC = 0.32 * REAL(NR)
C
C ..... CALCULATING THE FREQUENCIES
C
      DIF = -M+1
```

```
      DO 10 I = 1 , M
         F(I) = FC + DIF * DF
         DIF = DIF + 2.0
 10   CONTINUE
C
                          WRITE(6,*)(F(I),I=1,M)
C
      ES = 1.0
C
C     ----------          2*PI
C
      TPI = 8.0*ATAN(1.0)
      NSMPS = NR
C
      A = 0.0
      B = TB
      TS = 1.0
      DT = (B-A)/REAL(NR)
      ISD1 = 5383
      ISD2 = 8323
C
      IGRN1 = 124597
      IGRN2 = 369258
C
      DO 15 I = 1 , 23
         SC(I) = 0.0
  15  CONTINUE
C
                  DO 70 K = 1 , NRUNS
C
       L = 0
C
       NFAMP = 0
C
       ERCNT = 0.0
C
       CALL RAMPS(MODE1,NMSGS,MNDSCT,AMP,NDSCAR,IGRN1,IGRN2)
C
       CALL RDMSG(MD3,NMSGS,ND,SC,MSG)
C
                      DO 50 I = 1 , NMSGS
C
C     MODULATE & ADD NOISE(XAVG=0.0,XSTD = SQRT(N0/2)
C
       NMGAMP = NDSCAR(I) + 1
C
       DO 95 I,N = 1 , NMGAMP
          AMPMG(I,N) = AMP(NFAMP+I,N)
  95   CONTINUE
C
```

```
      JS = MSG(I) + 1
C
      NFAMP = NFAMP + NMGAMP
C
        CALL MGWNS(MD2,NR,TB,DT,SNR,F(JS),MSGMIN,ISD1,NDSCAR(I),AMPMG)
C
C-------------------------
C    RECEIVER SECTION
C-------------------------
C
C    FIRST: WE CORRELATE AND THEN WE INTEGRATE
C
      DO 40 J = 1 , M
C
          CALL CORLT(NR,TB,DT,F(J),MSGMIN,RMSGI,RMSGQ)
C
          CALL INTGRT(NR,DT,RMSGI,RSLT1)
C
          CALL INTGRT(NR,DT,RMSGQ,RSLT2)
C
          RESLT(J) = (RSLT1)**2 + (RSLT2)**2
C
  40  CONTINUE
C
C-------------------------
C    DECISION DEVICE
C-------------------------
C
          CALL DIGST(M,RESLT,MDEC,JUNK)
C
C-----------------------------------------------
C
      IF (JS .NE. MDEC) THEN
          ERCNT = ERCNT + 1.0
      ENDIF
C
  50                  CONTINUE
C
          PE = ERCNT/REAL(NMSGS)
          WRITE(6,*)SNR,PE
C
          SNR = SNR + 2.0
  70  CONTINUE
C-----------------------------
      STOP
      END
C
C-------------------------------------------------------------
C        END OF THE MAIN PROGRAM
C-------------------------------------------------------------
```

This program is developed to simulate the Parallel Quadrature Receiver on an IBM370 mainframe computer system. The principle of operation of this program was descriped in chapter two of this thesis.

```
*****************************************************************
                Parallel Quadrature Receiver
*****************************************************************
C
C    ********************************************************
C    RANDOM GENERATION OF THE SIGNAL
C    ********************************************************
C
      DIMENSION MSGMIN(300),MSG(100000),AMP(7*100000)
      DIMENSION NDSCAR(100000),AMPMG(7),RMSGI(300),RMSGQ(300)

      REAL NC,DT,PI,T,FC,F1,F2,ES,SNR,TS,MSGMIN,AMP,AMPMG
      REAL RMSGI,RMSGQ,SC(23),RSLT1,RSLT2
      REAL RESLT(16),F(16)

      INTEGER NDSCAR,MSG
C
      NMSGS  = 100000
      NRUNS =  21
C
      M =  16
      ND = 4
C
      SNR = 0.0
C
      MODE1 = 1
      MNDSCT = 7
      MD2 = 1
      MD3 = 1
C
      MNR = NR / 2
      DF = 0.01 * REAL(NR)
      NC = 2 * DF
      TB = REAL(NC)/ (2.0*DF)
      FC = 0.25 * REAL(NR)
C
C ..... CALCULATING THE FREQUENCIES
C
      DIF = -M + 1
      DO 10 I = 1 , M
          F(I) = FC + DIF * DF
          DIF = DIF + 2.0
 10   CONTINUE
C
```

```
                        WRITE(6,*)(F(I),I=1,M)
C
C   ..............          2*PI
C
      TPI = 8.0*ATAN(1.0)
      NSMPS = NR
C
      A = 0.0
      B = TB
      TS = 1.0
      DT = (B-A)/REAL(NR)
      ISD1 = 5383
      ISD2 = 8323
C
      IGRN1 = 124597
      IGRN2 = 369258
C
      DO 15 I = 1 , 23
         SC(I) = 0.0
   15 CONTINUE
C
      WRITE(6,*)'SIX PHASE DISCONT. FIX .POS..NMSGS=',NMSGS,',PQR, R=0'
C
                  DO 70 K = 1 , NRUNS
C
       L = 0
C
       NFAMP = 0
C
       ERCNT = 0.0
C
      CALL RAMPS(MODE1,NMSGS,MNDSCT,AMP,NDSCAR,IGRN1,IGRN2)
C
      CALL RDMSG(MD3,NMSGS,ND,SC,MSG)
C
                      DO 50 I = 1 , NMSGS
C
C    MODULATE & ADD NOISE(XAVG=0.0,XSTD = SQRT(N0/2)
C
      NMGAMP = NDSCAR(I) + 1
C
      DO 95 LN = 1 , NMGAMP
         AMPMG(LN) = AMP(NFAMP+LN)
   95 CONTINUE
C
      JS = MSG(I) + 1
C
      NFAMP = NFAMP + NMGAMP
C
        CALL MGWNS(MD2,NR,TB,DT,SNR,F(JS),MSGMIN,ISD1,NDSCAR(I),AMPMG)
```

```
C
C-------------------------
C    RECEIVER SECTION
C-------------------------
C
C    FIRST: WE CORRELATE AND THEN WE INTEGRATE
C
      DO 40 J = 1 , M
C
          CALL CORLT(NR,TB,DT,F(J),MSGMIN,RMSGI,RMSGQ)
C
          CALL INTGRT(NR,1,MNR,DT,RMSGI,RSLT1)
C
          CALL INTGRT(NR,MNR,NR,DT,RMSGI,RSLT2)
C
          CALL INTGRT(NR,1,MNR,DT,RMSGQ,RSLT3)
C
          CALL INTGRT(NR,MNR,NR,DT,RMSGQ,RSLT4)
C
          RESLT(J) = (RSLT1)**2+(RSLT2)**2+(RSLT3)**2+(RSLT4)**2
C
   40 CONTINUE
C
C-------------------------------
C    DECISION DEVICE
C-------------------------------
C
          CALL DLGST(M,RESLT,MDEC,JUNK)
C
C-------------------------
C
      IF (JS .NE. MDEC) THEN
          ERCNT = ERCNT + 1.0
      ENDIF
C
   50                 CONTINUE
C
          PE = ERCNT/REAL(NMSGS)
          WRITE( 6,*)SNR,PE
C
          SNR = SNR + 2.0
   70 CONTINUE
C
C-----------------------------
      STOP
      END
C
```

This program is developed to simulate the New FSK Multisampler Receiver on an IBM370 mainframe computer system. The principle of operation of this program was descriped in chapter four of this thesis.

```
C   ====================
C   =====                =====
C   ===      THE NEW       ===
C   ==     MULTISAMPLER FSK   ==
C   ===      RECEIVER        ===
C   =====                =====
C   ====================
C
C ***************************************************************
C *  RANDOM # OF DISCONTINUITIES WITHIN EACH BIT
C *  WITH A RANDOM PLACE OF OCURRANCE WITHIN THE
C *  BIT DURATION. THE STRUCTURE ALLOWS FOR VARI-
C *  ABLE OVERLAPPING SCHEMES FOR  COMPUTATIONAL
C *  EFFICIENCY.
C ***************************************************************
C
C
      REAL MSGMIN(480),AMP(7*100000),AMPMG(7),Y(2),SC(23)
      REAL F(16),FS(16),DT(16),FPR(16),FERR(16),TMPAR(80)
      REAL NC,PI,TB,FCES,SNR,TS
      INTEGER NDSCAR(100000),MSG(100000),NR(16),LNGEST(16)
C
      NMSGS  = 100000
      NRUNS =   21
C
      M =  16
      ND = 4
C
      SNR =  0.0
C
      MODE1 = 2
      MNDSCT = 1
      MD2 = 1
      MD3 = 1
C
      DF = 3.0
      NC = 6.0
      TB = REAL(NC)/(2.0*DF)
      FC = 75.0
      ES = 1.0
      LGDF = 2
      CNTDF = 50
C
      A = 0.0
```

```
      B = TB
      TS = 1.0
C
C ... CALCULATING THE FREQUENCIES
C
      DIF = 1-M
      DO 10 I = 1,M
         F(I)  = FC + DIF*DF
         LNGEST(I) = CNTDF + DIF * LGDF
         NR(I) = 4*INT(F(I))
         DIF   = DIF + 2.0
         FS(I) = REAL ( NR(I) )
         DT(I) = (B-A)/FS(I)
C
                  WRITE( 6,*)'F(I)= ',F(I),'NR(I)= ',NR(I)
                  WRITE( 6,*)'FS(I)= ',FS(I),'DT(I)= ',DT(I)
 10   CONTINUE
C
      WRITE(6,*)(F(I),I= 1,M)
C
C   ----------          2*PI
C
      TPI = 8.0*ATAN(1.0)
C
C ------ MODEL ORDER
C
      IP = 2
C
      ISD1 = 1234567
      ISEED2 = 3746561
C
      IGRN1 = 124597
      IGRN2 = 369258
C
      DO 15 I = 1 , 23
         SC(I) = 0.0
 15   CONTINUE
C
                  DO 70 K = 1 , NRUNS
C
       L = 0
C
       NFAMP = 0
C
       ERCNT = 0.0
C
       NCNT = 0
C
       CALL RAMPS(MODEL,NMSGS,MNDSCT,AMP,NDSCAR,IGRN1,IGRN2)
C
```

```
      CALL RDMSG(MD3,NMSGS,ND,SC,MSG)
C
        DO 50 I = 1 , NMSGS
C
C    MODULATE & ADD NOISE(XAVG=0.0,XSTD = SQRT(N0/2)
C
      NMGAMP = NDSCAR(I) + 1
C
      DO 95 LN = 1 , NMGAMP
         AMPMG(LN) = AMP(NFAMP+LN)
  95  CONTINUE
C
      JS = MSG(I) + 1
C
      NFAMP = NFAMP + NMGAMP
C
              FR = F(JS)


      DO 40 J = 1,M

          CALL MGWNS(MD2,NR(J),TB,DT(J),SNR,FR,MSGMIN,
     *          ISD1,NDSCAR(I),AMPMG)
          CALL BURG(MSGMIN,NR(J),IP,Y)
          CALL FEST(Y,FP,NCNT)
          FPR(J) = FP * FS(J)
C
          FERR(J) = ABS(FPR(J)-F(J))
C
  40  CONTINUE
C
      I2 = (I/2000)*2000
      IF ( I2 .EQ. I ) THEN
          WRITE( 6,*) I
          WRITE(22,*) I
      ENDIF
C
C
C-------------------------------------
C       DECISION SECTION
C-------------------------------------
C
C
      CALL DIGST(M,FERR,JUNK,MDEC)
C
      IF ( MDEC .NE. JS ) ERCNT = ERCNT + 1.0
C
C ---------------------------------------------
C
      ISD1 = ISD1 + 860
```

```
  50 CONTINUE
C
          PE = ERCNT / REAL(NMSGS)
          WRITE(6,*)NCNT
          WRITE(6,*)SNR,PE
C
          SNR = SNR + 2.0
C
  70 CONTINUE
C-------------------------
       STOP
       END
C
C-----------------------------------------------
C          END OF THE MAIN PROGRAM
C-----------------------------------------------
C
```

These subroutines have been developed to be used in the simulation programs of the tested receivers, on an IBM370 mainframe computer system.

```
C
C
C
C          GAUSIAN NOISE CORRUPTION
C          = = = = = = = = = = = = = = = = = = = = =
C-----------------------------------------------
C       A SUBROUTINE TO GIVE THE RANDOMLY GENERATED
C       SIGNAL, A RANDOM GAUSIAN NOISE, AND A RAYLEIGH
C       DISTRIBUTED AMPLITUDE
C   MODE2  = POSITION OF OCCURRENCE OF THE PHASE DISCONT.
C      (1)= RANDOM POSITION
C      (2)= FIXED POSITIONS
C   NR     = # OF SAMPLES
C   TB     = THE BIT PERIOD
C   DT     = THE SAMPLE DURATION
C   SNR    = THE SIGNAL TO NOISE RATIO TO BE USED FOR THE
C          NOISE LEVEL GENERATION
C   FC     = THE BIT MODULATION SIGNAL FREQUENCY
C   MSGMIN = THE RECEIVED SIGNAL AFTER NOISE, DISCONTINUITY
C          AND RAYLEIGH AMPLITUDE CORRUPTION
C   ISEED  = THE NEW SEED FOR THE GAUSIAN NOISE GENERATION
C   NDSCT  = THE NUMBER OF PHASE DISCONTINUITIES TO BE PUT
C          IN THE MODULATED SIGNAL
C   AMP    = THE RAYLEIGH DISTRIBUTED AMPLITUDES VECTOR
C
C            YOU WANT TO CHANGE IN THE ARRAY SIZES
C            ONLY IF YOU CHANGED: (1) THE # OF DISCONT.,
C            OR, (2) THE NUMBER OF SAMPLES
C-----------------------------------------------
C
      SUBROUTINE MGWNS(MODE2,NR,TB,DT,SNR,FC,MSGMIN,ISEED,NDSCT,AMP)
      DIMENSION R(300),MSGMI(300),MSGMIN(NR),AMP(2),AMP10(2)
      INTEGER LBEAR(3)
      REAL R,PI,MSGMI,MSGMIN,T
C
      TPI = 8.0*ATAN(1.0)
      NR4 = NR - 4
      NDSCT1 = NDSCT + 1
      NDSCT2 = NDSCT + 2
C
      DO 10 I = 1 , NDSCT1
         AMP(I) = SQRT(2.0/TB)*AMP(I)
         AMP10(I) = 10.0*AMP(I)
  10  CONTINUE
C
```

```
      AINC = TPI*FC*DT
      THETA = TPI*A
      ANGLE = THETA
C
      CALL RNSET(ISEED)
      CALL RNNOR(NR,R)
C
      XSTD =SQRT((ES/2.0)*FS*10.**(-SNR/10.))
      CALL SSCAL(NR,XSTD,R,1)
      ISEED = ISEED + 860
C
C ... TO CHOOSE FOR A RANDOM POSITION OF THE OCCURANCE OF THE
C    DISCONTINUITIES (MODE2 = 1), OR A FIXED POSITION OF
C    OCCURRENCE (MODE2=2), IN THE BIT DURATION.
C
      LBEAR(1) = 0
      LBEAR(NDSCT+2) = NR
C
      IF ( MODE2 .EQ. 1 ) THEN
C
          IF ( NDSCT .GE. 1 ) THEN
C
              DO 20 N = 2,NDSCT1
                  LBEAR(N) = INT( NR4 * RNUNF() ) + 2
  20          CONTINUE
C
          ENDIF
C
          CALL SORT(NDSCT2,LBEAR)

      ELSEIF ( MODE2 .EQ. 2 ) THEN

          DO 30 N = 2,NDSCT1
              LBEAR(N) = (N-1)*(NR/NDSCT1)
  30      CONTINUE

      ENDIF
C
C ... RAYLEIGH DISTRIBUTED AMPLITUDE SEGMENTS & CORRUPTION WITH
C    NOISE
C
      DO 60 J = 1 , NDSCT1
          DO 50 K = (LBEAR(J))+1,LBEAR(J+1)
              MSGMI(K) = AMP(J)*COS(ANGLE)
              IF( R(K) .GT. AMP10(J) ) R(K) = AMP10(J)
              MSGMIN(K) = MSGMI(K) + R(K)
              ANGLE = ANGLE+AINC
  50      CONTINUE
C
          A = RNUNF()
```

```
          THETAI = TPI*A
          ANGLE  = ANGLE + THETAI
   60 CONTINUE
C
C  AT THIS INSTANT, WE HAVE GOT OUR RECEIVED SIGNAL
C
      RETURN
      END
C
C
C
C             CORROLATION
C            = = = = = = = = =
C-----------------------------------------------
C       A SUBROUTINE TO MULTIPLY MY RECIEVED SIGNAL WITH
C       A COS AND A SIN TERMS (I.E. CORRELATE )
C-----------------------------------------------
C
      SUBROUTINE CORLT(NR,TB,DT,FC,MGMIN,RMSGI,RMSGQ)
      DIMENSION MGMIN(NR),RMSGI(NR),RMSGQ(NR)
      REAL R,PI,MGMIN,RMSGI,RMSGQ
      PI = 4.0*ATAN(1.0)
      T = 1.0
C
      AMP = SQRT(2.0/TB)
      AINC=2.*PI*FC*DT
      THETA = 0.0
      ANGLE = THETA + TS
C
      DO 20 K = 1,NR
         RMSGI(K) = MGMIN(K)*AMP*COS(ANGLE)
         RMSGQ(K) = MGMIN(K)*AMP*SIN(ANGLE)
         ANGLE = ANGLE + AINC
   20 CONTINUE
C
C  AT THIS INSTANT, WE HAVE GOT OUR RECEIVED SIGNAL, MULTIPLIED
C  BY COS AND SIN TERMS
C
      RETURN
      END
C
C
C             INTEGRATION
C            = = = = = = = = =
C-----------------------------------------------
C       A SUBROUTINE TO INTEGRATE THE GIVEN FUNCTION OVER
C       THE GIVEN PERIOD USING THE TRAPEZOID METHOD. THE
C       FUNCTION VALUES AT DIFFERENT EQUALLY SPACED POINTS
C       IN THE PERIOD OF INTEGRATION ARE TO BE GIVEN IN THE
C       FORM OF AN ARRAY CALLED F.
```

```
C-------------------------------------------------------
C
      SUBROUTINE INTGRT(NR,DT,F,RESULT)
      DIMENSION F(NR)
      REAL F,DT,RESULT
C
      SUM = 0.5*(F(1)+F(NR))
      DO 50 K = 2,NR-1
         SUM = SUM + F(K)
   50 CONTINUE
      RESULT = SUM * DT
C
C  AT THIS INSTANT, WE HAVE GOT OUR RECEIVED SIGNAL, MULTIPLIED
C  BY COS AND SIN TERMS, AND INTEGRATED OVER THE GIVEN INTERVAL.
C
      RETURN
      END
C
C            RANDOM RAYLEIGH AMPLITUDE GENERATOR
C           = = = = = = = = = = = = = = = = = = = = = = = = = =
C-------------------------------------------------------
C
C  A SUBROUTINE TO GENERATE RANDOM AMPLITUDES OF THE DIFFERENT
C  SEGMENTS OF BITS DEPENDING ON THE # OF DISCONTINUITIES WITHIN
C  A CERTAIN BIT.
C    MODE   = THE MODE OF OPERATION OF THE SUBROUTINE :
C       1 = RANDOM # OF DISCONTINUITIES WITHIN THE BIT DURATION
C       2 = CONSTANT # OF DISCONTINUITIES WITHIN THE BIT DURATION
C    NMSGS  = THE # OF MESSAGES FOR WHICH SEGMENTS THE RAYLEIGH
C          AMPLITUDES TO BE GENERATED
C    MNDSCT = THE MAX. # OF DISCONTINUITIES WITHIN A CERTAIN BIT
C    NAMPS  = THE TOTAL # OF AMPLITUDES THAT HAVE BEEN GENERATED
C    AMP    = AN ARRAY OF THE VALUES OF THE GENERATED AMPLITUDES
C    NDSCAR = AN ARRAY OF THE # OF DISCONTINUITIES OF EACH MESSAGE
C    IGRN1 & IGRN2 = THE SEED VALUES OF THE RAYLEIGH AMPLITUDE
C                GENERATORS
C
C            YOU WANT TO CHANGE IN THE ARRAY SIZES ONLY
C            IF YOU CHANGED: (1) THE # OF DISCONT., OR.
C            (2) THE NUMBER OF MESSAGES.
C-------------------------------------------------------
C
      SUBROUTINE RAMPS(MODE,NMSGS,MNDSCT,AMP,NDSCAR,IGRN1,IGRN2)
      REAL AMP((MNDSCT+1)*NMSGS),P(2*100000),Q(2*100000)
      INTEGER NDSCAR(NMSGS)
      NAMPS = 0.0
C
      IF ( MODE .EQ. 1 ) THEN
         DO 15 IDS = 1,NMSGS
            A = RNUNF()
```

```
            NDSCT = INT(MNDSCT*A)
            NDSCAR(IDS) = NDSCT
            NAMPS = NAMPS + NDSCT + 1.0
 15    CONTINUE
C
      ELSEIF ( MODE .EQ. 2 ) THEN
          DO 20 IDS = 1,NMSGS
            NDSCT = MNDSCT
            NDSCAR(IDS) = NDSCT
            NAMPS = NAMPS + NDSCT + 1.0
 20   CONTINUE
C
      ENDIF
C
      CALL RNSET(IGRN1)
      CALL RNNOR(NAMPS,Q)
C
      CALL RNSET(IGRN2)
      CALL RNNOR(NAMPS,P)
C
      DO 25 IAM = 1,NAMPS
         AMP(IAM) = SQRT((Q(IAM))**2 + (P(IAM))**2)
 25   CONTINUE
C
      IGRN1 = IGRN1 + 34739
      IGRN2 = IGRN2 + 41385
C
      RETURN
      END
C
C            RANDOM MESSAGE GENERATOR
C           = = = = = = = = = = = = = = = = = = =
C-----------------------------------------------------------------
C
C  A SUBROUTINE TO GENERATE RANDOM MESSAGES OF ONE AND ZERO
C
C     MODE   = MODE OF GENERATION OF THE MESSAGES
C       (1)= RANDOM GENERATION
C       (2)= FIXED GENERATION ( A SQUARE WAVE )
C     NMSGS  = THE # OF RANDOM MESSAGES TO BE GENERATED     ; INPUT
C     SC     = THE HEART OF THE MESSAGE VECTOR GENERATOR    ; INPUT
C     N      = THE DIMESION OF THE MESSAGE SPACE, M = 2**N  ; INPUT
C     MSG    = THE VECTOR OF THE RANDOM MESSAGES THAT
C            HAVE BEEN GENERATED                           ; OUTPUT
C
C-----------------------------------------------------------------
C
      SUBROUTINE RDMSG(MODE,NMSGS,N,SC,MSG)
      REAL SC(23)
      INTEGER MSG(NMSGS)
```

```
C
      IF ( MODE .EQ. 1 ) THEN

         DO 20 I = 1 , NMSGS
            MSG(I) = 0
            DO 10 J = 1 , N
               CALL SYMBOL(SC,K)
               MSG(I) = MSG(I) + K*(2**(J-1))
 10         CONTINUE
 20      CONTINUE
      ELSEIF ( MODE .EQ. 2 ) THEN
         DO 30 I = 1 , NMSGS
            IF ( (I/2)*2 .EQ. I ) THEN
               MSG(I) = 0
            ELSE
               MSG(I) = 1
            ENDIF
 30      CONTINUE
      ENDIF
C
      RETURN
      END
C
C-------------------------------------
C SYMBOL GENERATOR SUBROUTINE :
C          SCRAMBLER
C     K : TIME INDEX
C
C INPUT  : SC(23) ; SCRAMBLER REGISTER
C
C OUTPUT : A    ; SYMBOL BITS
C-------------------------------------
C
      SUBROUTINE SYMBOL(SC,I)
      REAL SC(23),D(2),X
C
      DO 10 I=1,2
         X=I+SC(18)+SC(23)
         IF (X .EQ. 1 .OR. X.EQ. 3) THEN
            D(I)=1
         ELSE
            D(I)=0
         ENDIF
C
         DO 20 J=22,1,-1
            SC(J+1)=SC(J)
 20      CONTINUE
C
         SC(1)=D(I)
 10   CONTINUE
```

```
C
      L = D(I)
C
      RETURN
      END
C
C                SORT
C                = = = =
C-------------------------------------------------------
C
C  A SUBROUTINE TO SORT THE INPUT ARRAY IN AN ASCENDING OR A
C  DESCENDING ORDER (USING THE BUBLE SORT ALGORITHM):
C    N = THE LENGTH OF THE ARRAY TO BE SORTED      ; INPUT
C    A = THE INPUT ARRAY TO BE SORTED. THE ELEMENTS
C       ARE FIRST INPUTTED IN THIS ARRAY, AND THEN
C       THE SORTED ELEMENTS ARE OUTPUTTED VIA IT   ; INPUT/OUTPUT
C
C-------------------------------------------------------
C
      SUBROUTINE SORT(N,A)
      REAL A(N)
C
      DO 20 J = N,2,-1
         I = 1
         DO 10 M = J,2,-1
            IF ( A(I) .GT. A(I+1) ) THEN
                  SAVE = A(I)
                  A(I) = A(I+1)
                  A(I+1) = SAVE
            ENDIF
            I = I + 1
   10    CONTINUE
   20 CONTINUE
C
      RETURN
      END
C
C-------------------------------------------------
C  A SUBROUTINE TO DECIDE WHICH IS THE LARGEST ELEMENT
C  IN AN ARRAY.
C
C      N     = LENGTH OF THE ARRAY
C      A     = ARRAY TO BE PROCESSED
C      LRGST  = THE POSITION OF THE LARGEST ELEMENT
C      LSMLST = THE POSITION OF THE SMALLEST ELEMENT
C-------------------------------------------------
C
      SUBROUTINE DLGST(N,A,LRGST,LSMLST)
      REAL A(N)
C
```

```
      RMAX = A(1)
      RMIN = A(1)
      LSMLST = 1
      LRGST = 1
C
      DO 10 I = 1,N
         IF ( A(I) .LT. RMIN ) THEN
             LSMLST = I
             RMIN = A(I)
         ENDIF
C
         IF ( A(I) .GT. RMAX ) THEN
             LRGST = I
             RMAX = A(I)
         ENDIF
 10   CONTINUE
C
      RETURN
      END

C
C= = = = = = = = = = = = = = = = = = = = = = = = = = = = = = = = = = =
C   AUTOCORRELATION METHOD OF SPECTRAL ESTIMATION
C    THE EXTENDED YULE-WALKER EQUATION SOLUTION
C              ARMA METHOD
C= = = = = = = = = = = = = = = = = = = = = = = = = = = = = = = = = = =
C
      SUBROUTINE BURG(SIP1,NS,IP,PHI)
C     REAL SIP1(60),SIP2(64),PHI(2)
      REAL SIP1(480),SIP2(484),PHI(2)
      R1 = 0.0
      R2 = 0.0
      R3 = 0.0
      R4 = 0.0
      NLAGS = 2.0*IP
      NSLGS = NS + NLAGS
      NLAGS1 = NLAGS + 1
C
      DO 15 I = 1,NLAGS
         SIP2(I) = 0.0
C      SIP2(I+NSLGS) = 0.0
 15   CONTINUE
C
      DO 20 I = NLAGS1,NSLGS
         SIP2(I) = SIP1(I-NLAGS)
 20   CONTINUE
C
      DO 25 I = NLAGS1,NSLGS
         R1 = R1 + SIP2(I) * SIP2(I-1)
         R2 = R2 + SIP2(I) * SIP2(I-2)
```

```
          R3 = R3 + SIP2(I) * SIP2(I-3)
          R4 = R4 + SIP2(I) * SIP2(I-4)
   25  CONTINUE
C
       DELTA = -1.0/(R2*R2-R1*R3)
C
C
       PHI(1) = (R2*R3 - R1*R4) * DELTA
       PHI(2) = (R2*R4 - R3*R3) * DELTA
C
C
C
       RETURN
       END
C
C
C
C    MEM ESTIMATION SUBROUTINE THROUGH BURG'S METHOD
C          OF SPECTRAL ESTIMATION
C             BURG ALGORITHM
C
C
       SUBROUTINE SURG(Y,N,IP,A)
       DIMENSION Y(N),A(IP),EFK1(420),EBK1(420),AA(420,420),
      *RHO(420),EBK(420),EFK(420)
C
       RHO0=0.

       DO 10 I=1,N
          RHO0=RHO0+(Y(I))**2/FLOAT(N)
   10  CONTINUE

       DO 20 I=2,N
          EFK1(I)=Y(I)
          EBK1(I-1)=Y(I-1)
   20  CONTINUE

       DO 80 K=1,IP
          SUMN=0.
          SUMD=0.

          DO 30 I=K+1,N
             SUMN=SUMN+EFK1(I)*EBK1(I-1)
             SUMD=SUMD+(EFK1(I))**2+(EBK1(I-1))**2
   30     CONTINUE

C         SUMD=SQRT(SUMD1*SUMD2)
          AA(K,K)=-2*SUMN/SUMD

          IF(K.EQ.1)THEN
```

```
            RHO(K)=(1.-(AA(K,K))**2)*RHO0
          ENDIF

          IF(K.GT.1)THEN
            RHO(K)=(1.-(AA(K,K))**2)*RHO(K-1)
          ENDIF

          IF(IP.EQ.1)THEN
            GOTO 90
          ENDIF

          IF(K.EQ.1)THEN
            GOTO 50
          ENDIF

          DO 40 J=1,K-1
            AA(J,K)=AA(J,K-1)+AA(K,K)*AA(K-J,K-1)
40      CONTINUE

50      DO 60 I=K+2,N
            EFK(I)=EFK1(I)+AA(K,K)*EBK1(I-1)
            EBK(I-1)=EBK1(I-2)+AA(K,K)*EFK1(I-1)
60      CONTINUE

          DO 70 I=K+2,N
            EFK1(I)=EFK(I)
            EBK1(I-1)=EBK(I-1)
70      CONTINUE

80    CONTINUE

90    SIG2=RHO(IP)

        DO 100 I=1,IP
          A(I)=AA(I,IP)
C       WRITE(6,*)A(I)
100   CONTINUE

        RETURN
        END
C
C
C           FREQUENCY ESTIMATION
C         ------------------------------------------
C ************************************************
C     A SUBROUTINE TO ESTIMATE A CERTAIN
C     FREQUENCY FROM SOME GIVEN PARAMETERS
C     OF SOME AR OR ARMA MODELS SUBROUTINE
C
C     TEST =  FREQUNCY ESTIMATION
```

```
C
C    PHI  =  THE SET OF THE MODEL COEFFICIENTS
C    FP   =  THE ESTIMATED FREQUENCY
C    NCNT =  THE NUMBER OF AMBIGIOUS POINTS
C
C ***************************************************
C
C
      SUBROUTINE FEST(PHI,FP,NCNT)
      REAL PHI(2),FP,TPI,TS
      INTEGER NCNT
C
      TPI = 8.0*ATAN(1.0)
      TS = 1.0
C
        IF ( ABS(PHI(2)) .LE. 0.000001 )     PHI(2) = 0.000001
C
          IF ( PHI(2) .LE. 0.0 ) THEN
               NCNT = NCNT+1
               GOTO  123
C       ENDIF
        ENDIF
C
C
        R = SQRT ( PHI(2) )
        CSB = -PHI(1)/(2.0*R)
C
        ARG = 0.5*(R+1./R)*CSB
        ABSARG = ABS ( ARG )
C     IF (( ABSARG .GT. 1.0 ) .OR. ( ABSARG .LT. 0.0 )) THEN
        IF ( ABSARG .GT. 1.0 ) THEN
            NCNT = NCNT + 1
            GOTO 123
        ENDIF
        FP = (1.0/(TPI*TS))*ACOS(ARG)
C
  123  CONTINUE
C
C
      RETURN
      END
C
```

# APPENDIX B

## Generation of the Rayleigh Distributed Amplitude:

Due to the existence and reception of the signal in a multipath environment, the parameters of the transmitted pulse may be affected. One of the effects of such a case will be in the amplitude of the received signal. The amplitude will have a Rayleigh distribution. In order to generate a Rayleigh distributed amplitude, we have to follow a certain transfomation procedure. This will be a transformation of the Gaussian random variables into Rayleigh random variable. The probability density function of a Gaussian random variable has the form:

$$f_X(x) = \frac{1}{\sqrt{2\pi}\sigma}\exp\left(\frac{-(x-m)^2}{2\sigma^2}\right)$$

where $\sigma^2$ is the variance of the random variable, and $m$ is the mean value. When the mean is zero, the Gaussian distribution will have the parobability density function (*pdf*) of the form:

$$f_X(x) = \frac{1}{\sqrt{2\pi}\sigma}\exp\left(\frac{-x^2}{2\sigma^2}\right)$$

It is known that if two random varibles $X$ and $Y$ are gausian distributed, indepedent, with zero mean and equal variances, then the transformation $z$:

$$z = \sqrt{x^2 + y^2}$$

has a Rayleigh probability density function.

Using the previous argument, two independent Gaussian random variables $x$ and $y$, with zero mean, and equal variance, will have a joint probability density function of the form:

$$f_{X,Y}(x,y) = f_X(x)\, f_Y(y) = \frac{1}{2\pi\sigma^2} \exp\left[\frac{-(x^2+y^2)}{2\sigma^2}\right]$$

The new random variable $Z$ will have the distribution of the form:

$$f_Z(z) = \begin{cases} \dfrac{z}{\sigma^2} \exp\left(\dfrac{-z^2}{2\sigma^2}\right) & ; \quad z \geq 0 \\ 0 & ; \quad z < 0 \end{cases}$$

This new random variable Z can, again, be transformed to the variable $A$, and the following relation will hold:

$$A = Z/\sigma \quad ,$$

or

$$Z = \sigma A \quad .$$

This transformation will produce a probability density function, of the random variable A. Since:

$$f_A(a) = f_Z(h(a)) \left|\frac{\partial h(a)}{\partial a}\right| \quad ,$$

where $h = g^{-1}(a)$, is the inverse transformation of $a$.

Hence,

$$f_A(a) = a \cdot \exp\left(-a^2/2\right)$$

In order for the signal to have a correct SNR value, the power of the Rayleigh distributed amplitude has to be taken into account, when generating the signal. This means that the mean square value of the Rayleigh distributed amplitude has to be equal to one, in order for the signal amplitude to be equal to 2E/T, which will satisfy the FSK transmitted signal structure, mentiond in Chapter Two of this thesis.

# APPENDIX C

**Relation between $\sigma_n^2$ and SNR:**

Since

$$\sigma_n^2 = \frac{N_o f_s}{2}$$

where $N_o$ is the noise power spectral density, and $f_s$, is the sampling frequency, then,

$$N_O = \frac{2\,\sigma_n^2}{f_s} \tag{C.1}$$

And, since

$$SNR = 10 \log\left(\frac{E_s}{N_o}\right)$$

then,

$$\frac{E_s}{N_o} = 10^{\left(\frac{SNR}{10}\right)} \tag{C.2}$$

Using Eqn. (C.1) above, we get

$$\frac{E_s}{N_o} = \frac{E_s\, f_s}{2\sigma_n^2} \tag{C.3}$$

Equating the right hand sides of Equations (C.2) and (C.3), we get

$$\sigma_n^2 = \frac{E_b f_s}{2 \cdot 10^{\left(\frac{SNR}{10}\right)}} \tag{C.4}$$

Equation (C.4), was used in generating the Gaussian noise that was added to the signal during the simulation.

# References


1. J. Proakis, *Digital Communications*, McGraw-Hill, 1989.
2. R.C. Higgins, "Performance Degradation in a Quadrature Receiver for CW Signals Corrupted by Multipath," *J. Accoust. Soc. Am.*, Vol. 69, No. 3, pp. 728-731, 1981.
3. H. Stark and F. Tuteur, *Modern Electrical Communications, Theory and Systems*, Printice-Hall Inc., 1979.
4. S. Haykin, *Communication Systems*, Wiley, Singapore, 1983.
5. K. J. Friederichs, "Error Analysis for Non-Coherent M-ary Orthogonal Communications Systems in the Presence of Arbitrary Gaussian Interference," *IEEE Trans. Comm.*, Vol. COM-34, pp. 817-821, 1986.
6. R.C. Higgins, "Quadrature Receivers Connected in Parallel to improve Detection Performance in a Multipath Environment," *J. Accoust. Soc. Am.*, Vol. 71, No. 2, pp. 395-401, 1982.
7. E. K. Al-Hussaini, "Parallel Quadrature Receivers for M-ary NCFSK Signals Through Multipath Fading Channels," *Arabian Jorn. Sci. Eng.*, Vol. 14, No. 4, Oct. 1989.
8. T. Y. Al-Jama'an, *New Digital Frequency Locked Loop Using the Maximum Entropy Method*, MSc. Thesis, Elect. Eng. Dept., King Fahd University of Petroleum and Minerals, Saudi Arabia, June 1989.
9. M. S. El-Hennawey and C. Carter, "ARMA Processing as applied to the Spectral Estimation of SARSAT Signals", *CRL Report Series*, No. CRL-119, McMaster University, Oct. 1983.
10. M. S. El-Hennawey and C. Carter, "On the Estimation of Carrier Frequency of Single Tone and Pulse-Modulated Signals: A Parametric Approach with MEM

and ARMA", *CRL Report Series*, No. CRL-137, McMaster University, Jan. 1985.

11. M. S. El-Hennawey and C. Carter, "MEM and ARMA Estimation of Signal Carrier Frequency", *IEEE Trans. Acoustics, Speech, and Signal Processing*, Vol. ASSP-34, pp. 618-621, June 1986.
12. L. Marple, "A New Autoregressive Spectrum Analysis Algorithm," *IEEE Trans. Acoustics, Speech, and Signal Processing*, Vol. ASSP-28, pp. 441-453, Aug. 1980.
13. N. Wiener, *Extrapolation, Interpolation and Smoothing of Stationary Time Series with Engineering Applications*, Wiley and Sons, New York, 1949.
14. S. L. Marple, Jr., "Frequency Resolution of High Resolution Spectrum Analysis Techniques," in *Proc. 1st RADC Spectrum Estimation Workshop*, 1978, pp. 19-35.
15. S. Haykin (Ed.), *Non Linear Methods of Spectral Analysis*, Springer Verlag, 1979.
16. Anathasios Papulis, *Probability, Random Variables and Stochastic Processes*, McGraw-Hill International Book Co., 1981.
17. J. Burg, " Maximum Entropy Spectral Analysis," *Proc. 37th Meeting Society of Exploration Geophysics*, Oklahoma City, Oklahoma, Oct. 1967.
18. E. Parzen, *Multiple Time Series in Multivariate Analysis*, by P. Krishnaiah, Academic Press, New York, 1969.
19. G. Box and G. Jenkins, *Time Series Analysis, Forecasting and Control*, Holden Day, 1976.
20. T. J. Ulrych and T. N. Bishop, "Maximum Entropy Spectral Analysis and Autoregressive Decomposition," *Rev. Geophysics*, Vol. 13, pp. 183-200, 1975.

21. G. Jenkins and D. Watts, *Spectral Analysis and its Applications*, Holden Day, 1986.

22. J. Cadzow, "Spectral Estimation: an Overdetermined Rational Model Estimation Approach," *Proc. IEEE*, Vol. 70, pp. 907-939, Sept. 1982.

23. B. Friedlander, "A Recursive Maximum Likelihood Algorithm for ARMA Spectral Estimation," *IEEE Trans. on Information Theory*, Vol. IT-30 No. 3, July 1982.

24. William T. Barnett, " Multipath Fading Effects on Digital Radio," *IEEE Trans. on Comm.*, COM-27, Vol. 11, pp. 1842-1848, Dec. 1979.

25. J. K. Chamberlain and et al. "Receiver Techniques for Microwave Digital Radio," *IEEE Communications Magazine*, Vol. 11, pp. 43-54, Nov. 1986.

26. Curtis A. Siller, Jr., "Multipath Propagation," *IEEE Communications Magazine*, 22(2), pp. 6-15, Feb. 1984.

27. Yoshimasa Daido, Sadao Takenaka, Eisuki Fukuda, Toshiaki, and Hiroshi Nakamora, "Multilevel QAM Modulation Techniques for Digital Microwave Radios," *IEEE Journal on Selected Areas in Comm.*, SAC-5, Vol. 3, pp. 336-341, April 1987.

28. G. D. Forney et al. " Efficient Modulation for bandlimited Signals," *IEEE Journal on Selected Areas in Comm.*, SAC-2, Vol. 5, pp. 632-647, Sept. 1984.

29. Jerry D. Gibson, *Principles of Digital and Analog Communications*, Macmillan Publishing Co., 1990.

30. Leon W. Couch II. *Digital and Analog Communication Systems*, Macmillan Publishing Co., 1987.

31. Edward A. Lee and avid G. Messerschmitt, *Digital Communication*, Kluwer Academic Publishers, 1988.

32. William C. Lindsey and Marvin K. Simon, *Telecommunication Systems Engineering*, Printice-Hall Inc., 1973.

33. Chun Loo and Norman Secord, "Computer Models for Fading Channels with Applications to Digital Transmission," *IEEE Trans. on Vehicular Tech.* Vol. 40(4), pp. 700-707, Nov. 1991.

34. C. W. Lundgren and W. D. Rummler, " Digital Radio Outage Due to Selective Fading - Observation vs. Prediction from Laboratory Simulation," *The Bell Systems Technical Journal*, Vol. 58(5), pp. 1073-1103, May-June 1979.

35. Michael J. Miller and Syed V. Ahamed, *Digital Transmission Systems and Networks*, Computer Science Press, 1987.

36. Christoff K. Pauw and Donald L. Schilling, "Probability of Error for M-ary PSK and DPSK on a Rayleigh Fading Channel," *IEEE Trans. on Comm.*, Vol. 36(6), pp. 755-756, June 1988.

37. William D. Rummler, "More on the Multipath Fading Model," *IEEE Trans. on Comm.*, COM-29, pp. 346-352, March 1981.

38. William D. Rummler, R.P. Goutts and M. Liniger, "Multipath Channel Models for Microwave Digital Radio," *IEEE Communications Magazine*, Vol. 24(11), pp. 30-42, Nov. 1986.

39. Bernard Sklar, *Digital Communications Fundamentals and Applications*, Printice-Hall International, Inc., 1988.

40. David R. Smith, *Digital Transmission Systems*, Van. Nostrand Reinold Co., 1985.

41. Seymour Stien, "Fading Channel Issues in Systems Engineering," *IEEE Journal on Selected Areas in Comm.*, SAC-5(2), pp. 68-89, Feb. 1987.